
The Consequences of Aneuploidy in Human Cells

DISSERTATION DER FAKULTÄT FÜR BIOLOGIE
DER LUDWIG-MAXIMILIAN-UNIVERSITÄT MÜNCHEN



vorgelegt von
Diplom-Biologin
Silvia Stinglele (geb. Coenen)

Dezember 2012

EIDESSTATTLICHE ERKLÄRUNG

Hiermit erkläre ich an Eides statt, dass ich die vorliegende Dissertation selbstständig und ohne unerlaubte Hilfe angefertigt habe. Ich habe weder anderweitig versucht eine Dissertation einzureichen oder eine Doktorprüfung durchzuführen, noch habe ich diese Dissertation oder Teile derselben einer anderen Prüfungskommission vorgelegt.

München, den

Promotionsgesuch eingereicht am: 18.12.2012

Datum der mündlichen Prüfung: 06.03.2013

Erster Gutachter: Prof. Dr. Stefan Jentsch

Zweiter Gutachter: Prof. Dr. Peter Becker

Die vorliegende Arbeit wurde zwischen Februar 2008 und Dezember 2012 unter der Anleitung von Zuzana Storchova (Ph.D.) am Max-Planck-Institut für Biochemie in Martinsried durchgeführt.

Wesentliche Teile dieser Arbeit sind in der folgenden Publikation veröffentlicht und zusammengefasst:

Stingele S*, Stoehr G*, Peplowska K, Cox J, Mann M, Storchova Z (2012). "Global analysis of genome, transcriptome and proteome reveals the response to aneuploidy in human cells." *Mol Syst Biol* **8**: 608.

Stingele S, Stoehr G, Storchova Z (2012). "Activation of autophagy in cells with abnormal karyotype." *Autophagy* **9**(2).

** these authors contributed equally to this work*

Note on results obtained in collaboration:

Analysis of data and generation of graphs depicted in Fig. 15, 16, 17, 18, 19, 20, 23, 24, 25, 32 and 33 were performed by our collaborator Gabriele Stoehr (group of Matthias Mann).

Mass spectrometry methods, reagents and machines used by the collaborators are not described in this thesis but referenced in (Stingele, Stoehr et al. 2012).

CONTENTS

1 Abstract	1
2 Introduction	2
2.1 Chromosomal abnormalities	2
2.2 Origins of aneuploidy	4
2.3 Aneuploidy and gene expression levels	7
2.4 Cell proliferation and physiology of aneuploids	8
2.5 Aneuploidy and tumorigenesis	12
2.6 Aneuploidy and chromosomal instability	14
2.7 Protein stress	15
2.8 Protein degradation	16
2.8.1 Proteasomal degradation.....	16
2.8.2 Autophagic degradation.....	18
3 Aim of research	22
4 Results	23
4.1 Construction of aneuploid cell lines	23
4.2 Description and characterization of cell lines	24
4.2.1 HCT116 cell lines.....	24
4.2.2 RPE-1 cell lines - generation and verification	27
4.3 Aneuploid cell lines display a growth delay	28
4.4 The growth delay is due to a prolonged G1 and S phase	30
4.4.1 Aneuploid cells grow slower due to increased time in interphase	30
4.4.2 Aneuploid cells display an increased G1 population	31
4.4.3 Aneuploid cell lines display prolonged G1 and S phase.....	33
4.5 Aneuploid cell lines adjust their protein levels	34
4.5.1 Correlation studies of replicates	34
4.5.2 Matching HCT116 5/4 DNA, mRNA and protein information.....	35
4.5.3 Comparison of mRNA and protein levels of chromosome 5.....	37
4.5.4 Confirmation of data in other cell lines.....	38
4.6 Kinases and subunits of protein complexes are preferentially adjusted in aneuploid cells	41
4.6.1 Analysis of subunits of protein complexes.....	41
4.6.2 Analysis of protein kinases	43
4.7 Aneuploid cells show a distinct cellular response	44
4.8 Aneuploid cells show increased autophagic and proteasomal activity	48
4.8.1 Aneuploid cell lines show up-regulation of autophagic proteins	48
4.8.2 Proteasomal activity is increased in some aneuploid cell lines	49

4.8.3 Autophagic activity is increased in aneuploid cell lines	50
4.9 Aneuploid cell lines show increased p62-dependent autophagy	52
4.9.1 p62 levels are increased in aneuploid cells	52
4.9.2 p62 aggregates colocalize with ubiquitin	53
4.10 Aneuploid cells do not show increased sensitivity to autophagy inhibition	54
4.10.1 Sensitivity of aneuploid cells to autophagy inhibiting drugs	54
4.10.2 Knockdown of p62 is not detrimental to aneuploid cells	54
4.11 Proteins coded on chromosome 5 are not increased after the inhibition of autophagy	56
5 Discussion	58
5.1 Mammalian aneuploid model systems	59
5.2 G1 and S phase delay in aneuploid cell lines	61
5.3 Analysis of transcriptome and proteome in aneuploid cell lines	64
5.4 Pathway analysis in aneuploid cell lines	67
5.5 Analysis of protein degradation mechanisms in aneuploid cell lines	70
5.6 p62 dependent autophagy is increased in aneuploid cell lines	72
6 Experimental procedures	77
6.1 Material	77
6.1.1 Chemicals, media and reagents	77
6.1.2 Buffers	78
6.1.3 Plasmids and bacteria	80
6.1.4 Kits	80
6.1.5 Technical equipment	80
6.1.6 Software	81
6.1.7 Antibodies	81
6.2 Methods	83
6.2.1 Cell culture	83
6.2.2 Molecular biology standard techniques	84
6.2.3 Generation and characterization of cell lines	86
6.2.4 Growth and Cell Cycle Studies	88
6.2.5 Autophagy and proteasome studies	90
6.2.6 Experimental setup for genome, transcriptome and proteome analysis	92
6.2.7 Analysis of genome, transcriptome and proteome data	94
7 References	97
8 Abbreviations	109
9 Acknowledgements	113
10 Curriculum vitae	115

1 ABSTRACT

Aneuploidy is a change in number or structure of one or more chromosomes that are not a multiple of the whole chromosome set. One of the best known pathological aneuploidies is trisomy 21 (Down syndrome), with chromosome 21 present in three instead of two copies. Patients with Down syndrome display severe mental retardation and growth defects. In fact, most abnormal aneuploid karyotypes lead to spontaneous abortions during embryogenesis, indicating that aneuploidy is not well tolerated in humans. Aneuploidy was also shown to be a common hallmark of cancer tissues; however, the debate is ongoing whether aneuploidy is rather a by-product or a trigger of tumorigenesis. Even though aneuploid karyotypes were already identified more than 100 years ago little is understood about cellular physiology of aneuploidy cells, especially in humans. To uncover the consequences of numerical aneuploidy in human cells, I generated aneuploid cell lines derived from the human cell lines HCT116 and RPE-1 hTERT. First, we showed that aneuploid cells proliferate slower compared to their disomic counterparts. A detailed cell cycle analysis revealed that this delay was due to a prolonged G1 and S phase, whereas G2 and M phase remained unperturbed. Furthermore, we conducted an in depth genome wide comparison of DNA, mRNA and protein levels in aneuploid cells. Using CGH, mRNA array and SILAC technology, we quantified the changes in DNA, mRNA and protein abundance. We revealed that extra chromosomes are actively transcribed and translated. However, the abundance of some proteins, particularly subunits of protein complexes and protein kinases, are adjusted towards disomic levels. Additionally, we asked how the cellular physiology is affected by the addition of a specific chromosome. Two scenarios are possible: either the cellular response depends on the additional chromosomes or all aneuploid cells show the same changes of cellular physiology. Indeed, we found that all aneuploid cell lines show similar physiological responses, irrespective of the type of additional chromosome. All aneuploid cell lines down-regulate DNA and RNA metabolism and up-regulate among others energy metabolism, lysosome function and membrane biosynthesis pathways. Lysosomes which are involved in autophagy are besides the ubiquitin-proteasome system important for cellular protein turn over. We found p62-dependent selective autophagy increased in all analyzed cell lines with extra chromosomes suggesting a role of p62-dependent selective autophagy in maintenance of protein homeostasis upon expression of extra protein in these cell lines.

2 INTRODUCTION

Passing hereditary information faithfully from mother to daughter cell is crucial for all living organisms. Before each cell division, cells duplicate their hereditary information, which is then later equally distributed onto the daughter cells, thus generating two cells with exactly the same genetic information. Eukaryotes store their hereditary information on separate chromosomes within their nuclei. Diploid organisms contain two of each chromosome type ($2N$) (Fig. 1). A normal human cell exhibits 23 pairs of chromosomes, 22 pairs of autosomes with identical genetic information and one pair of heterosomes. The heterosome pairs, XX and XY, determine the sex, whereas the autosomes are present equally in males and females. In comparison to diploids, haploid cells contain only one set of chromosomes ($1N$). Genome integrity is maintained by checkpoints which ensure the generation of two daughter cells with identical genetic material.

2.1 Chromosomal abnormalities

Numerical or structural changes of chromosomes can result from errors during amplification and segregation of the hereditary information. Depending on the type of error cells with aberrant chromosome content are either aneuploid or polyploid.

Polyploidy describes a chromosome content which is a multiple of the parental euploid karyotype. There are different types of polyploidy, such as triploid cells containing three or tetraploids containing four chromosome sets. Even though tetraploidy leads to death in early developmental stages during embryogenesis (Kaufman 1991) polyploidy is a common phenomenon in nature. As polyploid plants and their fruits are bigger in size generation of a polyploid karyotype is used for breeding (e.g. wheat and banana)(Elliott 1958). Furthermore, polyploidy is common in many human tissues and organs, as for example tetraploid hepatocytes (Guidotti, Bregerie et al. 2003), polyploid megakaryocytes (Raslova, Roy et al. 2003) and embryonic polyploid trophoblasts (Sarto, Cominato et al. 1982). However, the function of polyploidy in these tissues remains unclear.

In contrast, aneuploidy is a change in number or structure of chromosomes that are not a multiple of the whole chromosome set. Aneuploidy can arise by chromosome non-disjunction either after mitotic division of cells or after meiosis leading to aneuploid gametes. Fusion of an aneuploid gamete with a normal haploid gamete can lead to the offspring of an aneuploid embryo. One of the best known embryonic aneuploidies is

trisomy 21 (Down syndrome), with chromosome 21 present in three instead of two copies (Fig. 1). Embryos with Down syndrome display severe growth defects. Other identified viable aneuploid disorders are trisomy 13 and 18. No other aneuploid disorders were found to be compatible with life and most aneuploidies affecting the whole organism are lethal. In fact, most spontaneous abortions are due to an abnormal aneuploid karyotype (Toikkanen, Joensuu et al. 1993). Likewise, trisomic mice die during embryogenesis and the only viable trisomy is trisomy 19, leading to death shortly after birth (Magnuson, Smith et al. 1982). Accordingly, aneuploidy in flies (Lindsley, Sandler et al. 1972) and nematodes leads to developmental defects and lethality (Hodgkin, Horvitz et al. 1979).

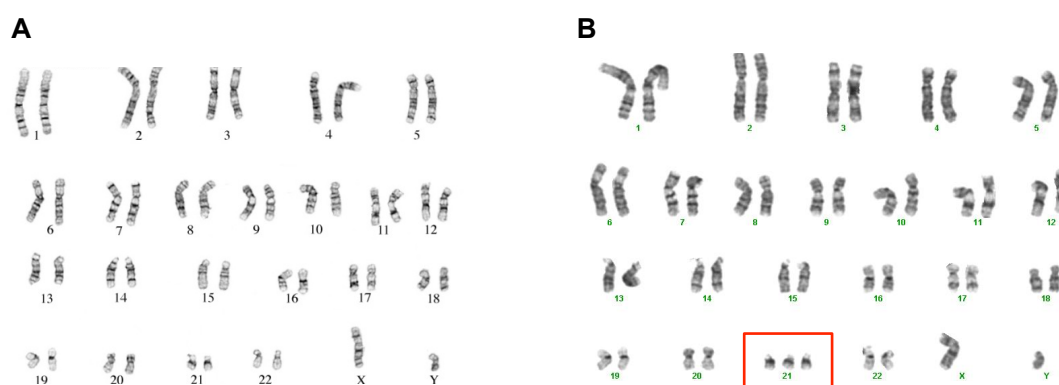


Fig. 1: Human diploid (A) and aneuploid trisomy 21 (B) karyotype. In diploid cells, all 23 chromosomes are present in two copies (2N), except the heterosomes in males (A). Aneuploid cells display a karyotype with a change in number or structure of single or multiple chromosomes that are not a multiple of the whole chromosome set. Trisomy 21 patients display a karyotype with three copies of chromosome 21 (marked in red) instead of two (B).

However, aneuploid cells can also arise during cell division of somatic cells. Aneuploidy was shown to be a common hallmark of cancer. In fact, 90% of solid tumors are aneuploid (Storchova and Kuffer 2008). In 2007, Yuorov and colleagues found that 30-35% of all brain cells in healthy humans are aneuploid, but it is not known whether these cells are able to propagate. Interestingly, an increased frequency of aneuploid cells was found in brains of Alzheimer's disease patients. The exact function of aneuploid cells in human brains remains unclear (Yuorov, lourov et al. 2007) (Yuorov, Vorsanova et al. 2009).

It is important to separate aneuploidy from chromosomal instability (CIN) which is as well as aneuploidy a frequent hallmark of cancer (Holland and Cleveland 2009). Whereas aneuploidy describes the present state of the genomic material, chromosomal instability describes ongoing missegregation of different chromosomes (Holland and Cleveland 2009). Therefore, chromosomally unstable cells are always aneuploid as e.g. shown in cancerous tissues (Nagaoka, Hassold et al. 2012) whereas aneuploid cells are not always chromosomally unstable, as shown in cells from Down syndrome patients.

2.2 Origins of aneuploidy

Whole chromosome aneuploidies result from chromosome segregation errors. Chromosome missegregation can either happen randomly or due to mutations leading to defects in spindle assembly checkpoint (SAC), sister chromatid cohesion or merotelic attachment (Fig. 2). In contrast to whole chromosome aneuploidies structural aneuploidies can result from errors in DNA replication and repair. These currently known mechanisms of aneuploidization in somatic cells are summarized in the following paragraphs.

The SAC is a checkpoint that creates a wait signal during mitosis until the kinetochores of all chromosomes are properly attached to microtubules. Even one kinetochore that is not attached to a microtubule is sufficient to trigger the SAC signal (Rieder, Cole et al. 1995). A complete knockout of many spindle checkpoint genes such as genes encoding for Bub3 and Mad2 were shown to be embryonic lethal (Dobles, Liberal et al. 2000; Kalitsis, Earle et al. 2000). However, mice with impaired SAC survive and their cells can divide even though the chromosomes are not aligned properly leading to chromosomally instable cells (Fig. 2A). This was shown by Michel and colleagues who generated *Mad2* haplo-insufficient mice which developed lung tumors at high rates and respective cells displayed high levels of chromosomally instable aneuploid cells (Michel, Liberal et al. 2001). Similarly, mice heterozygous for *Bub1*, *BubR1* and *Bub3* develop high levels of aneuploidies and spontaneous or induced tumor development (Dai, Wang et al. 2004; Baker, Jeganathan et al. 2006; Jeganathan, Malureanu et al. 2007).

A second mechanism which defect results in chromosomal missegregation, is sister chromatid cohesion. Two newly replicated sister chromatids are kept together by evolutionary conserved protein complexes called cohesins. This protects the sisters chromatids from premature segregation, which may result in aneuploidy (Fig. 2B). The cohesin rings are cleaved by separase at anaphase onset. Sister chromatid cohesion is necessary to create tension by keeping the sister chromatids together while the microtubules attached to the kinetochores pull them apart (Peters 2012). Aneuploidy was found to be increased in yeast cells with defects in proteins involved in chromatid cohesion (Guacci, Koshland et al. 1997; Michaelis, Ciosk et al. 1997). In concordance, it was shown that inactivation of *STAG2*, a subunit of the cohesion complex, leads to aneuploidy in human cells (Solomon, Kim et al. 2011). Moreover, a recent screen sequenced somatic mutations of chromosomally instable colorectal cancer cell lines. Intriguingly, authors revealed that identified mutated genes coded for yeast homologues that were found to regulate sister chromatid cohesion (Barber, McManus et al. 2008). In line, separase levels were found to be increased in breast cancer tissues (Zhang, Ge et al. 2008) and *STAG2* levels were decreased in human cancer cell lines, indicating an *in*

vivo role of cohesion in tumorigenesis. Moreover, age dependent defects of cohesion during oogenesis in elderly women were found to increase levels of aneuploid oocytes resulting in higher levels of aneuploid embryos (Lister, Kouznetsova et al. 2010). Furthermore, it was shown that sister chromatid cohesion is important to prevent merotelic attachment (Cimini 2008).

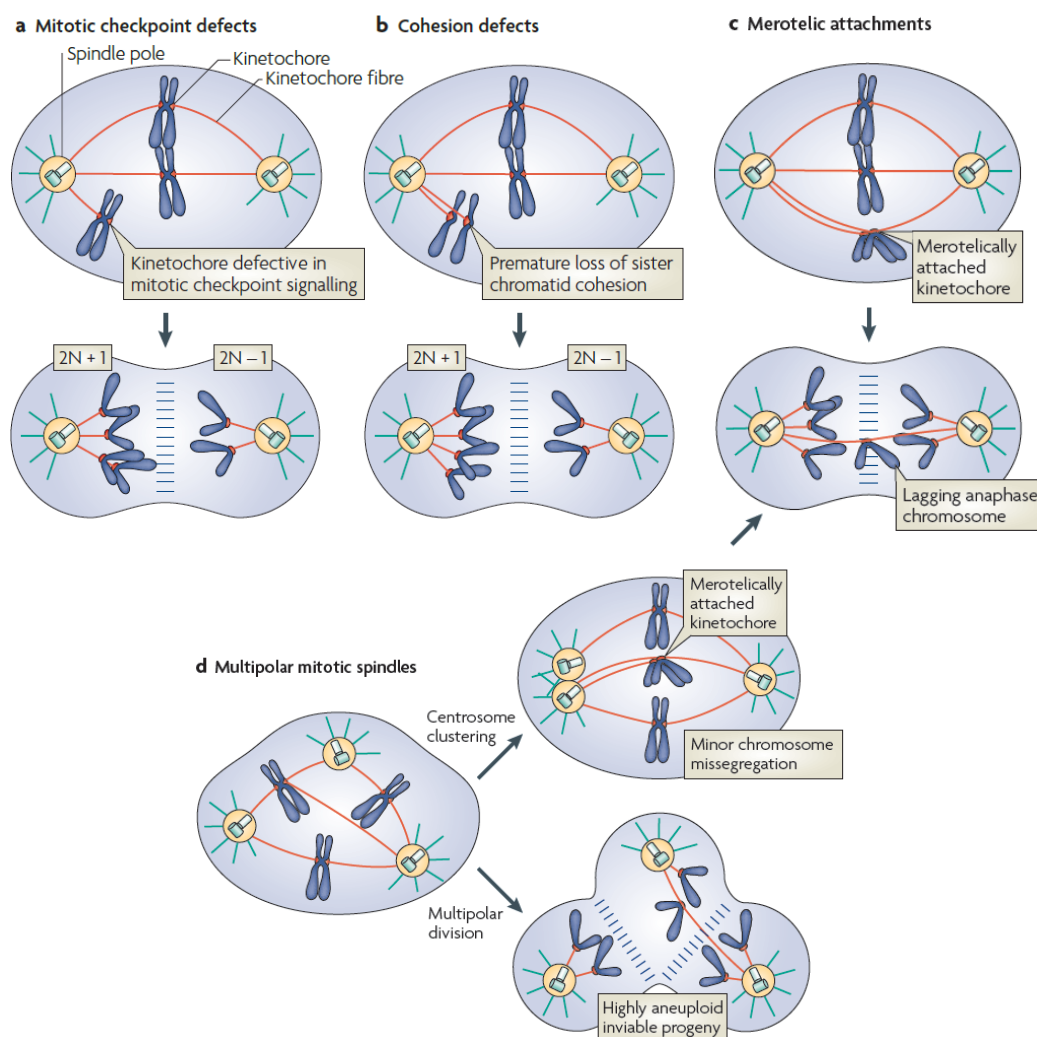


Fig. 2: Origins of whole chromosome aneuploidies. Chromosome missegregation can lead to whole chromosome aneuploidy. Three known mechanisms can lead to chromosome missegregation. Spindle assembly checkpoint defects (A), Cohesion defects (B) and merotelic attachment (C+D). Merotelic attachment can either arise randomly (C) or is happening more frequently in cells with multiple centrosomes. These cells either display a multipolar division and die in most of the cases or are able to cluster their centrosomes, which then tend to merotelic attachment (D). Figure adapted from: (Holland and Cleveland 2009)

Merotelic attachment classifies the attachment of one sister chromatid to microtubules from both spindle poles. Besides resulting from chromatid cohesion defects merotelic attachment can also arise spontaneously. In many cases this type of error is not recognized by the SAC, because both kinetochores are attached to microtubules under

sufficient tension. Therefore, merotelic attachment remains often uncorrected. Attachment defects result in lagging chromosomes (chromosomes that are not properly aligned) and consequently chromosome missegregation and aneuploidy (Fig. 2C) (Cimini, Howell et al. 2001). Recently, it was shown that cells with multiple centrosomes tend to missegregate their chromosomes due to a high frequency of merotelic attachment (Ganem, Godinho et al. 2009). Authors propose that chromosomes connect to microtubules from two different spindle poles during an intermediate multipolar stage during cell division. Then multipolarity is resolved to bipolarity by clustering of centrosomes and merotelic attachment leads to chromosome missegregation. This explains why cells with multiple centrosomes are usually highly chromosomally unstable (Sato, Mizumoto et al. 2001; Lingle, Barrett et al. 2002). This finding is in contrast to the long standing hypothesis that cells with multiple centrosomes become aneuploid due to multipolar division by distributing the chromosomes on more than two daughter cells (Holland and Cleveland 2009). Since Ganem and colleagues could show that cells derived from multipolar division undergo apoptosis (Ganem, Godinho et al. 2009) generation of aneuploidy is probably rather due to merotelic attachment (Fig. 3D). It was proposed that aneuploidy results out of tetraploidy as tetraploid cells are chromosomally unstable and lose chromosomes over time (Mayer and Aguilera 1990; Fujiwara, Bandi et al. 2005). Interestingly, tetraploid cells with doubled centrosome number passing intermediate stages of multipolarity were shown to have elevated levels of lagging chromosomes which were not detectable in tetraploid cells with only two centrosomes (Ganem, Godinho et al. 2009).

Many aneuploid cells do not display numerical aneuploidies but structural aneuploidies. The origin of these gross chromosomal rearrangements (GCRs) in aneuploid cells is mostly unclear. It is known that DNA damaging agents such as γ -irradiation and hydroxyurea induce chromosomal rearrangements (Suzuki, Ojima et al. 2003) suggesting that rearrangements might be a result of improper repair of DNA lesions. Defects such as mutations or deletions of proteins involved in homologous recombination leads to genomic instability as well. Moreover, perturbations of DNA replication results in elevated levels of chromosomal rearrangements (Huang and Koshland 2003). Lagging chromosomes often form micronuclei after cell division. Replication of this trapped DNA is often defective and results in a pulverization of the chromosome which is later reassembled leading to structural aneuploidy (Crasta, Ganem et al. 2012).

2.3 Aneuploidy and gene expression levels

The hallmark of aneuploidy is an altered karyotype with either amplified or deleted genome regions if compared to euploidy. The question arises whether changes in gene copy number lead to a proportional scaling of expression-levels. Transgene experiments adding single genes to a cell provide evidence that at least for single genes protein levels scale according to gene copy number (reviewed in (Birchler 2010)).

First studies in aneuploid plants showed expression levels of most transcripts do not scale according to gene copy number (Guo and Birchler 1994). Whereas, studies of aneuploid yeast and mouse cells showed mRNA are transcribed in a dosage dependent manner (Amano, Sago et al. 2004; Upender, Habermann et al. 2004; Torres, Sokolsky et al. 2007; Williams, Prabhu et al. 2008). How transcriptional levels are changed in aneuploid cells was also addressed by scientists studying dosage compensation of sex chromosomes. Dosage compensation describes a mechanism compensating gene expression dosage of sex chromosomes to maintain equal gene expression levels in male and female organisms (Zhang and Oliver 2007). In mammals, females are able to inactivate randomly one of their X chromosomes by methylation of DNA and histones to compensate the extra load of gene numbers in comparison to males. In contrast, gene expression levels of the X chromosome in male fruit fly are up-scaled. Gene expression levels in male *Drosophila* are maintained by the male-specific lethal (MSL) complex. The complex contains MOF, an acetyltransferase, which is believed to activate gene expression by acetylating histone H4 at lysine 16 (Akhtar and Becker 2000). Dosage compensation is achieved at transcriptional levels and not post translationally (Belote and Lucchesi 1980). Similar compensation mechanisms could also influence gene expression patterns of different gene copy numbers in aneuploid cells. To address this possibility, Zhang and colleagues performed a genome wide transcriptome analysis of *Drosophila* S2 cells containing segmental aneuploidies, comparing gene expression levels to gene copy number. Interestingly, they found that transcripts of aneuploid gene regions are dosage compensated and that this dosage compensation on mRNA level is not dependent on the MSL complex (Zhang, Malone et al.). Differences in gene expression studies can be various and variations observed between mammals and flies are probably rather due to evolutionary divergence and therefore are probably due to different strategies how organisms cope with their extra load of genetic material.

Most studies analyzed transcriptional levels in aneuploids. However, buffering mechanisms for subunit proteins of macromolecular complexes in aneuploid maize and flies were described already more than 30 years ago (Birchler and Newton 1981; Devlin, Holm et al. 1982). In line, two studies in aneuploid yeast showed that even though transcripts were present according to the gene copy number some proteins were at

levels as expected for euploid cells. Accordingly, 20% of proteins did not scale proportionally with their gene copy number, but were present at lower levels. Intriguingly, all compensated proteins identified, are subunits of protein complexes (Torres, Sokolsky et al. 2007; Torres, Dephoure et al. 2010). However, another study analyzing aneuploid yeast with complex karyotypes found no significant compensation of a specific protein group (Pavelka, Rancati et al. 2010), which may be due to differences in karyotype complexity. The reason why some proteins do not scale according to gene copy number remains unknown. Three reasons may lead to this protein compensation. Subunits of protein complexes may not be translated into proteins, are less stable or are actively degraded. Data by Torres and colleagues as described above suggests that aneuploid yeast require proteasomal degradation to proliferate as well as haploid yeast (Torres, Dephoure et al. 2010), indicating that subunits may be actively degraded.

In conclusion, aneuploid cells show most studies showed that transcriptional levels scale with gene copy number. It was suggested that specific proteins such as subunits of macromolecular complexes are compensated to a level lower as expected for gene copy number. However, detailed studies on protein levels especially in human aneuploid cells are missing.

2.4 Cell proliferation and physiology of aneuploids

Most whole embryo aneuploidies in humans lead to miscarriages and viable aneuploid humans display mental retardation and growth defects. In line with these findings, cultured fibroblasts derived from Down syndrome patients grow slower in comparison to diploid fibroblasts (Segal and McCoy 1974). Similarly, aneuploid MEF and artificially generated aneuploid yeast cells grow significantly slower compared to their non-aneuploid counterparts (Torres, Sokolsky et al. 2007; Williams, Prabhu et al. 2008; Pavelka, Rancati et al. 2010).

Pathway analyses were performed to gain first insights into how aneuploidy affects cellular physiology. There are two possibilities how extra protein could influence cellular physiology. First, depending on the set of altered proteins distinct cellular pathways could be influenced. Amplification of a chromosome containing e.g. a negative regulator of a pathway could lead to an inhibitory effect of this pathway due to its increased expression. This would mean that a specific loss or gain of a chromosome with its specific genes would lead to a distinct de-regulated pathway pattern which should be different in every individual aneuploidy. Second, aneuploid cells could also show similar cellular physiology independent of the type of extra chromosome. This may be the case if cellular physiology

is rather altered by common characteristics of aneuploid cells such as protein stress. Detailed studies on deregulated pathways in aneuploid cells were performed so far only in yeast (Torres, Sokolsky et al. 2007; Pavelka, Rancati et al. 2010). Whereas Pavelka et al. could not find a common pattern of pathway regulation in aneuploid yeast Torres et al. observed a transcriptional regulation pattern similar to the environmental stress response (ESR). The effect of aneuploidy on cellular physiology was also tested in transformed as well as cancerous human cell lines which contained a transferred chromosome. Multiple transcripts were deregulated across the whole genome however, no common aneuploidy specific pathway pattern was reported (Upender, Habermann et al. 2004). Similarly, studies in *Drosophila* cells did not reveal any aneuploidy specific response (Zhang, Malone et al. ; Stenberg, Lundberg et al. 2009). In contrast it was just recently published that aneuploid yeast (single chromosome aneuploidies as well as complex aneuploidies), plant, mice and human cells show highly related gene expression patterns (Sheltzer, Torres et al. 2012), indicating that differences in most studies are probably due to differences in data analysis. However, fly cells may have alternate mechanisms how to deal with aneuploidy.

There is indication, that aneuploid yeasts have an altered energy metabolism which may cause reduced growth rates. Aneuploid yeast showed down-regulation of proteins involved in energy metabolism under growth limiting conditions. Moreover, aneuploid yeast assimilates higher levels of glucose and creates less biomass per glucose compared to wild-type yeast. In line, two gene loci of the two glucose transporters, Hxt6 and Hxt7 were amplified, confirming that aneuploid yeast needs more glucose for survival (Torres, Sokolsky et al. 2007). On the other hand, aneuploid MEF cells showed no significant increase in glucose uptake, but instead lactate uptake was elevated in comparison to disomic MEFs. Additionally, glutamine consumption was significantly increased as well as ammonium production (Williams, Prabhu et al. 2008). However, why cells show these differences in metabolite production and consumption remains unclear but there are hypothesis that transcription, translation and degradation of protein encoded on the extra chromosome require energy, which leads to an increased need for energy metabolites (Williams, Prabhu et al. 2008).

Further studies were conducted to test if either DNA or mRNA and protein affect cellular growth. First, extra DNA was added to haploid yeast cells using a yeast artificial chromosome (YAC) containing non-transcribed human and mouse DNA. Cells harbouring these YACs showed no growth delay, indicating that growth defects are due to changed mRNA or protein abundance (Torres, Sokolsky et al. 2007) and not to the additional DNA. To test if proteins are harmful to aneuploid cells same authors treated cells with drugs affecting protein homeostasis. Indeed, they could show that aneuploid

cells are more sensitive to several drugs such as cycloheximide, thiolutin, hygromycin, rapamycin, geldanamycin and MG132. Moreover, aneuploid yeast cells were more sensitive to higher temperatures. All these treatments affect cellular protein homeostasis. Cycloheximide, hygromycin as well as rapamycin inhibit protein synthesis. Geldanamycin inhibits Hsp90, an important chaperone that is actively transcribed after heatshock, whereas increased temperature triggers the heat shock response. MG132 inhibits the proteasome and sensitivity suggests an important function of the proteasome in aneuploid yeast. Accordingly, a recent study indicates that increased proteasome activity allows aneuploid yeast cells to grow faster. Aneuploid yeast was shown improved growth-rates upon several gene-deletions, including *UBP6*, which encodes a de-ubiquitinating enzyme (Torres, Dephoure et al. 2010). Authors speculate that deletion leads to a higher turnover of protein by the proteasome (Torres, Dephoure et al. 2010) and therefore, a relief of the protein burden on cellular physiology. Taken together, data suggests that aneuploid cells are indeed challenged with protein stress, which is probably due to the extra protein expressed in aneuploid cells. However, why most of these drugs affect aneuploid cell proliferation remains unknown.

In contrast to these studies, Pavelka and colleagues could not show a common sensitivity of aneuploid yeast cells towards certain drugs (Pavelka, Rancati et al. 2010). Authors studied proliferation capacity of aneuploid yeasts under various drug treatments such as drugs used as chemotherapeutics or antifungal drugs. Here aneuploid strains show a high diversity of sensitivity towards various drugs which was dependent on the type of extra chromosomes. Whereas some of the aneuploid strains grew worse, other aneuploid strains displayed growth benefits compared to their euploid counterpart when treated with some drugs, such as rapamycin, bleomycin and thiolutin. Rapamycin as well as thiolutin however, had anti-proliferative effects in the study conducted by Torres and colleagues. Differences between these two studies may result from differences in complexity of aneuploidy. Pavelka and colleagues used yeast with complex aneuploid karyotype ranging between 1N and 3N whereas Torres et al added single chromosomes to haploid yeast. The study by Pavelka and colleagues indicates that altered gene expression may lead to phenotypic variation. Therefore, a complex aneuploid karyotype could lead to an evolutionary advantage of cells towards specific stresses. Evolutionary aspects of this study are further discussed in the chapter “Aneuploidy and tumorigenesis”

The first study in mammalian cells revealed three drugs, AICAR, chloroquine and 17-AAG affecting growth of aneuploid MEF cells as well as aneuploid cancer cell lines (Tang, Williams et al. 2011). As described above, yeast aneuploid cells seem to have an altered energy metabolism, which would be in line with the sensitivity to AICAR, a drug which activates AMPK and induces energy stress (Corton, Gillespie et al. 1995).

Moreover, aneuploid yeasts were shown to be more sensitive to the inhibition of Hsp90 by geldanamycin. In accordance, this mammalian cell study shows that inhibition of Hsp90 by 17-AAG, a derivative of geldanamycin, affects growth of aneuploid cells. However, geldanamycin itself was not tested. In contrast to aneuploid yeast cells, mammalian cells were sensitive to chloroquine. Chloroquine is an anti-malarial drug which was shown to inhibit autophagy. However, aneuploid yeast cells were shown to be sensitive to MG132, a proteasome inhibitor. This indicates that aneuploid yeast and mammalian cells require different protein degradation pathways for proliferation. Besides these three drugs a series of drugs was tested inducing genotoxic, proteotoxic as well as energy stress. Intriguingly, most protein stress inducing drugs did not affect growth of aneuploid cells, therefore, being not as striking as in the yeast study. Differences between studies in mammalian and yeast cells may be due to differences in protein homeostasis. Mammalian cells may have alternative pathways to bypass the inhibition of another one.

In conclusion, there is indication that aneuploid cells display a common aneuploidy specific cellular response, which may be conserved. Furthermore, aneuploid cells display marked growth defects, which are probably based on an increased need in energy due to transcription, translation and degradation of extra protein. However, this hypothesis is mainly based on correlative studies and detailed experiments elucidating underlying mechanisms are yet missing.

2.5 Aneuploidy and tumorigenesis

Even though, aneuploidy was found to be a hallmark of cancerous tissues already 100 years ago (Boveri 1912) the relationship between aneuploidy and tumorigenesis remains elusive. Since mice with high level of chromosome missegregation develop cancer with high frequency, it is hypothesized that aneuploidy can trigger tumor formation. Multiple observations made in the last century indicate that there is a relationship between aneuploidy and tumorigenesis.

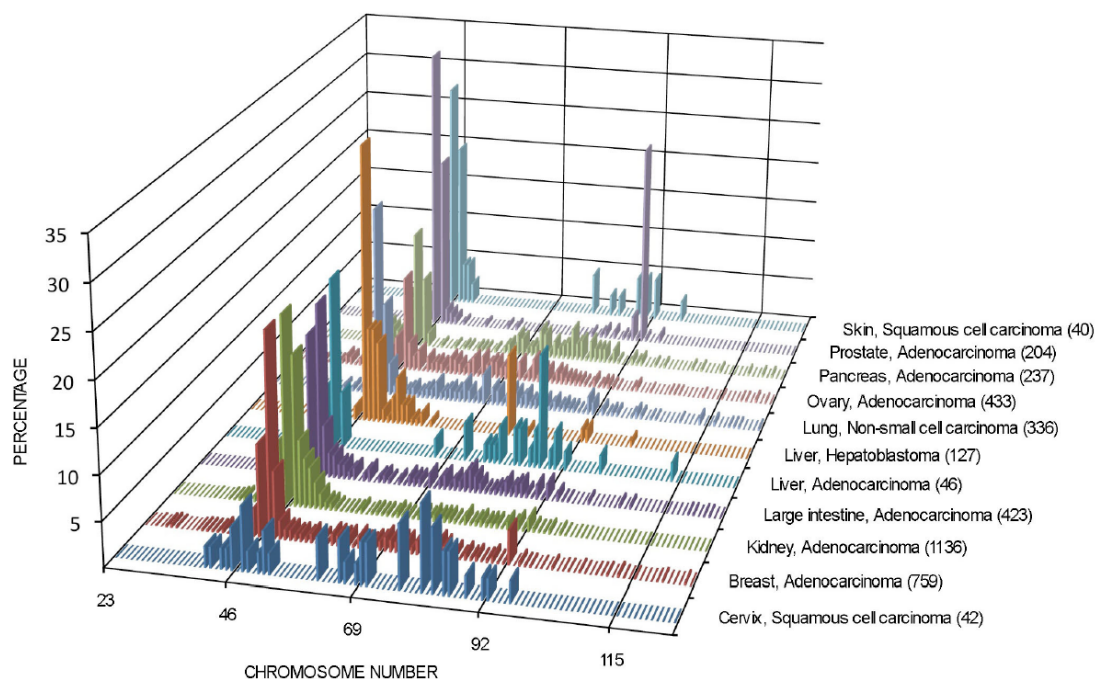


Fig. 3: Aneuploidy and tetraploidy in human cancers. Displayed are karyotypes as listed in the Mittelman database, sorted by cancer types. The graph clearly shows that multiple cancer types contain high level of aneuploidies. Highest peaks are found around diploidy (46 chromosomes), likely indicating missegregation events. In some of the cancer types, karyotypes vary below tetraploidy (92 chromosomes). Figure adapted from (Storchova and Kuffer 2008).

As shown in Fig. 3, karyotyping of multiple human tumors showed that cancer tissues contain a highly variable chromosome content, ranging from hypertetraploidy (more than the doubled chromosome number) to hypodiploidy (chromosome number less than diploid karyotype), with an accumulation of cells with a karyotype ranging around diploidy and tetraploidy (Mittelman data base), (Storchova and Kuffer 2008). Tumor cells of some tissues seem to propagate the aberrant karyotype stably whereas others tumor cells are chromosomally instable resulting in tissues containing cells with various karyotypes (Lengauer, Kinzler et al. 1997).

Moreover, the oncogene *c-MYC* (chromosome 8) is often amplified in various cancer types (Escot, Theillet et al. 1986; Nesbit, Tersak et al. 1999) and accordingly,

chromosome 8 amplification is one of the most frequent aneuploidies (10-20%) found in acute myeloid leukaemia (AML) (Paulsson and Johansson 2007). A recent study on somatic copy number alterations in cancer showed that 25% of cancer cells display either whole arm or whole chromosome aneuploidies, whereas only 10% of cells contain small, site specific changes, so called focal SCNAs (Beroukhim, Mermel et al. 2010). As described above, changes in the levels or function of spindle assembly checkpoint (SAC) proteins is a possible mechanism for chromosome missegregation and thus can lead to aneuploidy. Interestingly, defects in the SAC, such as low BUB1 levels were observed in several colorectal cancer cell lines (Cahill, Lengauer et al. 1998). Jeganathan and colleagues (Jeganathan, Malureanu et al. 2007) generated mice expressing reduced levels of BUB1. These mice develop spontaneous tumors with a high level of aneuploidy. MEF cells isolated from the mutant mice exhibit high rates of chromosome missegregation. Similarly, mice heterozygous for *Mad2*, *BubR1* and *Bub3* are prone to spontaneous or induced tumor development (Dai, Wang et al. 2004; Baker, Jeganathan et al. 2006). Furthermore, MAD2 overexpression is a common phenomenon in human tumors (Sotillo, Hernando et al. 2007) and leads to chromosomal instability (Hernando, Nahle et al. 2004). It was shown that overexpression of MAD2 leads to aneuploidy as a consequence from a checkpoint override and promotes tumorigenesis in mice (Sotillo, Hernando et al. 2007), Weaver and colleagues have shown that *Cenp-E*^{+/-} mice developed high levels of tumors with an aneuploid phenotype (Weaver and Cleveland 2007; Weaver, Silk et al. 2007). Although these data support the hypothesis that aneuploidy leads to tumorigenesis, it remains unclear whether the cancer phenotypes observed in these mice models are due to the aneuploidy or due to another unknown functions of the spindle assembly checkpoint proteins. Another study performed in 2005 by Fujiwara and colleagues could show that injection of *p53*^{-/-} tetraploid cells into mice lead to a high frequency of malignant mammary epithelial cancers. Moreover, tumors tissues were highly aneuploid (Fujiwara, Bandi et al. 2005). Since, tetraploidy presents a rather instable state (Storchova and Pellman 2004) it is not surprising that these developing tumors were aneuploid. In contrast to other studies, this study indicates that aneuploidy itself can lead to cancer formation. In conclusion, many studies suggest a role of aneuploidy in tumorigenesis. However, if aneuploidy triggers

2.6 Aneuploidy and chromosomal instability

It was proposed that numerical aneuploidy leads to increased chromosomal instability. A recent study showed that aneuploid yeasts indeed display an increased level of chromosome missegregation, DNA damage and mitotic recombination in comparison to haploid yeasts (Sheltzer, Blank et al. 2011). Moreover, it was shown that chromosomal instability is dependent on the type of aneuploidy. Therefore, chromosomal instability was relatively low if aneuploidy was close to haploidy. However, the closer the aneuploid karyotype was to the 2N state, the more increased their level of chromosomal instability (Zhu, Pavelka et al. 2012). Inherent instability of aneuploid may provide an explanation how aneuploidy could trigger tumor formation. Intriguingly, chromosomal instability was shown to lead to a poor prognosis and high level of resistance to chemotherapeutics (Gao, Furge et al. 2007; Choi, Seo et al. 2009). Additionally, as aneuploid yeasts were shown to be less chromosomally stable than haploids they may adapt easier to various stresses due to higher genomic variability. This is in line with studies by Pavelka and colleagues who found that aneuploid yeast displayed growth advantages compared to their euploid counterparts if treated with certain drugs (Pavelka, Rancati et al. 2010). Since aneuploid yeasts used in this study were naturally generated and contain more complex aneuploidies, one could speculate that evolutionary progress could already take place during generation of aneuploid strains. Besides aneuploid cells may evolve due to external stresses, they may also evolve to internal factors (e.g. the reason for their slow growth). As another study showed that after cultivation of aneuploid yeast, some yeast strains were able to improve their growth to a similar level as their euploid counterpart. After analysis of these fast growing aneuploid yeast strains authors identified multiple changes and most often a deletion of the gene encoding for Ubp6, a de-ubiquitinating enzyme. Authors hypothesize that deletion of *UBP6* leads to a higher turnover of protein by the proteasome. This increased protein degradation abolishes the burden of extra protein on the cell and enables increased growth (Torres, Dephoure et al. 2010). Therefore, after cultivation of aneuploid yeast, cells displayed genomic changes that were shown to be beneficial for their growth. Accordingly, also aneuploid MEF cells were able to immortalize faster than normal diploid MEFs (Williams, Prabhu et al. 2008). Immortalization results from mutations and modulations of genes leading to increased proliferation rate. Therefore, increased immortalization rate may be due to a higher level of chromosomal instability as observed for aneuploid yeast.

In conclusion, aneuploid yeast cells were shown to display increased chromosomal instability. This may allow aneuploid cells to adapt faster to certain stresses than their euploid counterparts, providing an interesting evolutionary model. In line, increased chromosomal instability of aneuploid cells could also explain how aneuploidy leads to

tumorigenesis. However, reasons for increased chromosomal instability and DNA damage in aneuploid cells remain elusive and further research is needed to dissect the underlying molecular mechanisms.

2.7 Protein stress

Current research indicates that aneuploid cells suffer from protein overexpression due to their extra genetic material. A surplus of proteins can be harmful to a cell due to several reasons. Overexpression of proteins can lead to protein missfolding and aggregation which can be harmful for cellular homeostasis. Proteins with long hydrophobic chains can interfere with protein function of other proteins and aggregate, which in turn can lead to the disruption of important cellular functions (Chiti, Stefani et al. 2003; Stefani and Dobson 2003). Missfolding of a single protein can lead to the destabilization of other proteins and thus start a reaction that may have detrimental effects for a cell (Gidalevitz, Ben-Zvi et al. 2006; Gidalevitz, Krupinski et al. 2009). The hallmark of several neurodegenerative diseases such as Parkinson's, Huntington's and Alzheimer's disease is an accumulation of aggregating proteins (Bossy-Wetzel, Schwarzenbacher et al. 2004). Why these protein aggregates are toxic to the cell is not yet completely understood. Olzscha and colleagues showed that artificially constructed amyloids promoted interactions and sequestered other cellular proteins that were large in size and rich in unstructured regions. Most of these proteins that were sequestered with the artificially constructed amyloids have important functions and authors hypothesize that aggregation of these proteins may lead to the proteotoxicity and disruption of important cellular functions (Olzscha, Schermann et al.). Protein aggregation diseases usually affect neurons indicating that neurons are more prone to accumulate missfolded proteins (Drummond and Wilke 2008). Aggregation diseases occur in aging organisms because orchestration of proteostasis decreases with age (Balch, Morimoto et al. 2008) resulting from the decreasing function of protein degradation and folding machinery (Sherman and Goldberg 2001; Morimoto 2008). Moreover, proteotoxicity was recently hypothesized to play a role in aging since pathways that prevent proteotoxicity were found to be important for longevity in *C. elegans* (Taylor and Dillin 2011).

To avoid proteotoxic effects, cells developed sophisticated regulatory mechanisms controlling protein translation, folding, segregation and degradation (Balch, Morimoto et al. 2008). The rate of protein translation as the first step of protein quality control can be adapted by multiple means and affect proteins either globally or specifically (Gebauer and Hentze 2004). Reducing the translational rate could provide more time for protein folding and degradation and therefore affect protein homeostasis. Some proteins fold

spontaneously after translation, whereas others need to be folded by chaperones (Morimoto 2008). Upon thermal shock all cells from prokaryotes to eukaryotes react by overexpressing heat shock proteins (HSPs), which are chaperones that enable the cell to refold missfolded proteins (Ellis, van der Vies et al. 1989) (Lindquist and Craig 1988; Morimoto 2008). There are several different heat shock proteins that are classified by their molecular weight, such as Hsp90 and Hsp70. The main regulators of the heat shock response are transcription factors (HSFs) that allow expression of heat shock response proteins (Akerfelt, Morimoto et al. ; Morimoto 2008). Some cellular proteins are translated by ribosomes associated with endoplasmic reticulum (ER) and translocated into the ER lumen, where they are folded. The ER contains chaperones to fold proteins within the ER. Faulty protein folding in the ER triggers a stress response pathway called the unfolded protein response (UPR) (Schroder and Kaufman 2005; Walter and Ron 2011). Only correctly folded proteins are transported to their final destination by the ER. If a protein remains missfolded it is delivered to the proteasome and degraded via ER associated degradation (ERAD) (Hurtley, Bole et al. 1989; Ellgaard and Helenius 2003). Cells usually undergo apoptosis after persistent ER stress (Tabas and Ron 2011). Thus, maintenance of correct protein levels and folding is essential for the cells and old, aberrant or malfunctional proteins as well as proteins that remain missfolded despite the above mentioned protein quality control system must be degraded. This is achieved by the two major protein degradation machineries, the ubiquitin-proteasome-system (UPS) and autophagy (Ciechanover 2005).

2.8 Protein degradation

2.8.1 Proteasomal degradation

One of the best studied protein degradation machineries is the ubiquitin-proteasome-system (UPS). Degradation of proteins via the UPS is a tightly regulated process that is carried out in several steps. High selectivity is maintained by tagging substrates with ubiquitin, which marks them for the degradation by the 26S proteasome (Hochstrasser 1996; Hershko and Ciechanover 1998). Ubiquitin, as the name indicates, is ubiquitously expressed and highly conserved among eukaryotes. It is a globular 76 amino acid protein, which can be covalently attached to a lysine (K) of the target protein via its C-terminus. Ubiquitination involves an enzymatic E1-E2-E3 cascade (Fig. 4). Initially, an ubiquitin activating enzyme (E1) enzyme forms a high energy thioester with ubiquitin's C-terminus in an ATP dependent reaction. The ubiquitin moiety is subsequently transferred to the active cysteine of an ubiquitin conjugating enzyme (E2). Finally, ubiquitin is conjugated to the ϵ -amino group of a lysine residue in the substrate protein. This step is

catalyzed by ubiquitin ligases (E3) (Hershko and Ciechanover 1998; Glickman and Ciechanover 2002).

Substrates can undergo several rounds of ubiquitination, resulting in the formation of ubiquitin chains. Depending on the lysine residues in ubiquitin used for conjugation, chains with several linkage types and therefore topologies can be formed. The type of ubiquitin modification results in diverse biological outcomes. K48-linked polyubiquitin chains for example target proteins for degradation via the 26S proteasome (Hicke and Dunn 2003), whereas monoubiquitination can regulate the substrate activity, and K63-linked chains mediate processes in transcription (Muratani and Tansey 2003), DNA repair (Hoegel, Pfander et al. 2002) and endocytosis (Hicke and Dunn 2003). Ubiquitination is a reversible process. Ubiquitin deconjugation is performed by de-ubiquitinating enzymes (DUBs) (Amerik and Hochstrasser 2004; Nijman, Luna-Vargas et al. 2005).

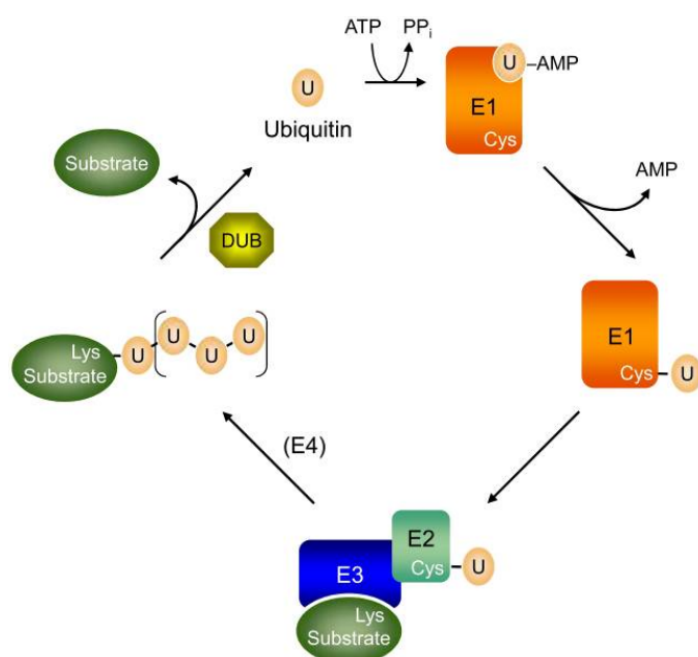


Fig. 4: The ubiquitin conjugation pathway.

Ubiquitin is activated in an energy dependent step by the enzyme E1, involving an AMP-ubiquitin intermediate. Ubiquitin is then transferred to the cysteine of an E2. The E3 ligase catalyzes finally the conjugation of ubiquitin to the substrate. The E3 ligase can also conjugate the ubiquitin to another ubiquitin, thereby forming ubiquitin chains. Polyubiquitylated substrates are recognized and degraded by the 26S proteasome. Ubiquitination can be reversed by de-ubiquitinating enzymes (DUBs). Figure adapted from (Hochstrasser 2009).

Substrates modified with K48-linked polyubiquitin chains are recognized by the 26S proteasome. The 26S proteasome consists of two subassemblies, the 20S core particle and the 19S regulatory particle. The 20S core particle is barrel shaped and consists of four rings, two outer α -rings and two inner β -rings, which themselves consist of seven subunits. The inner β -rings contain the active sites. The 19S regulatory particle recognizes ubiquitinated substrates via several ubiquitin binding domains, resulting in their unfolding and translocation into the 20S core particle. To mediate these tasks, the 19S regulatory particle requires energy, which is provided by its six ATPase subunits.

After the cleavage of the substrate, the proteasome releases the resulting peptides as well as free ubiquitin, which can later be reused (Glickman and Ciechanover 2002).

2.8.2 Autophagic degradation

As the Greek name indicates, autophagy ("self-eating") is a catabolic process that mediates degradation of proteins or organelles by the lysosome (Mizushima and Levine), (Yang and Klionsky). Most cells display basic levels of autophagy that can be further activated by several conditions such as starvation. Under starvation conditions, cells degrade old proteins to provide amino acids for new protein synthesis. Therefore, autophagy acts as a recycling process to maintain cellular physiology. Autophagy research was initially uncovered in budding yeast and multiple autophagy-related (ATG) genes were identified (Klionsky, Cregg et al. 2003). Autophagy research in mammalian cells becomes more and more popular as autophagy plays numerous functions in cell physiology and pathology. Three different classes of autophagy are currently known: chaperone-mediated autophagy, microautophagy and macroautophagy, the latter being best studied.

Chaperone-mediated autophagy (Fig. 5A) is a process that enables degradation of specific proteins by sequestering them directly into the lysosome. Only proteins containing a KFERQ-sequence can be recognized and targeted by this pathway (Dice 2007), (Orenstein and Cuervo)(Kaushik, Bandyopadhyay et al.). The cytosolic chaperone Hsc70 (heat shock cognate 70) recognizes the KFERQ-sequence (Chiang, Terlecky et al. 1989) and targets the substrates to the receptor Lamp2a which is located at the lysosomal membrane (Cuervo and Dice 1996) where the substrate is transported into the lysosome after unfolding (Salvador, Aguado et al. 2000). Chaperone-mediated autophagy was shown to be most active after oxidative stress (Kiffin, Christian et al. 2004) or upon starvation. Only long starvation phases from more than 10 hours (Backer and Dice 1986) to 3 days (Cuervo, Knecht et al. 1995) induce chaperone mediated autophagy.

Microautophagy (Fig. 5B) engulfs proteins by invagination of the lysosomal membrane. Details are so far poorly understood and not further discussed here.

Macroautophagy (Fig. 5C), hereafter referred to as autophagy, is the best studied lysosomal degradation process. Target proteins are engulfed by a double layered membrane called the autophagosome and transferred to the lysosome. During the transfer, autophagosome and lysosome fuse to form the autolysosome and the proteins are released for degradation. Despite intense research in the last years, the exact

orchestration of proteins and their functions remain to be resolved. In the following paragraphs I will focus on the autophagic machinery in mammalian cells.

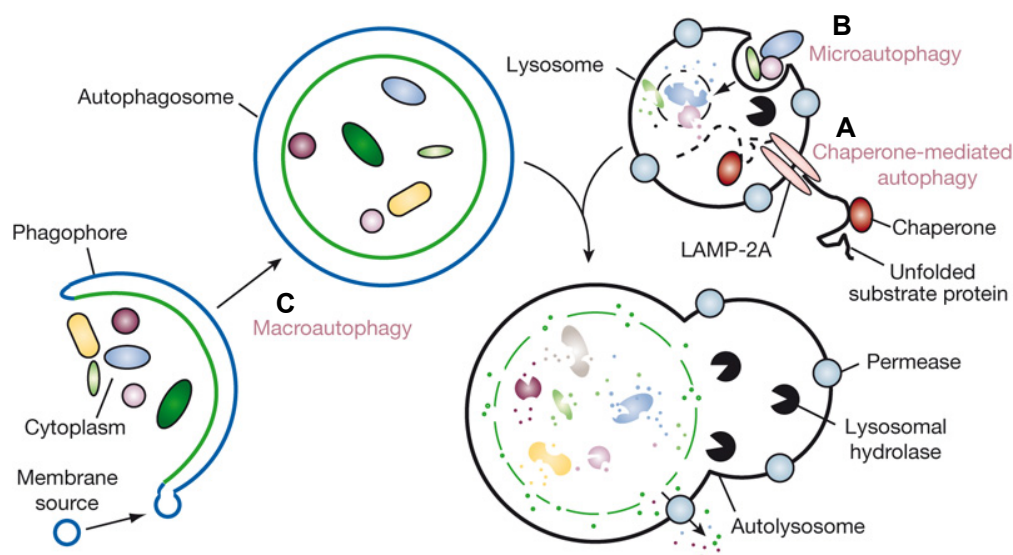


Fig. 5: Autophagy in mammalian cells. Depicted are the three known forms of autophagy: Chaperone-mediated autophagy (A), Microautophagy (B) and Macroautophagy (C). During chaperone-mediated autophagy, Hsc70 is targeting proteins via the KFERQ-motif; the target proteins are transferred into the lysosome by Lamp2a mediated transport. During microautophagy, the lysosomal membrane directly engulfs proteins. Macroautophagy requires the formation of an autophagosome that collects proteins and/or organelles and releases them into the lysosome by fusion. Proteins are degraded by lysosomal hydrolases and permeases. Figure adapted from (Mizushima, Levine et al. 2008).

2.8.2.1 The autophagy machinery

The induction of autophagy is mediated by the ULK1-kinase, which acts downstream of TOR complex1 (TORC1) that negatively regulates autophagy (Mizushima). ULK1 is in a complex with mATG13 and FIP200 (an orthologue of yeast Atg17), which are both essential for autophagy. During activation of autophag, e.g. under starvation, suppression of mTORC1 causes dephosphorylation of ULK1, which is needed to activate autophagy (Jung, Jun et al. 2009)(Hosokawa, Hara et al. 2009). Membrane nucleation is the initial step of autophagy that enables autophagosome assembly. The origin of the double layered membrane remains unresolved however, there is evidence that it is derived from the ER membrane (Hayashi-Nishino, Fujita et al. 2009)(Yla-Anttila, Vihinen et al. 2009). Three class III PtdIns3K complexes are known to be involved in the formation of autophagosomes, the ATG14L complex (Matsunaga, Saitoh et al. 2009), the UVRAG complex (Itakura, Kishi et al. 2008) and the negatively regulating Rubicon complex (Matsunaga, Saitoh et al. 2009), each of the complexes containing hVSP34 and Beclin1 (homologue of yeast Atg6). To form an autophagosome, the double layered membrane

needs to grow to a vesicle. In this elongation step, two ubiquitin-conjugating-like systems are essential. The ubiquitin-like modifier ATG12 is activated by the E1-like enzyme ATG7, transferred to ATG10, which is an E2-ligase and conjugated to ATG5 (Mizushima, Sugita et al. 1998)(Yang and Klionsky). LC3 is an ubiquitin-like protein and required for the formation of the autophagosome. LC3 is synthesized as pro-LC3 and cleaved to LC3-I by ATG4B. Then, LC3-I is activated by ATG7 and transferred to the E2-ligase ATG3, which conjugates LC3-I to phosphatidylethanolamine (PE) (Tanida, Tanida-Miyake et al. 2002)(Tanida, Tanida-Miyake et al. 2001). The LC3-PE conjugate, also named LC3-II, is localized in the autophagosomal membrane. The two distinct forms of LC3 (LC3-I and LC3-II) are commonly used as autophagic markers (Klionsky, Abeliovich et al. 2008). Subsequently, the autophagosome and the lysosome fuse with each other to release proteins for degradation. This process requires the protein RAB7 (Gutierrez, Munafo et al. 2004). The protein FYCO1 recognizes RAB7, binds to LC3 and facilitates microtubule plus end-directed vesicle transport (Pankiv, Alemu et al. 2010). The fusion process is positively regulated by the UVRAG complex. Finally, after fusion, inner membrane LC3-II as well as other proteins are degraded by the lysosomal hydrolases whereas the outer membrane LC3 gets recycled (Tanida, Ueno et al. 2008).

2.8.2.2 Selective autophagy

Macroautophagy was for a long time believed to degrade long lived and bulk proteins non-specifically. However, recent research revealed that autophagy can target specific proteins, or even aggregates (aggrephagy), pathogens (xenophagy) and organelles such as mitochondria (mitophagy) and peroxisome (pexophagy) (Xie and Klionsky 2007)(Johansen and Lamark). In the recent years, receptors were identified that interact with cellular cargo to target it for degradation. The characteristics of all so far identified receptors are: interaction with LC3 by the LC3-interacting region (LIR domain), the ability to aggregate, and the ability to specifically recognize their substrates. The best characterized receptor for selective autophagy is p62/SQSTM1, hereafter referred to as p62. As other receptors, p62 can bind to LC3 via its LIR domain, which is a 22 amino acid long, linear motif (Pankiv, Clausen et al. 2007). Another important domain for its function is the ubiquitin binding UBA domain, which enables binding to ubiquitinated proteins. p62 can bind to ubiquitin chains with a preference for K63-linked ubiquitin chains (Long, Gallagher et al. 2008; Kirkin, McEwan et al. 2009). It was shown that only mono-ubiquitination of normally long-lived cytoplasmic proteins is sufficient to trigger degradation by autophagy (Kim, Hailey et al. 2008). The "Phox and Bem1p domain" (=PB1 domain) of p62 promotes oligomerization and probably aggregation, therefore allowing the formation of aggregates with its target proteins (Lamark, Perander et al. 2003)(Kirkin, McEwan et al. 2009). As already mentioned above, p62 can target and

resolve protein aggregates (Bjorkoy, Lamark et al. 2005)(Komatsu, Waguri et al. 2007), (Pankiv, Clausen et al. 2007) and it colocalizes with ubiquitin positive foci in neurodegenerative disease tissues (Kuusisto, Salminen et al. 2002)(Kuusisto, Salminen et al. 2001). Thus, p62-histochemistry has been proposed as a marker for several aggregation diseases (Kuusisto, Kauppinen et al. 2008). Accordingly, autophagy deficient mice lacking ATG5 and ATG7 displayed signs of neurodegenerative diseases and accumulated ubiquitin positive inclusion bodies in neurons and hepatocytes without an expression of aberrant proteins that are known to form aggregates (Komatsu, Waguri et al. 2006)(Hara, Nakamura et al. 2006). Early studies of p62 deficient mice showed that they are prone to develop high levels of diabetes and obesity (Rodriguez, Duran et al. 2006) but no signs for neurodegenerative diseases as found for ATG5 and ATG7. This was also confirmed by Komatsu and colleagues, who could not find any ubiquitin positive inclusion bodies neither in liver nor in brain tissue after genetic ablation of p62 (Komatsu, Waguri et al. 2007), which could be explained by loss of aggregation capacity that is mediated by the PB1 domain of p62. However, in p62 double knockout mice, brain cells show phenotypes of Alzheimer diseased brain with increase in K63-linked ubiquitin depending on age (Wooten, Geetha et al. 2008). This observation could also be explained by another protein that takes over the function of p62 in p62 deficient cells, such as NBR1, which was found to have similar functions (Kirkin, Lamark et al. 2009). Besides p62 other receptors were identified that target cellular material to the autophagosome, such as NBR1 (Kirkin, Lamark et al. 2009), HDAC6 (Iwata, Riley et al. 2005) and NIX, that was shown to target mitochondria (Novak, Kirkin et al.). So far the field of selective autophagy research is just arising. Elucidating selected targets of these autophagy receptors remains an interesting field of research.

3 AIM OF RESEARCH

Aneuploidy is detrimental in human embryos and was shown to be a common hallmark of cancerous tissues. So far little is known how aneuploidy affects pathological phenotypes. Therefore, gaining insights on cellular physiology of aneuploid cells may be useful for understanding the phenotypes of aneuploidy linked diseases and for providing new strategies for drug development.

Aneuploidy leads to growth defects as shown for cells isolated from trisomy 21 patients, aneuploid mice and aneuploid yeasts. Furthermore, it was shown that in aneuploid mammalian cells transcripts scale proportionally to gene copy number, therefore transcribing the additional information from the extra chromosome. However, so far only little is known about how protein levels scale in aneuploid human cells.

In this study my aim was first, to generate and characterize human cell lines with one or two extra chromosomes derived from the cell lines HCT116 and RPE-1 hTERT. Then we planned to evaluate growth characteristics of these generated tri- and tetrasomic cell lines and pinpoint their growth delay to a specific cell cycle phase. Finally, our aim was to compare DNA, mRNA and protein levels in direct comparison to each other. Therefore, I performed a quantitative analysis of DNA, mRNA and protein abundance changes using aCGH, mRNA array and SILAC technology. Thanks to the progress of large scale proteomics analysis in the recent years, we were able to compare whole genome wide protein levels of aneuploid cell lines to their disomic counterpart and between different aneuploid cell lines. We were interested whether protein levels scale proportionally with gene copy number, or whether we can find regulations for specific groups of proteins as suggested for yeast, plant and fly. Furthermore, we asked if tri- or tetrasomic cell lines show a distinct cellular response to the extra chromosome.

Determination of pathways that are deregulated in all aneuploid cells will lead to further research analyzing how aneuploid cells differ from diploids. Identifying these differences is crucial for understanding the impact of aneuploidy on cellular physiology.

4 RESULTS

Recent research showed that transcripts of yeast, mouse and human aneuploid cells scale according to gene copy number (Mao, Zielke et al. 2003; Amano, Sago et al. 2004; Torres, Sokolsky et al. 2007; Williams, Prabhu et al. 2008; Ried, Hu et al. 2012). However, not much is known about how protein levels are altered in human cells with an extra chromosome. To analyze protein expression levels and altered cellular physiology of aneuploid cells, cell lines were generated by adding extra chromosomes to the cell lines HCT116 and RPE-1 hTERT (hereafter referred to as RPE-1). This way we were able to construct cognate cell lines with an extra chromosome, which can be accurately compared to their parental cell lines.

4.1 Construction of aneuploid cell lines

Cell lines were constructed by adding an extra chromosome to chromosomally stable cell lines. To study the effect of an extra chromosome on cellular physiology it is important to carefully choose the parental cell lines since cell lines should be diploid and segregate their chromosomes faithfully. As recipient cell lines the cell line HCT116 and RPE-1 hTERT (hereafter referred to as RPE-1) were employed. Both cell lines are frequently used for genome instability research due to their genome stability and near diploid karyotype. Aneuploid cell lines were generated by microcell fusion technique (Fournier 1981) as described in Material and Methods. Cells were treated with antibiotics to select for aneuploid cells. Cell colonies arising after cultivation were expanded, collected and characterized by aCGH and chromosome paints analysis.

4.2 Description and characterization of cell lines

4.2.1 HCT116 cell lines

One cell line which was used to generate aneuploid cells was HCT116. HCT116 is a male, colorectal cancer cell line (ATCC), displaying a high frequency of microsatellite instability (MIN) but low levels of chromosomal instability (CIN) (Lengauer, Kinzler et al. 1997). Cell lines with the addition of chromosome 3 and chromosome 5 were constructed by microcell fusion and were kindly provided by M. Koi (Koi, Umar et al. 1994; Haugen, Goel et al. 2008). To track cells for cell cycle studies, our laboratory (Christian Kuffer) created a stable HCT116 cell line with GFP-tagged histone 2B (H2B) (hereafter referred to as HCT116 H2B-GFP). To this cell line, chromosome 5 was added by using microcell fusion technique to generate HCT116 H2B-GFP cell lines with an extra chromosome.

4.2.1.1 Verification of aneuploid karyotype by M-FISH and paints analysis

The aneuploid karyotype of all created cell lines was verified by paints analyses and for HCT116 with extra chromosome 5 also by Multiplex-FISH (M-FISH). To confirm the successful chromosome transfer, the extra chromosome and one control chromosome of mitotic spreads were stained using paints probes, with DAPI counterstaining of all chromosomes (Fig. 6A). Furthermore, the exact karyotype of the HCT116 cell line with extra chromosome 5 and its parental HCT116 cell line was determined by detailed M-FISH analysis which was performed by Chrombios GmbH (Fig. 7B). The cell line HCT116 with extra chromosome 5 was used for detailed proteome analysis.

Paints analysis revealed that the cell line with the added chromosome 3 contains one additional copy of chromosome 3 (hereafter referred to as HCT116 3/3), whereas the cell line with added chromosome 5 contains two additional copies of chromosome 5 (hereafter referred to as HCT116 5/4). A part of chromosome 5 is translocated to another chromosome, which was present in all analyzed cells. Two different cell line types were generated for the cell line HCT116 H2B-GFP with added chromosome 5, one with one additional chromosome 5 (hereafter referred to as HCT116 H2B-GFP 5/3) and one with two additional chromosomes 5 (hereafter referred to as HCT116 H2B-GFP 5/4). The original HCT116 cell line was described to display the karyotype: 45,X,-Y,dup(10)(q24q26),der(16)t(8;16)q13;p13,der(18)t(17;18)(q21;p11.3) (Masramon, Ribas et al. 2000). M-FISH analysis confirmed the translocation for chromosome 8 to chromosome 16, as well as the translocation from chromosome 17 to 18 in HCT116 as well as HCT116 5/4 cell lines. Moreover, analysis confirmed the two extra copies of chromosome 5 in HCT116 5/4 and the chromosome which contains the translocated part of chromosome 5 was clearly identified as chromosome 16. For each cell line 10

karyograms were evaluated by Chrombios GmbH. One representative karyogram is shown in Fig 6B. To summarize, paints as well as M-FISH analyses confirmed the successful transfer of chromosomes to HCT116 derived cell lines and the generation of aneuploid cell lines.

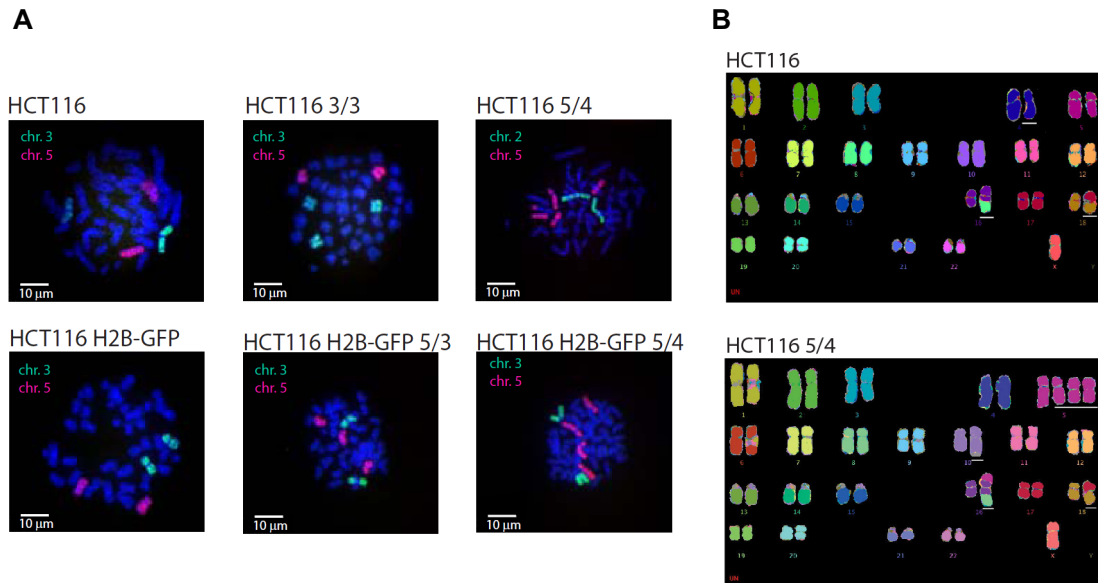


Fig. 6: Chromosome paint and M-FISH analysis. (A) Chromosome paint analysis of cell lines. Chromosome 5 is depicted in red and chromosome 2 or 3 in green. The HCT116 cell line with the extra chromosome 3 contains one additional chromosome (HCT116 3/3). The cell line with chromosome 5 contains two extra copies (HCT116 5/4). Two cell lines derived from HCT116 H2B-GFP were generated, one with one (HCT116 H2B-GFP 5/3) and one with two (HCT116 H2B-GFP 5/4) copies of chromosome 5. As expected, HCT116 and HCT116 H2B-GFP cell lines contain only two copies of every stained chromosome. **(B)** M-FISH analysis of HCT116 and HCT116 5/4. The M-FISH karyograms of both cell lines are identical except for the extra chromosomes 5. A part of chromosome 5 is translocated to chromosome 16. This translocation is also visible in the paints analysis.

4.2.1.2 Verification of DNA levels in aneuploid cells by aCGH analysis

The generated cell lines might have gained aberrations that are not seen by mere staining of the extra chromosome. To further characterize created cell lines, genomic profiles of all cell lines were examined by 4x44 K aCGH analysis performed by IMGM laboratories (Fig. 7). aCGH analysis confirmed the amplifications observed by M-FISH analysis. These changes are also present in all analyzed HCT116 cell lines. Only the cell line HCT116 5/4 displays chromosome 17 on normal levels compared to HCT116. Besides these changes, no other changes were observed of chromosomes that are expected to be disomic. The aCGH profile of the cell line HCT116 5/4 shows that most parts of chromosome 5 are amplified. However, some regions are present at lower levels displaying partial deletions. Also paints and M-FISH analysis showed that three of the four copies of chromosome 5 are smaller if compared to the fourth one, with one of the chromosome parts being translocated to chromosome 16. Since this cell line was used

4 RESULTS

for further detailed expression analysis, a 2x400 K high density aCGH analysis was conducted to exactly map the amplified chromosome regions (Fig. 8).

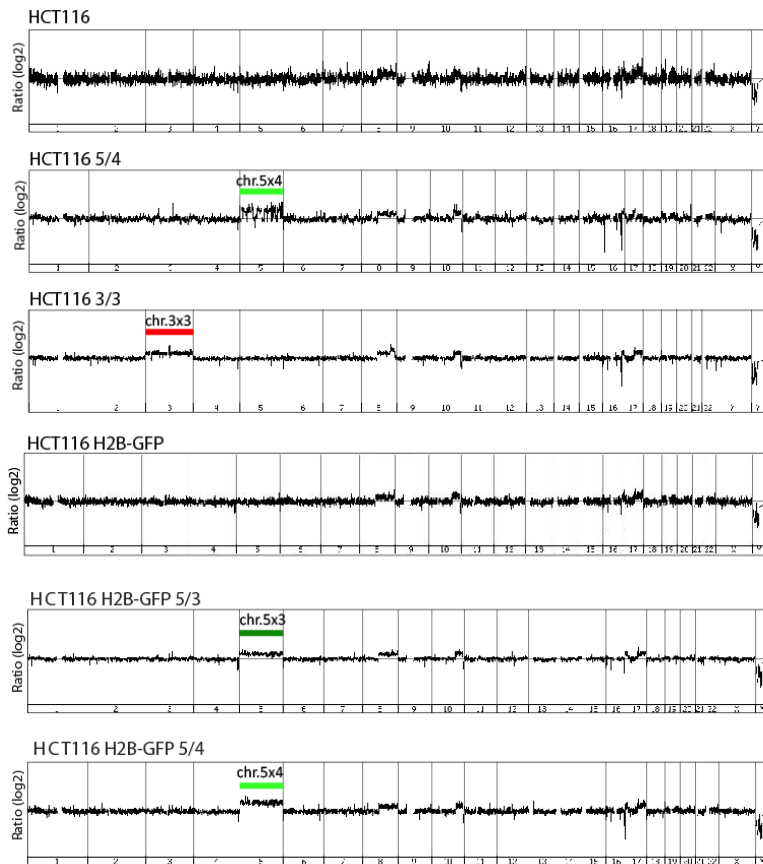


Fig. 7: aCGH analysis of HCT116 cell lines. DNA levels are depicted in log₂ scale and aligned according to their genome position. Chromosome 5 is marked in green and chromosome 3 in red. The cell line HCT116 shows amplification of parts of chromosome 8, 10 and 17 as well as deletion of the Y chromosome. These changes are also present in the aneuploid cell lines. Besides amplification of the extra chromosome, mostly generated cell lines do not differ from their origin cell line HCT116 comparing the aCGH profiles. Aneuploid cell lines show clear amplification of the extra chromosome. The cell line HCT116 5/4 however, contains some parts of chromosome amplified whereas other parts seem to be present as in cell lines disomic for chromosome 5.

4.2.1.3 High resolution aCGH analysis of HCT116 5/4 cell line

Chromosome regions of chromosome 5 that are not tetrasomic were mapped by performing a 2x400K high density aCGH analysis (Fig. 8). For this analysis the HCT116 genomic DNA was used as a direct reference sample in the experimental setup. High density aCGH data allowed a clear identification of disomic regions of chromosome 5 (blow out, Fig. 9). Gene regions that were not tetrasomic were excluded from the analysis. Moreover, corresponding mRNA and protein information was deleted from the dataset.

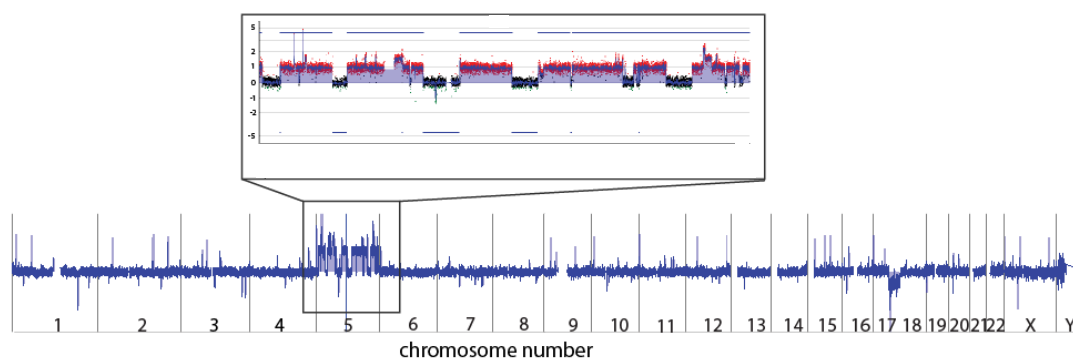


Fig. 8: 2x400K high density aCGH for the cell line HCT116 5/4. DNA levels are depicted in log₂ scale. HCT116 5/4 genomic DNA was directly compared to genomic DNA of HCT116. High density aCGH analysis was performed to exactly map the amplified and disomic chromosome regions of chromosome 5 as this cell line was used for detailed genome wide expression analysis. Chromosome 17 is amplified in HCT116 but not in HCT116 5/4 as shown by previous aCGH analyses, therefore it appears below zero. The amplification and the deletions of chromosome 5 are clearly visible

4.2.2 RPE-1 cell lines - generation and verification

The second cell line which was used to generate aneuploid cells is RPE-1. This cell line was employed to show that results from HCT116 derived cell lines were not cell line specific. The cell line RPE-1, is derived from female primary retinal pigment epithelium and was immortalized by stably expressing hTERT (ATCC). Similar to HCT116, RPE-1 is a near diploid cell line which propagates its genetic material stably (Jiang, Jimenez et al. 1999). The RPE-1 cell line is not derived from tumor tissues (ATCC). Therefore, cellular physiology of this cell line is expected to be more similar to the natural cellular status and is easier to cultivate than primary human cells from patient tissues which become senescent after short time. The RPE-1 as well as the RPE-1 H2B-GFP cell lines were kind gifts of Stephen Taylor (University of Manchester, UK). Chromosome 5 was added to the RPE-1 cell line and chromosome 21 was added to the RPE-1 H2B-GFP cell line by microcell fusion. Afterwards, aCGH analysis was conducted to confirm successful chromosome transfer (Fig. 9).

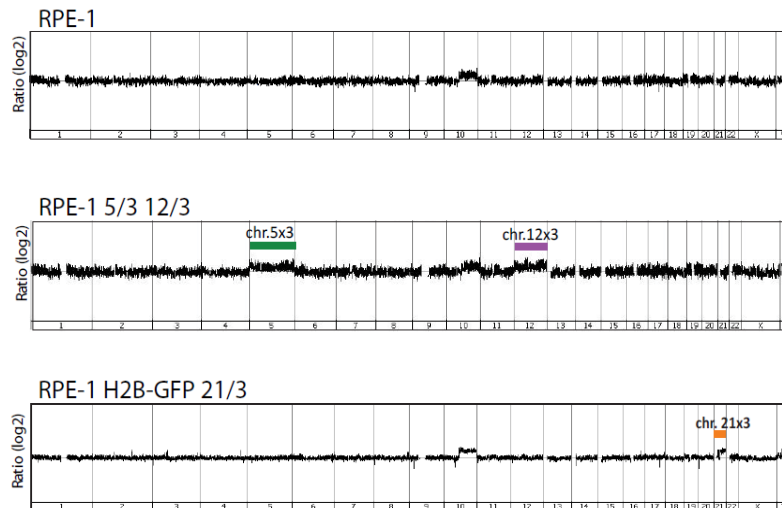


Fig. 9: aCGH analysis of RPE-1 cell lines. DNA levels are depicted in log₂ scale. The RPE-1 cell line shows partial amplification of chromosome 10, which is also found in all aneuploid RPE-1 cell lines. Analysis of RPE-1 with extra chromosome 5 showed that also chromosome 12 was amplified. The cell line with extra chromosome 21 only incorporated the long arm of the chromosome. Chromosome 5, 12 and 21 are depicted in green, purple and orange, respectively.

As seen in the aCGH plots, RPE-1 cell line also displays a partial amplification of chromosome 10, however no other changes were identified. This is also seen in aneuploid cell lines derived from the RPE-1 or RPE-1 H2B-GFP cell lines. Analysis of the aCGH profiles of cell lines with transferred chromosome revealed that chromosome 5 was successfully added to the cell line RPE-1. Unexpectedly, chromosome 12 was also amplified in this cell line (hereafter referred to as RPE-1 5/3 12/3. For the cell line with transferred chromosome 21 the aCGH analysis revealed that only the long arm of chromosome 21 was successfully added to the cell line. However, this should not affect the study of protein levels in aneuploid cells when included accurately into the analysis. Therefore, the created cell lines RPE1 5/3 12/3 and RPE-1 H2B-GFP 21/3 were used for proteome studies.

4.3 Aneuploid cell lines display a growth delay

As aneuploid cells such as yeast, mouse and human aneuploid cells were shown to grow slower compared to their euploid counterpart (Segal and McCoy 1974; Torres, Sokolsky et al. 2007; Williams, Prabhu et al. 2008) we monitored growth characteristics of our aneuploid cell lines. Growth curves were generated, counting cells during 1 to 5 days after seeding (Fig 10). Growth curves clearly show that aneuploid human cells derived from HCT116 grow slower compared to their disomic counterparts HCT116 or HCT116 H2B-GFP. The tetrasomic cell line with one added copy of chromosome 5 grows comparably faster to the cell line with two additional copies of the chromosome, indicating that the growth delay may be dosage dependent (Fig. 10, right panel). This is in line with the growth delay observed for other aneuploid cells (Segal and McCoy 1974; Torres, Sokolsky et al. 2007; Williams, Prabhu et al. 2008), which was also suggested to

4 RESULTS

be dosage dependent (Torres, Sokolsky et al. 2007). In conclusion, our aneuploid model cells show severe growth defects if compared to their disomic counterparts, which is in line with former studies.

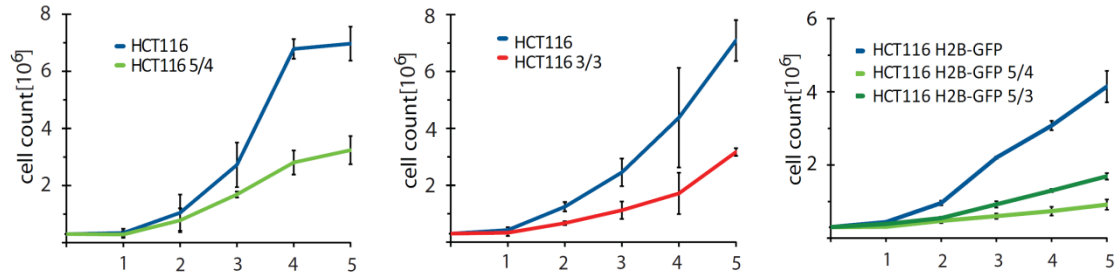


Fig. 10: Growth curves of HCT116 cell lines. 3×10^5 cells were seeded and counted every day. The cell line HCT116 grows faster than HCT116 5/4 (left panel) and HCT116 3/3 (middle panel). Also HCT116 H2B-GFP 5/3 and 5/4 grow slower compared to HCT116 H2B-GFP (right panel). The cell line with one extra copy of chromosome 5 HCT116 H2B-GFP 5/3 grows faster than the cell line with two extra copies of chromosome 5 HCT116 H2B-GFP 5/4. Experiments were performed in triplicates. The mean values are depicted; error bars show SD of mean.

4.4 The growth delay is due to a prolonged G1 and S phase

4.4.1 Aneuploid cells grow slower due to increased time in interphase

Growth defects of aneuploid yeast were shown to be due to a delay in G1 phase (Torres, Sokolsky et al. 2007). The cause for the growth delay of mammalian aneuploid cells however, remained unknown. A growth delay may be due to several reasons such as increased cell death level, prolonged cell cycle phase, complete arrest in a cell cycle phase or extensive cellular senescence. To address what is the origin of the reduced growth rate observed in cells with extra chromosome, cell death, cell senescence and live cell imaging experiments determining time in interphase and mitosis were performed (Fig. 11).

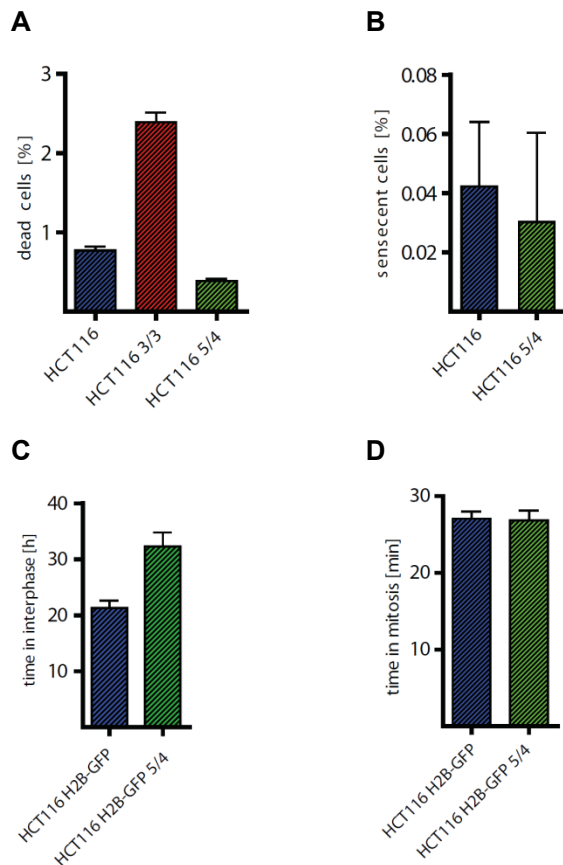


Fig. 11: Aneuploid cell lines grow slower due to prolonged interphase.

(A) Amount of dead cells was analyzed by propidium iodide (PI) exclusion experiment. HCT116 3/3 shows an increased level of dead cells whereas cell death level in HCT116 5/4 is lower than in HCT116. (B) HCT116 5/4 and HCT116 show similar levels of senescent cells, which were detected by β -galactosidase staining. (C) Live cell imaging following H2B-GFP positive nuclei by tracking the time from the onset of anaphase to the onset of the subsequent anaphase of the daughter cell revealed that HCT116 H2B-GFP 5/4 shows a significantly prolonged interphase compared to HCT116 H2B-GFP. (D) Time in mitosis, which was measured from the nuclear envelope breakdown (NEB) to the onset of anaphase was not perturbed in HCT116 H2B-GFP 5/4 compared to HCT116 H2B-GFP. All experiments were performed in triplicates, the mean values are plotted and the SEM is indicated by the error bars.

Cell death levels were measured by propidium iodide (PI) exclusion experiment using FACS analysis. Data shows that the growth delay is not due to an increase in cell death rate of aneuploid cells. Even though HCT116 3/3 displays an increased cell death level, HCT116 5/4 has a cell death level below HCT116 (Fig. 11A). Notably, cell death rates are relatively low in all analyzed cell lines, and can therefore not be the reason for the

slow growth of aneuploid cells. Moreover, there was no increased tendency of HCT116 5/4 to become senescent than HCT116 as confirmed by β -galactosidase assay (Fig. 11B). This assay makes use of the compound b-D-galactopyranoside (X-Gal) staining β -galactosidase which is highly expressed in senescent cells (Dimri, Lee et al. 1995). As a control cells were treated for 7 days with 0.2 μ M doxorubicin to induce senescence. Treated cells were clearly β -galactosidase positive, however, due to massive increase of cell size and unclear cell boundaries, data was not included in the graph. Live cell imaging analysis of nuclear H2B-GFP for 36 h, with automated image capture every 10 min revealed that HCT116 H2B-GFP 5/4 (mean = 32,32 h) spend longer time in interphase than HCT116 H2B-GFP (mean = 21,32 h) (Fig. 11C). This could be observed for HCT116 3/3 and HCT116 5/4 in comparison to HCT116 as well (data not shown). As these cell lines lack the nuclear marker H2B-GFP cells were imaged every 10 min in bright field for 72 h (data not shown). In contrast, time in mitosis was not prolonged in HCT116 H2B-GFP 5/4 (mean = 26.85 min) in comparison to HCT116 H2B-GFP (mean = 27.05 min) (Fig. 11D), as again analyzed by imaging H2B-GFP signal this time for 48 h every 4 min. As time in mitosis was similar in HCT116 H2B-GFP and HCT116 H2B-GFP 5/4, mitosis can be excluded as the cause for the growth delay. To summarize, growth delay was neither due to cell death nor senescence in HCT116 H2B-GFP 5/4 but prolonged interphase. Further analysis was applied to pinpoint the specific cell cycle phase which leads to the growth defect in cell lines with an extra chromosome.

4.4.2 Aneuploid cells display an increased G1 population

To specify cell cycle phases in the aneuploid HCT116 cell lines, first, cell cycle profiles of unsynchronized, cycling cells were generated by FACS analysis using propidium iodide staining. As seen in Fig. 12A, HCT116 5/4 showed an increased 2C peak whereas the 4C peak is decreased, meaning that more cells are in G1 phase compared to G2 and/or M phase.

Then the relative percentages of G1, S and G2/M phases from the cell lines HCT116, HCT116 5/4, HCT116 H2B-GFP, HCT116 H2B-GFP 5/3 and HCT116 H2B-GFP 5/4 were depicted (Fig. 12B). In line with the previous data, more cells of cell lines with extra chromosome aneuploids are present in G1 phase. This difference is significant between HCT116 and HCT116 5/4. At the same time fewer cells are present in G2 and/or M phase. Differences between HCT116 and HCT116 5/4 as well as between HCT116 H2B-GFP and HCT116 H2B-GFP 5/3 or HCT116 H2B-GFP 5/4 are significant. The effect seems to increase with the extra chromosome number since HCT116 H2B-GFP 5/4 displays more cells in G1 than HCT116 H2B-GFP 5/3. However, this effect was not

4 RESULTS

significant. In theory, the increase in G1 phase in aneuploid cells could be due to three reasons, first senescence, which displays the same DNA content as G1 phase, second slower progression through G1 phase or third faster progression through G2 and/or M phase. As shown above, time in mitosis was not altered between HCT116 H2B-GFP and HCT116 H2B-GFP 5/4. Moreover, senescence was not increased in HCT116 5/4 compared to HCT116. Therefore, as aneuploid cells display an increased cell population in G1 phase, data suggests that aneuploid cell lines spend more time G1 phase.

A

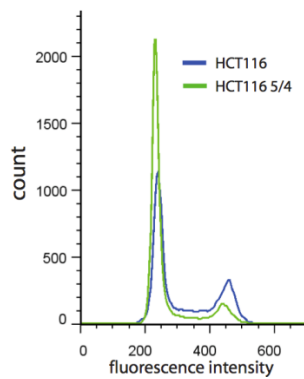
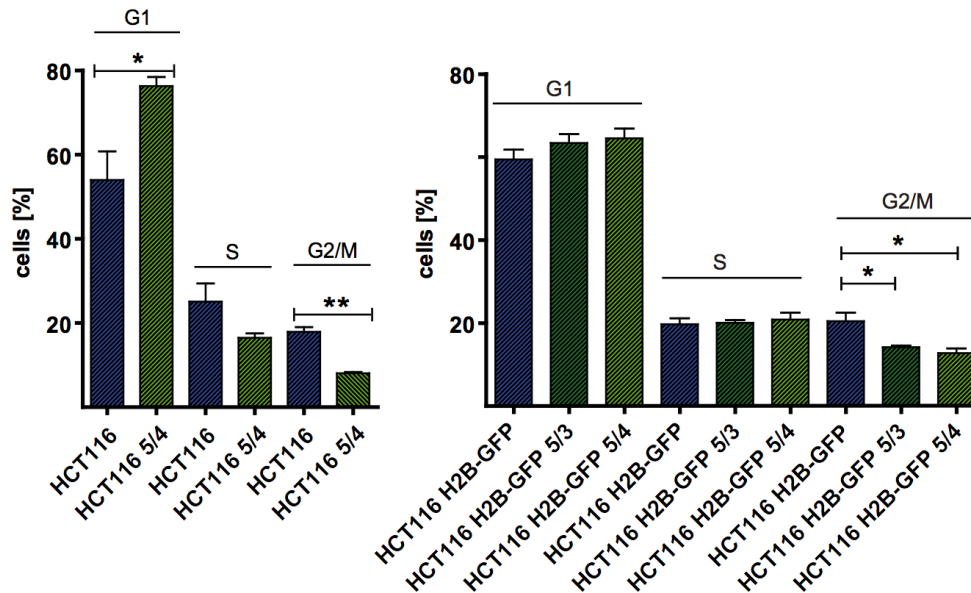


Fig. 12: FACS cell cycle profiles of cell lines: cell lines with extra chromosome display an increased 2C population whereas 4C population is decreased. (A) Representative FACS profiles of HCT116 (blue) and HCT116 5/4 (green). FACS cell cycle profile of HCT116 5/4 displays an increased 2C population compared to HCT116, whereas 4C peak is decreased. **(B)** Relative percentages of cells in G1 and G2 and/or M phase of HCT116, HCT116 5/4 (left panel), HCT116 H2B-GFP, HCT116 H2B-GFP 5/3 and HCT116 H2B-GFP 5/4 (right panel). HCT116 and HCT116 H2B-GFP are colored in blue, cell lines with extra chromosome in green. Significances are displayed as asterisk (unpaired *T*-test), the standard error is depicted in the error bars. All analyzed cell lines with extra chromosome showed increased 2C population, whereas the 4C population was decreased.

B



4.4.3 Aneuploid cell lines display prolonged G1 and S phase

To evaluate whether cells with extra chromosomes progress slower through G1 phase further experiments were conducted to pinpoint the duration of the different cell cycle phases. Therefore, cell cycle profiles by FACS analysis of HCT116 5/4 and HCT116 were taken every 1.5 hours after thymidine release for 24 hours (Fig. 13).

FACS cell cycle profiles obtained after thymidine release were evaluated by FlowJo software. Percentages of cells present in the specific cell cycle phases per time point were visualized in Fig. 13. Data shows that HCT116 5/4 spend longer time in S phase after thymidine release (Fig. 13B) compared to HCT116 (Fig13A). Moreover, G1 phase starts later than in HCT116 and is also prolonged compared to HCT116. In contrast, G2 and/or M Phase are not affected. Notably, HCT116 5/4 were not equally well synchronized as HCT116, this may be due to their prolonged cell cycle which may need longer synchronization. In conclusion, growth defects of aneuploid cell lines are due to their delay in G1 and S phase and not due to cell death or senescence.

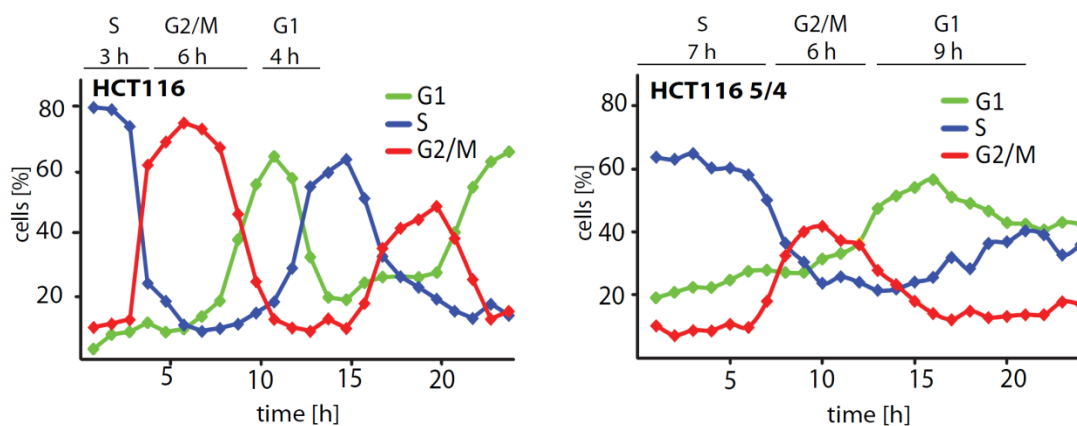


Fig. 13: G1 and S phase are prolonged in HCT116 5/4 compared to HCT116. Cell lines were synchronized with thymidine and released from S phase. Cells were taken every 1.5 hours and were then fixed, PI stained and cell cycle profiles were analyzed by FACS. Percentages of cells in G1, S and G2/M were evaluated and depicted in the shown graphs. HCT116 5/4 (left panel) clearly shows a prolonged S phase after release if compared to HCT116 (right panel). Moreover cells progress slower through G1 phase, whereas G2/M is not affected.

4.5 Aneuploid cell lines adjust their protein levels

mRNAs are expressed according to their gene copy number as described for trisomy 21 cells, aneuploid MEFs and yeast cells (Mao, Zielke et al. 2003; Torres, Sokolsky et al. 2007; Williams, Prabhu et al. 2008). However, detailed studies comparing DNA, mRNA and protein levels in aneuploid human cells are missing. To compare DNA, mRNA and protein levels of aneuploid cell lines with their disomic counterparts, aCGH analysis, mRNA array analysis as well as SILAC analysis were performed. Raw data was analyzed and processed by the MaxQuant software (Cox and Mann 2008). For normalization of aCGH data raw values were divided by their corresponding background signal. Then, aCGH and mRNA data of aneuploid cells were divided by aCGH and mRNA data from disomic cell lines, respectively, to allow comparison of abundance changes. As the median differed from zero, population was normalized by subtracting the median of the whole population from values. For analysis, DNA, mRNA and protein ratios were converted into log₂ ratios.

4.5.1 Correlation studies of replicates

The aneuploid cell line HCT116 5/4 in respect to HCT116 was studied in most detail, since the dynamic range of measured changes from the extra chromosome is the highest among all model aneuploids. mRNA array analysis for HCT116 5/4 and HCT116 were conducted in biological triplicates which were converted into log₂ ratios. Then, their medians were subtracted from each other. SILAC experiments were performed in biological triplicates including 6 measurements with one of them being a reverse labeling experiment. For the biological triplicates median ratios were calculated as well. Median ratios calculated from at least two biological replicates were used for analysis.

To test for variability between technical and biological replicates as well as forward and reverse labeling, direct comparison of proteins was conducted. Technical and biological replicates show a high Pearson correlation factor between 0.79 and 0.84 (Fig. 14A,B). Whereas technical replicates and biological replicates generated by forward labeling are quite similar, comparison of forward and reverse labeling revealed that some proteins do not follow similar trends (Fig. 14C). However, enrichment analysis on the outliers did not show any pathway significantly enriched (data not shown) which shows that labeling does not affect specific pathways in these cell lines these and therefore should not influence the following analyses.

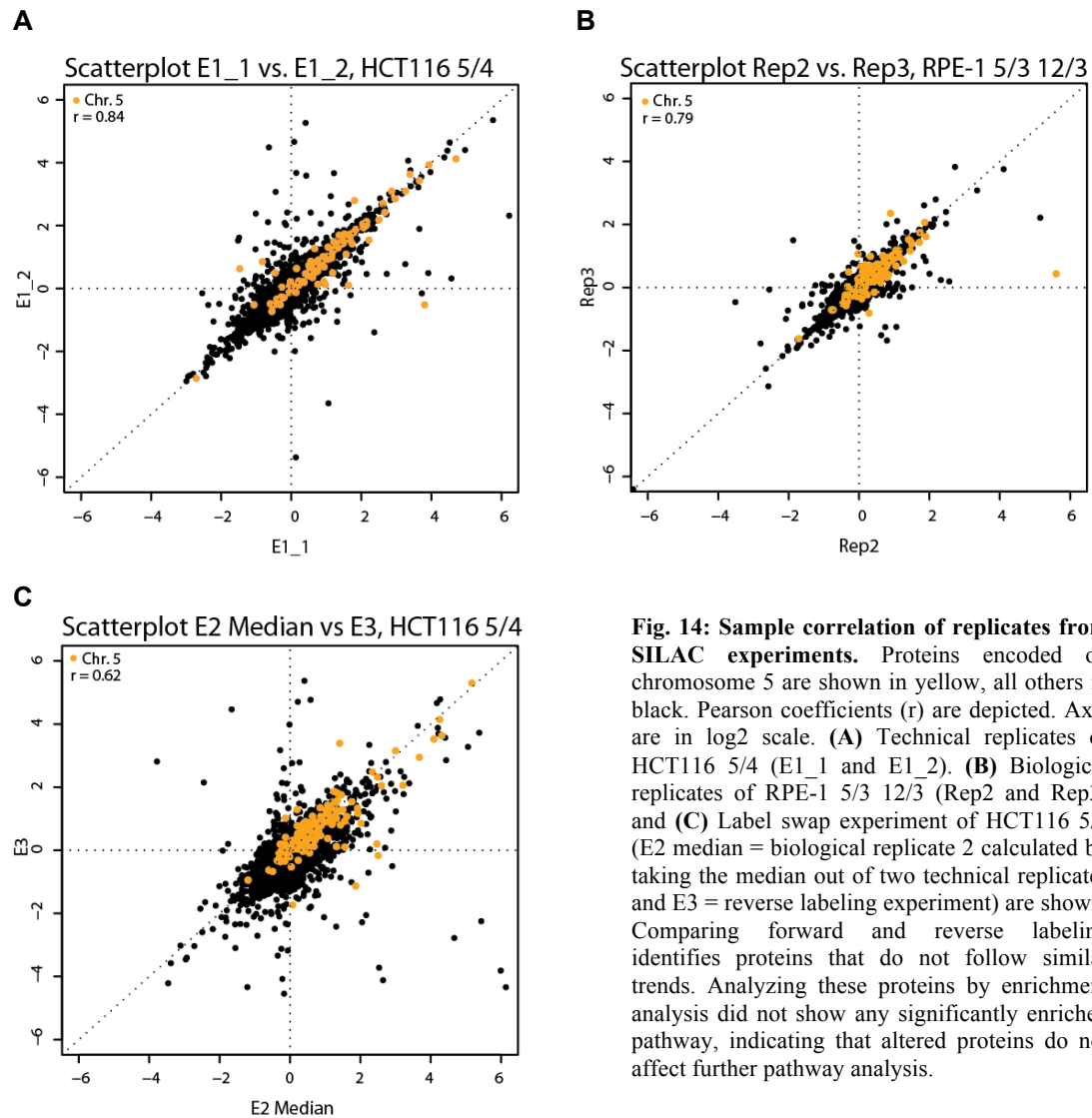


Fig. 14: Sample correlation of replicates from SILAC experiments. Proteins encoded on chromosome 5 are shown in yellow, all others in black. Pearson coefficients (r) are depicted. Axis are in log₂ scale. **(A)** Technical replicates of HCT116 5/4 (E1_1 and E1_2). **(B)** Biological replicates of RPE-1 5/3 12/3 (Rep2 and Rep3) and **(C)** Label swap experiment of HCT116 5/4 (E2 median = biological replicate 2 calculated by taking the median out of two technical replicates and E3 = reverse labeling experiment) are shown. Comparing forward and reverse labeling identifies proteins that do not follow similar trends. Analyzing these proteins by enrichment analysis did not show any significantly enriched pathway, indicating that altered proteins do not affect further pathway analysis.

4.5.2 Matching HCT116 5/4 DNA, mRNA and protein information

Aneuploid (HCT116 5/4) to diploid (HCT116) abundance changes of mRNA and DNA entries were directly matched to their corresponding protein entries using the annotated chromosomal position using the MaxQuant software (Cox and Mann 2008) (Fig. 15). Parts of chromosome 5 which were not at tetrasomic levels (threshold 0.65 (log₂ scale)) were removed from the analysis leading to a “filtered” dataset (Fig. 15, magnified chromosome region). Corresponding mRNAs and proteins were removed from the analysis as well. One may speculate that some amplified chromosome parts, which contain gene information coding for proteins that are harmful to a cell are preferentially lost. However, enrichment analysis of gene information coded on the disomic chromosome parts showed no enrichment for a specific category in the disomic chromosome parts compared to the tetrasomic gene information. Comparison of aneuploid to diploid abundance changes of DNA, mRNA and protein data shows that

4 RESULTS

mRNA as well as protein levels highly vary around zero. Closer look on chromosome 5 reveals that mRNA as well as protein levels of chromosome 5 are in average increased in HCT116 5/4. To study protein changes between HCT116 5/4 and HCT116 in detail density distribution graphs comparing protein abundance changes with their DNA and mRNA abundance changes were generated.

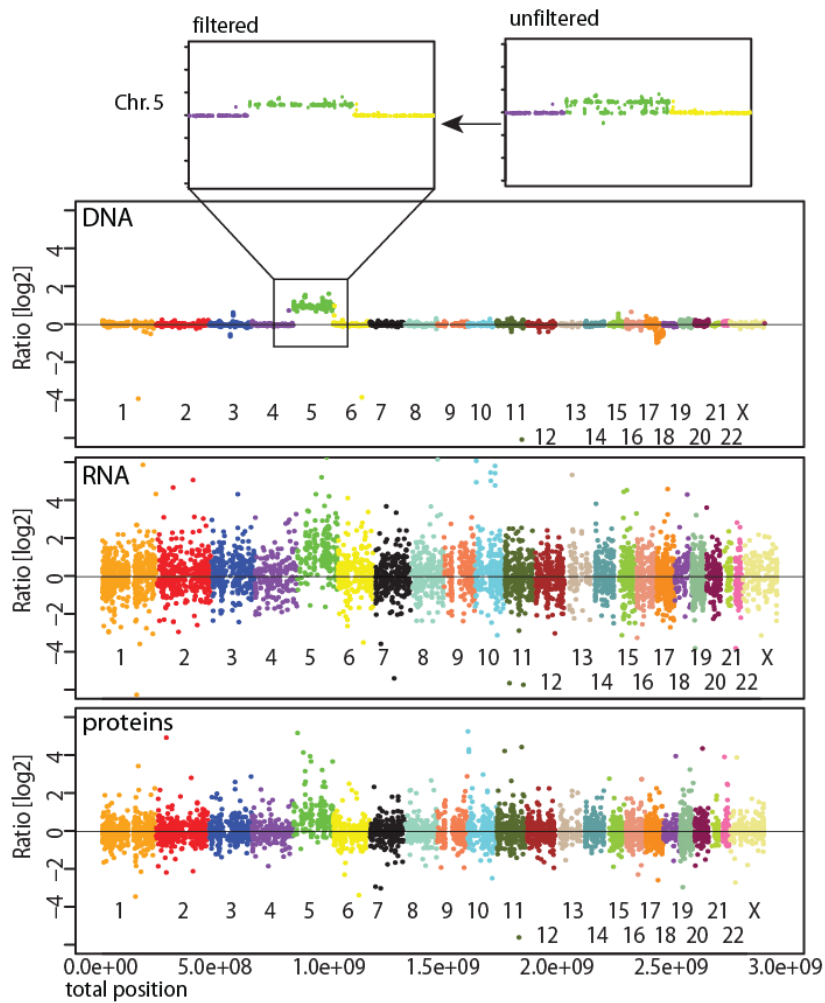


Fig. 15: Comparison of DNA, mRNA and protein data obtained from the HCT116 5/4 cell line. DNA, mRNA and protein abundance changes of HCT116 5/4 in relation to HCT116 are depicted. Data is presented at log₂ scale and aligned by chromosome position. Each dot represents either an abundance change ratio of DNA, mRNA or protein. DNA and mRNA abundance change ratios were matched to a corresponding protein. Parts of chromosome 5 that were not present at tetrasomic levels were removed from the analysis (magnified region). Data set with chromosome deletions is called “unfiltered” whereas the dataset with removed information is called “filtered”.

4.5.3 Comparison of mRNA and protein levels of chromosome 5

To allow accurate comparison of aneuploid to diploid abundance changes between mRNA and proteins, density distribution graphs were generated using the R software. Comparison of mRNA and protein abundance changes of chromosome 5 by density distribution graphs clearly shows that whereas mRNAs are present according to gene copy number (median = 1.0993) proteins are down-shifted towards levels as expected in disomic cells (median = 0.6943). This shift was only observed for the tetrasomic chromosome and not for disomic chromosomes. Therefore, the down-shift of protein abundance changes is a specific phenomenon of proteins encoded on the extra chromosomes (Fig. 16). Indeed, 53 (27%) out of 197 proteins encoded on the tetrasomic chromosome 5 are show at abundance changes as expected for disomic chromosomes (calculated by taking the median +/- twice the standard deviation). The calculated median of abundance changes from these proteins is 0.26, while median of their mRNA is 1.16. In conclusion, abundance changes of mRNAs encoded on the extra chromosome are present as expected for their gene copy number whereas the abundance changes of proteins are present at lower levels. This indicates that aneuploid cell lines adjust levels of proteins encoded on the extra chromosome.

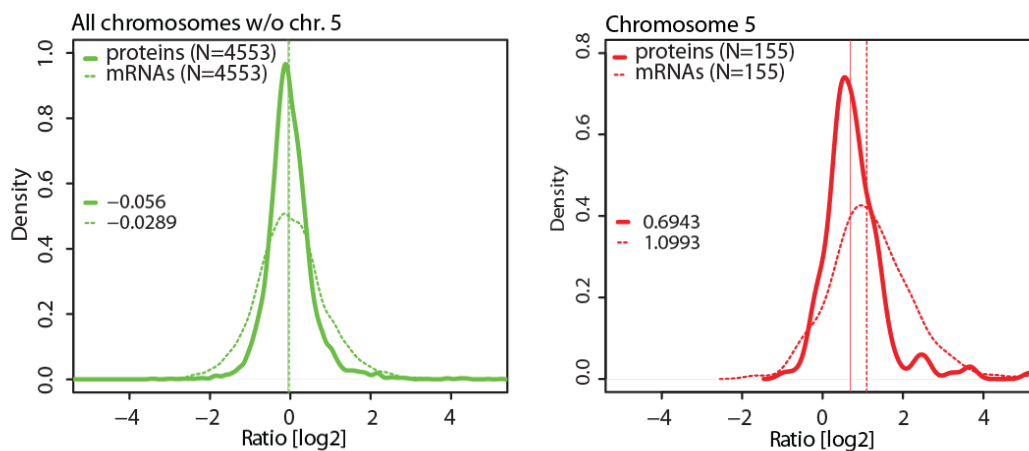


Fig. 16: Comparison of mRNA and protein abundance changes by density distribution graphs. Density distribution plots of mRNA and protein abundance changes from all chromosomes excluding chromosome 5 (left panel) and from chromosome 5 only (right panel). Protein levels from chromosome 5 are down-shifted compared to mRNA levels. Medians are depicted. Differences of protein and mRNA distribution of chromosome 5 are statistically significant (Wilcoxon rank sum test).

4.5.4 Confirmation of data in other cell lines

To confirm, that the down shift of protein abundance changes from proteins encoded on the extra chromosome is also observed in other aneuploid cell lines, SILAC experiments were performed for the cell lines HCT116 H2B-GFP 5/4, HCT116 H2B-GFP 5/3 and HCT116 3/3 (Fig. 17A).

As for HCT116 5/4 aneuploid to diploid ratios were generated and log₂ ratios were calculated. Then, abundance change ratios of proteins were matched and compared to their DNA abundance change ratios (Fig. 17). Furthermore, to show that the effects are not cell line specific, aneuploid RPE-1 cell lines were analyzed (RPE-1 5/3 12/3 and RPE-1 21/3) (Fig. 17B) and also their DNA abundance change ratios were matched to their protein abundance change ratios.

As described above, density distribution graphs were generated using abundance change ratios of genome and proteome information of HCT116 3/3, HCT116 H2B-GFP 5/3 and HCT116 H2B-GFP 5/4 cell lines in relation to HCT116 (Fig. 18A). Furthermore, to show that mRNA levels are present at gene copy number, mRNA array analysis was conducted for RPE-1 cell lines and mRNA aneuploid to diploid abundance changes were calculated. To clearly show that downshift of abundance changes is not already present at mRNA level mRNA and protein abundance changes were directly compared in density distribution graphs (Fig. 18B). Analysis of protein abundance changes from the extra chromosome in HCT116 3/3 showed similar trends as observed for HCT116 5/4. 25% of proteins encoded on chromosome 3 show abundance changes as expected for disomic chromosomes. In conclusion, aneuploid cells adjust proteins from the extra chromosome to a level as expected for disomic chromosomes. Moreover, this adjustment was present in all tested aneuploid cell lines with extra chromosomes, confirming that the abundance adjustment of proteins encoded on the extra chromosome is a general phenomenon.

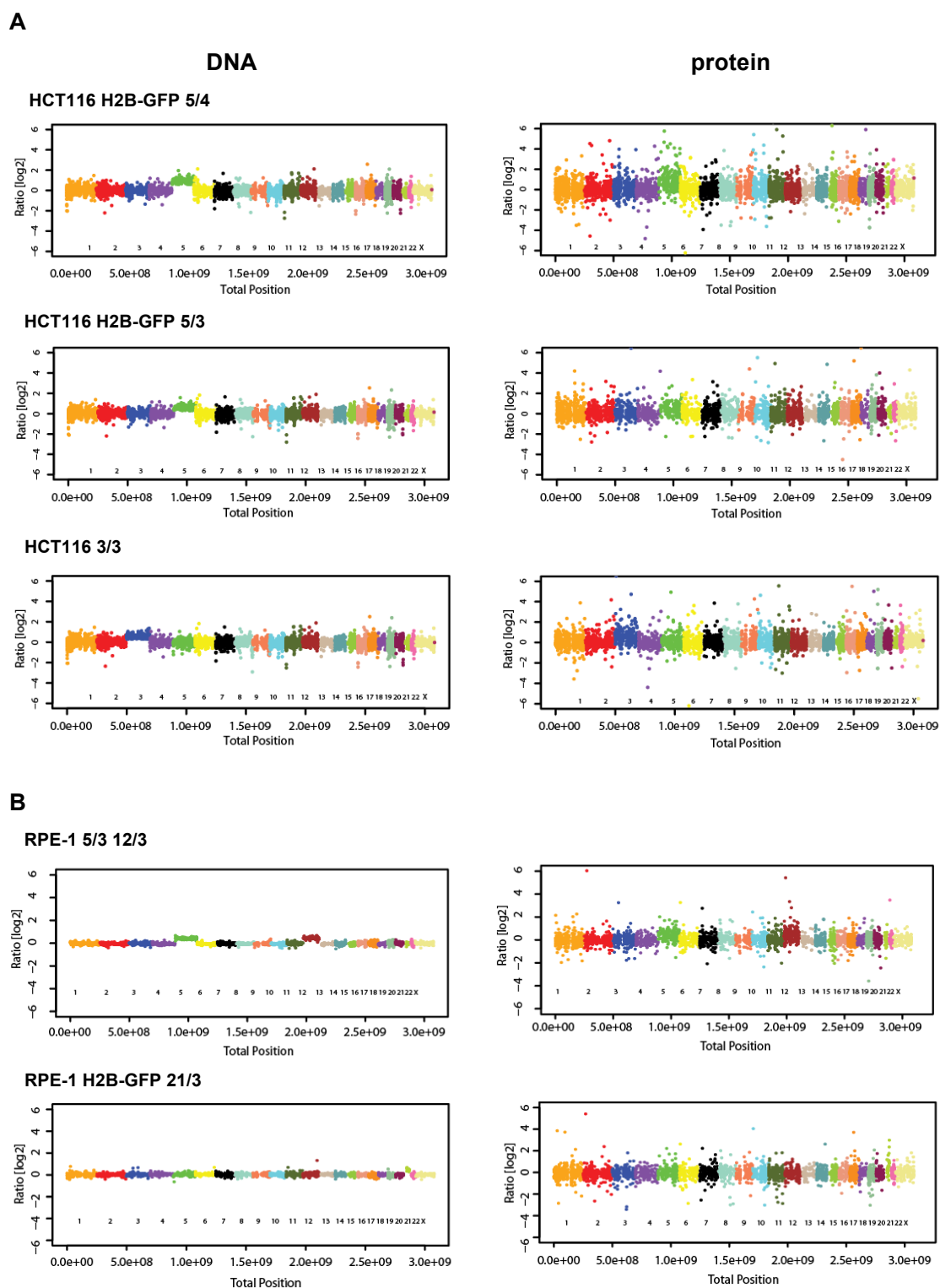


Fig. 17: Comparison of DNA and protein data from cell lines with extra chromosome. DNA and protein data of the cell lines are depicted in relation to HCT116 data as log₂ scale. Data is aligned by chromosome number. **(A)** DNA and protein data of the cell lines derived from HCT116: HCT116 H2BGFP 5/4, HCT116 H2BGFP 5/3, HCT116 3/3 and from RPE-1. **(B)** DNA and protein data of the cell lines derived from RPE-1: RPE-1 5/3 12/3 and RPE-1 H2B-GFP 21/3.

4 RESULTS

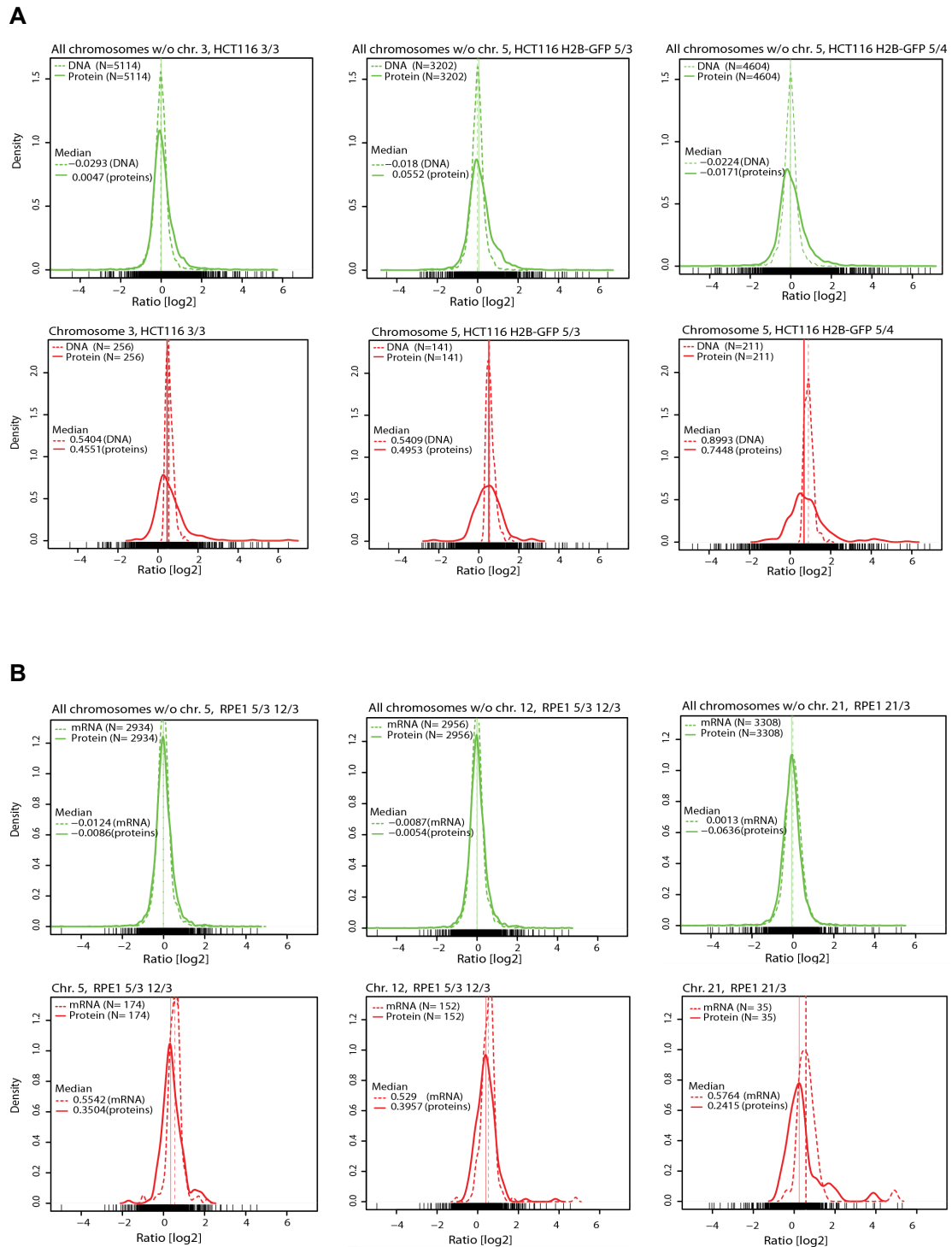


Fig. 18: Comparison of genome and transcriptome or genome and proteome of cell lines with extra chromosome. (A) Density distribution analysis of DNA and protein levels in HCT116 cell lines with extra chromosome. Comparison of DNA and protein levels from the extra chromosome (red, lower panel) or from all chromosomes except the extra chromosome. Data from cell lines HCT116 3/3, HCT116 H2B-GFP 5/3 and HCT116 H2B-GFP 5/4 are depicted. **(B)** Density distribution analysis of mRNA and protein levels in RPE-1 cell lines with extra chromosome. Compared are mRNA and protein levels from the extra chromosome (red, lower panel) or from all chromosomes except the extra chromosome. Data from cell lines RPE-1 5/3 12/3 and RPE-1 H2B-GFP 21/3, are depicted. Note that chromosome 12 and chromosome 5 are depicted individually. Abundance levels of proteins encoded on the extra chromosome are clearly shifted towards disomic levels.

4.6 Kinases and subunits of protein complexes are preferentially adjusted in aneuploid cells

4.6.1 Analysis of subunits of protein complexes

The theory that subunits of complexes are compensated to similar levels has been proposed already years ago (reviewed in (Veitia, Bottani et al. 2008)). Recently, it was suggested that in aneuploid yeast subunit proteins encoded on the extra chromosome are compensated (Torres, Sokolsky et al. 2007; Torres, Dephoure et al. 2010). Therefore, we tested if specific groups of proteins may be preferentially adjusted in our cell lines by analyzing if an annotated category is significantly different from the population.

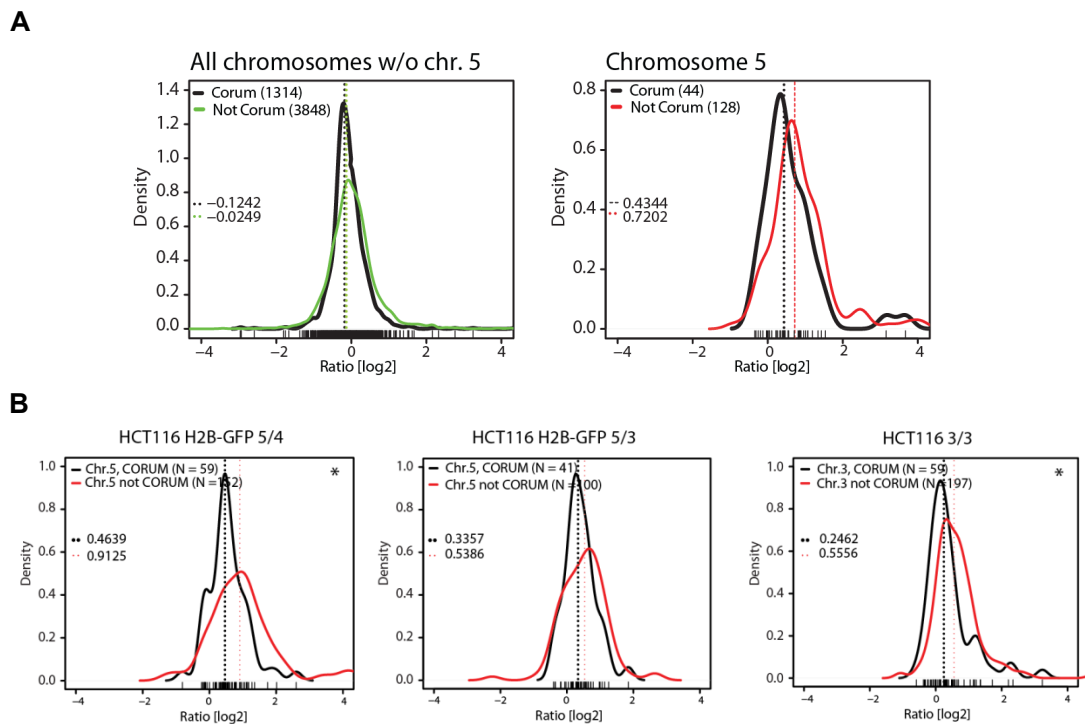


Fig. 19: Abundance of subunits of macromolecular complexes coded on the extra chromosome are regulated. (A) Density plots comparing subunits of macromolecular complexes (CORUM, black line) to the other proteins. Right panel shows the comparison of proteins from all chromosomes excluding chromosome 5. The left panel shows proteins from chromosome 5. Abundances of proteins encoded on chromosome 5 that are subunits of macromolecular complexes are clearly down-shifted. This shift is not observed for protein subunits encoded on all disomic chromosomes. Differences between populations are significant (Wilcoxon rank sum test). (B) Comparison of proteins from the amplified chromosome that are annotated as subunits of macromolecular complexes (CORUM, black line) compared to proteins that are not annotated in CORUM (red line). The cell lines HCT116 H2B-GFP 5/4, HCT116 H2B-GFP 5/3 and HCT116 3/3 are shown. The median is represented by dashed line. Asterisks indicate the significance (Wilcoxon rank sum test).

4 RESULTS

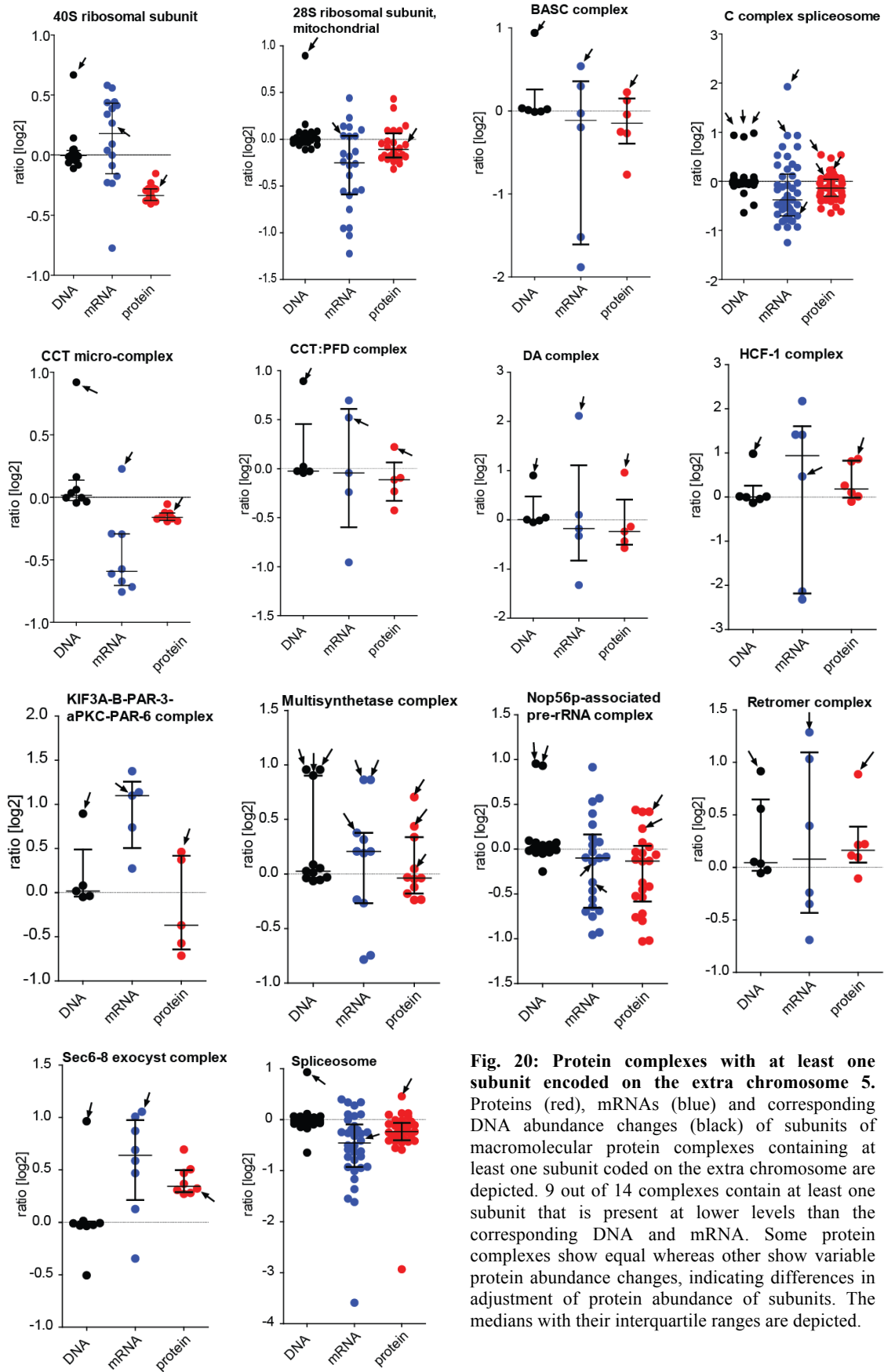


Fig. 20: Protein complexes with at least one subunit encoded on the extra chromosome 5. Proteins (red), mRNAs (blue) and corresponding DNA abundance changes (black) of subunits of macromolecular protein complexes containing at least one subunit coded on the extra chromosome are depicted. 9 out of 14 complexes contain at least one subunit that is present at lower levels than the corresponding DNA and mRNA. Some protein complexes show equal whereas other show variable protein abundance changes, indicating differences in adjustment of protein abundance of subunits. The medians with their interquartile ranges are depicted.

Indeed, abundance changes of protein subunits of macromolecular complexes (KEGG annotation: CORUM) significantly differed from the rest of the population, showing a clear downshift towards diploid level. Therefore, also mammalian aneuploid cells adjust protein subunits of complexes, similarly as suggested for yeast (Fig. 19A). In concordance, similar down-regulation was found in the cell lines HCT116 H2B-GFP 5/4, HCT116 H2B-GFP 5/3 and HCT116 3/3 (Fig. 19B). Due to the high dynamic range of the tetrasomic chromosome 5 (HCT116 5/4) and our in depth analysis which provides ≈ 6000 proteins for analysis, HCT116 5/4 cell line was used for detailed analysis of abundance changes of protein subunits. Protein complexes annotated in the CORUM database that contained at least 5 protein subunits with at least one subunit coded on chromosome 5 were studied in detail. DNA, mRNA and protein abundance changes of these subunits of protein complexes were compared in detail. This revealed that 9 out of 14 complexes show a lower protein abundance change of at least one subunit encoded on the extra chromosome compared to their DNA and mRNA abundance changes (Fig. 20). Even though not all complexes displayed similar protein abundance changes, abundance changes of subunits encoded on the extra chromosome was most often shifted towards the median of the other complex subunits. In conclusion, protein subunits are not expressed according to gene copy number but to a lower level in aneuploid cell lines. Protein subunits encoded on the extra chromosome are in most cases adjusted to a level more similar to other subunits of the same complex.

4.6.2 Analysis of protein kinases

Another protein-group that was significantly different from the population was the category “kinases”. Whereas mRNA abundances (mean = 0.9018) were more spread, protein abundances were tightly centered around diploid level (mean = 0.2612) (Fig. 21). Analysis of protein abundance changes of kinases encoded on the extra chromosome revealed that kinases with abundance changes similarly as their respective gene copy number contain kinases that display function in pathways that were shown to be up-regulated in aneuploid cell lines (e.g. JNK2). Kinases with protein abundance as expected for disomic chromosome, however, were not involved in any deregulated pathways. Due to lower protein number in proteome studies of other aneuploid cell lines and a small number of kinases encoding on extra chromosomes, this trend was not significant in any other aneuploid cell line. In conclusion, aneuploid cells show adjusted protein levels of proteins encoded on the extra chromosome with a preference for subunits of macromolecular complexes and most likely kinases.

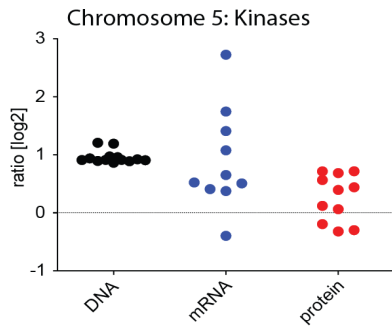


Fig. 21: Proteins kinases of the extra chromosome are regulated. Depicted are all kinases encoded on chromosome 5 in HCT116 5/4. DNA abundance is shown in black, mRNA abundance in blue and protein abundance in red. Data is shown in log₂ scale. Whereas mRNA levels are more spread, protein abundance is clearly down-shifted compared to DNA level.

4.7 Aneuploid cells show a distinct cellular response

Previous analysis on mRNAs in aneuploid yeast revealed changes in expression of some mRNA groups under growth limiting conditions, such as up-regulation of ribosome biogenesis and down-regulation of carbohydrate metabolism (Torres, Sokolsky et al. 2007). Furthermore, aneuploid cells display common characteristics which are not present in diploids, such as slow growth, sensitivity to protein stress, increased glutamine consumption as well as ammonium production (Torres, Sokolsky et al. 2007; Williams, Prabhu et al. 2008; Torres, Williams et al. 2010). These studies indicate that aneuploids show similarities in cellular physiology that differ from diploids. Moreover, it was shown that aneuploid plant, yeast and mouse cells show a similar cellular aneuploidy specific responses (Sheltzer, Torres et al. 2012).

To examine whether an extra chromosome causes a specific cellular response in the generated cell lines, pathway analysis was conducted. Therefore, SILAC data of various generated cell lines were analysed using the Perseus software (Cox and Mann 2012). The application “2-D annotation enrichment analysis” was used to study pathway regulations in aneuploid cells by testing if a category was significantly different from the rest of the population. This was done by applying a non-parametric two-sided Wilcoxon-Mann-Whitney test. A 2% Benjamini-Hochberg false discovery rate was used to control for multiple hypothesis testing. Then, by combining significant abundance changes a relative regulation value between -1 and 1 of the significant categories is calculated. Comparing the data analysis revealed that the up- and down-regulated pathways of two cell lines highly correlate. This means that all tested cell lines with extra chromosome show a distinct cellular response. A high correlation of up- and down-regulated pathways was also found between HCT116 and RPE-1 derived cell lines with extra chromosome (Fig. 22A right panel). This suggests that the observed cellular response to aneuploidy is a general phenomenon and not cell line specific. Additionally, identified pathways were not up- and down-regulated due to increased gene copy number of genes encoded on the added chromosomes. Excluding proteins encoded on the tetrasomic chromosome

from the pathway analysis did not change the observed up- and down-regulated pathways (Fig. 22B). Pathways that are deregulated in cell lines with extra chromosome are regulated on transcriptional, and not only posttranslational level (Fig. 22C,D) as transcriptome and proteome data correlate well, as shown for HCT116 5/4 (Fig. 22C). Moreover, comparing only transcriptome data of cell lines with extra chromosome derived from two different parental cell lines also shows a high similarity of pathway deregulation. Pathways that are up-regulated in cell lines with extra chromosome are: membrane metabolism, energy metabolism, endoplasmic reticulum (ER) and lysosome. Pathways that are down-regulated in cell lines with extra chromosome are pathways involved in DNA- and RNA-metabolism.

To analyze the most up- or down-regulated pathways more detailed, box plots were generated with the extracted categories from all analyzed cell lines (Fig. 23). Abundance changes of proteins from the annotated category were plotted next to their information on DNA abundance from the corresponding genome position. Analysis was conducted for the up-regulated pathways Fig 23A) “lysosome” and “carbohydrate catabolic process” and for the down-regulated pathways (Fig. 23B) “spliceosome” and “DNA replication”. Box plots confirmed the clear up- and down-regulation of the selected pathways. During this study, it was published that aneuploid MEF cells also display a distinct pattern of deregulated pathways which was similar in all tested aneuploid MEF cells (Sheltzer, Torres et al. 2012). In line with our data they observed similar pathways down regulated such as DNA replication and chromosome segregation, pathways which were up-regulated are extracellular region and response to stress. This indicates that aneuploid cells show deregulated pathway patterns that are similar between all tested aneuploids of the same species. This was shown for yeast, mouse and in this study for human aneuploid cells.

To summarize, aneuploid cell lines show a distinct pattern of pathway de-regulation which was similar even between aneuploids derived from different cell lines. Pathway deregulation of mRNAs correlated with pathway deregulation of proteins, suggesting that pathway deregulation can already be studied on mRNA level. The category “lysosome” was one of the most up-regulated categories, which was found in all tested aneuploids.

4 RESULTS

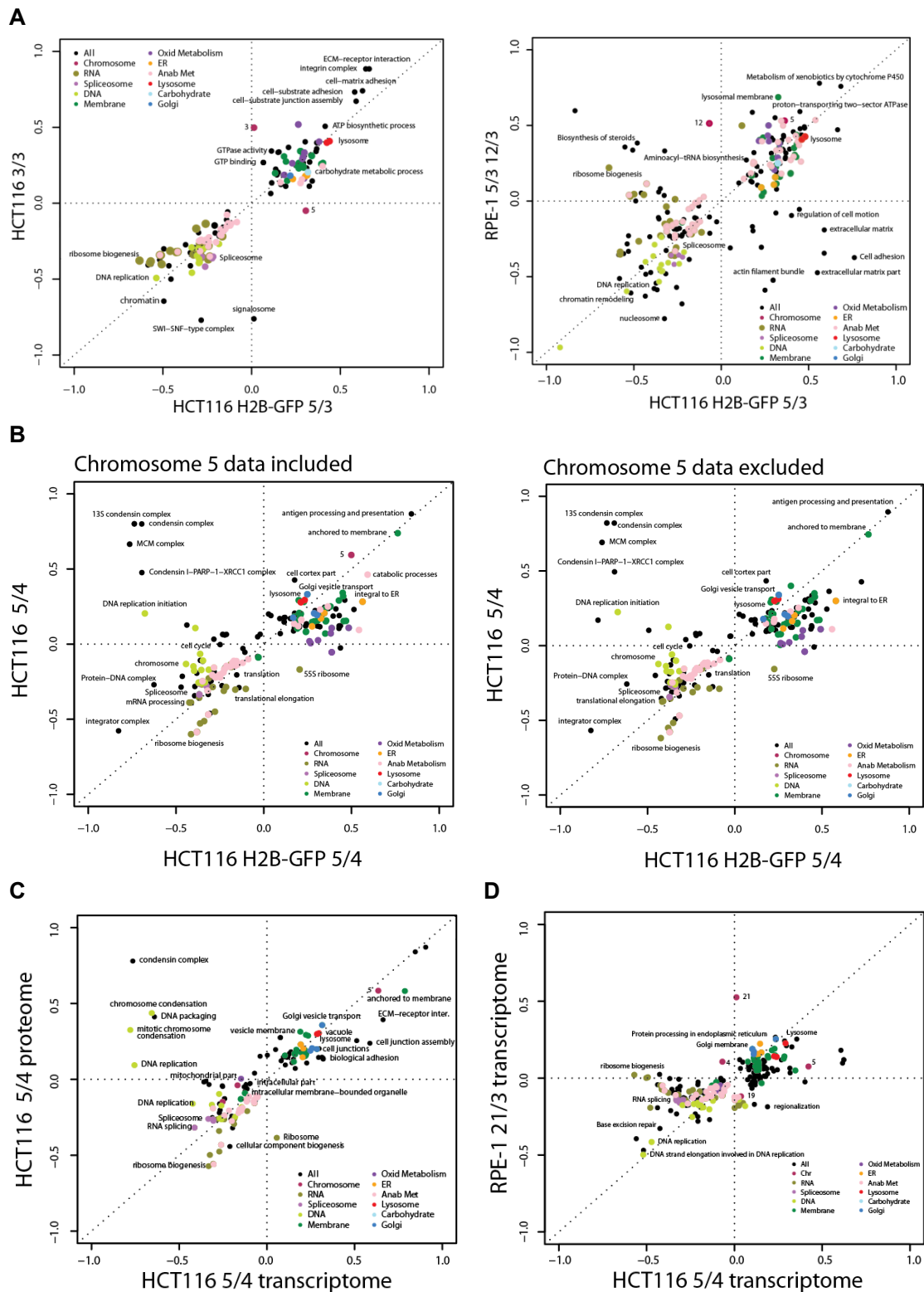


Fig. 22: Aneuploid cells display a distinct cellular response. Two-dimensional (2-D) annotation enrichment analysis. Altered pathways between aneuploid are plotted (Benjamini-Hochberg FDR threshold 0.02). **(A)** Deregulated pathways correlate between aneuploid HCT116 cell lines (left panel) and between aneuploid HCT116 and RPE-1 cell lines (right panel). Pathway deregulation does not depend on specific chromosome but rather represents a general response to the extra chromosome. **(B)** Cellular response does not depend on the increase in gene copy number of genes coded on the added chromosome, as excluding the protein data from the added chromosome did not affect the cellular response. **(C)** Comparison of pathway regulation based on mRNA and protein data of HCT116 5/4 shows striking similarity. **(D)** This similar regulation pattern was also identified when only transcriptome datasets of two different aneuploid cell lines were compared.

4 RESULTS

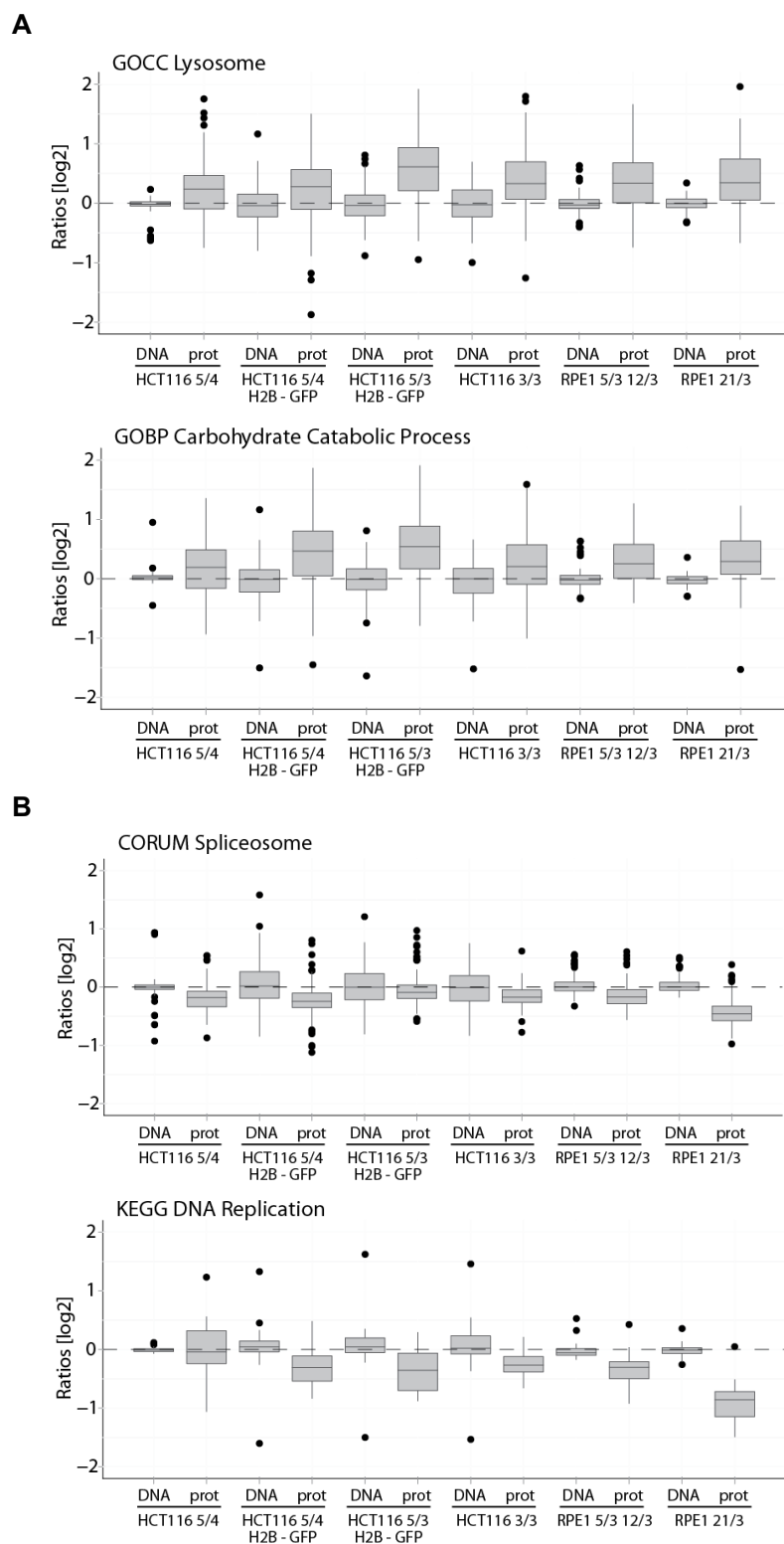


Fig. 23: Examples for up- and down-regulated pathways in cells with extra chromosome. Categories were extracted from the SILAC data and plotted in \log_2 scale. As a control DNA abundance changes of corresponding proteins were plotted next to the protein abundance changes. Differences between DNA and protein abundances were all significant (unpaired *T*-test with Welch's correction, $P < 0.05$). **(A)** Two examples for up-regulated pathways, "lysosome" and "carbohydrate catabolic process". **(B)** Two examples for down-regulated pathways, "spliceosome" and "DNA-replication".

4.8 Aneuploid cells show increased autophagic and proteasomal activity

4.8.1 Aneuploid cell lines show up-regulation of autophagic proteins

As described above, cell lines with extra chromosome express 75% of the protein encoded on the added chromosome according to gene copy number. However, 25% of protein is adjusted to lower levels. Moreover, all cell lines with extra chromosome up-regulate lysosomal proteins. The lysosome is a final step of a protein quality control system which degrades cellular material (Mizushima and Levine ; Yang and Klionsky 2010). The best studied lysosomal protein degradation pathway is macroautophagy, hereafter referred to as autophagy.

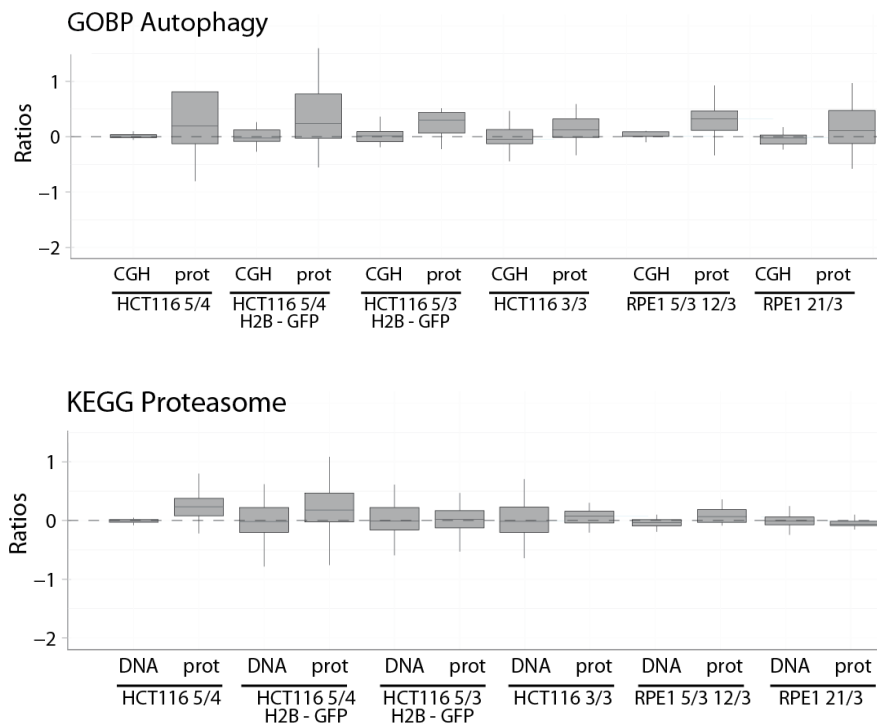


Fig. 24: Box plots of autophagic and proteasomal proteins in cells with extra chromosome. Box plots reveal that indeed autophagic proteins are up-regulated in most cell lines (upper panel). Only some cell lines with extra chromosome show up-regulated proteasomal proteins. This seems to be mainly true for cell lines with extra chromosome 5 (lower panel).

Since cell lines with extra chromosome show increased lysosomal pathways and proteins from the added chromosome are adjusted towards levels as expected for disomes, we

hypothesized that aneuploid cell lines can degrade specific proteins encoded on the extra chromosome by autophagy.

To first test whether proteins annotated in the category “autophagy” are up-regulated we generated boxplots with proteins and corresponding DNA levels comparing all aneuploid cell lines in relation to their respective control cell line with each other (Fig. 24, upper panel). This analysis indeed revealed that proteins of the category “autophagy” are up-shifted. To test whether proteasomal proteins are up-regulated in aneuploid cells as well, we plotted proteins from the category “proteasome” (Fig. 24, lower panel). Only some cell lines show up-regulated proteasomal protein levels. However, average levels of autophagic as well as proteasomal proteins were not significantly different to their aCGH levels for most cell lines (unpaired *T*-test), which is why they were not depicted in the 2-D annotation graphs. Analysis of proteasomal proteins with increased protein abundances of the category “proteasome” revealed that PSME1 (PA28 α) and PSME2 (PA28 β) were highly increased in the cell lines HCT116 5/4 and HCT116 H2B-GFP 5/4. PA28 is a part of the immunoproteasome. It was shown that PA28 activates the immunoproteasome and plays a role in MHC class I antigen presentation (Sijts and Kloetzel 2011). However, an up-shift of PA28 was mainly observed in the cell lines with extra chromosome 5 and may be a chromosome specific reaction.

To summarize, cell lines with extra chromosome show increased levels of proteins annotated in the category “autophagy”, only some cell lines showed increased protein levels of proteasomal proteins. However, up-regulation was in most cases insignificant.

4.8.2 Proteasomal activity is increased in some aneuploid cell lines

An increase in proteasomal degradation can either be achieved by up-regulating expression levels of proteasomal subunits or by increasing proteasomal activity itself. Therefore, proteasomal activity may be even increased without amplified proteasomal subunits. To test whether proteasomal activity is increased in aneuploids, cells were seeded in equal amounts at the day of the experiment and proteasome activity was measured by applying an assay that measures the chymotrypsin-like protease activity associated with the proteasome. This assay revealed that proteasomal activity was increased in the cell lines HCT116 3/3 and HCT116 5/4 when compared to disomic HCT116 (Fig. 25 left panel). However, the cell lines HCT116 H2B-GFP 5/3 and HCT116 H2B-GFP 5/4 did not show an increase in proteasomal activity (Fig. 25, right panel), even though HCT116 H2B-GFP 5/4 showed increased proteasomal protein levels. To conclude, proteasome activity was increased in two out of four tested aneuploid cell lines. Therefore, proteasomal degradation may play a role to maintain protein homeostasis in

some aneuploid cell lines. However, one has to note, that proteasomal degradation can be modulated at several steps (for details see discussion).

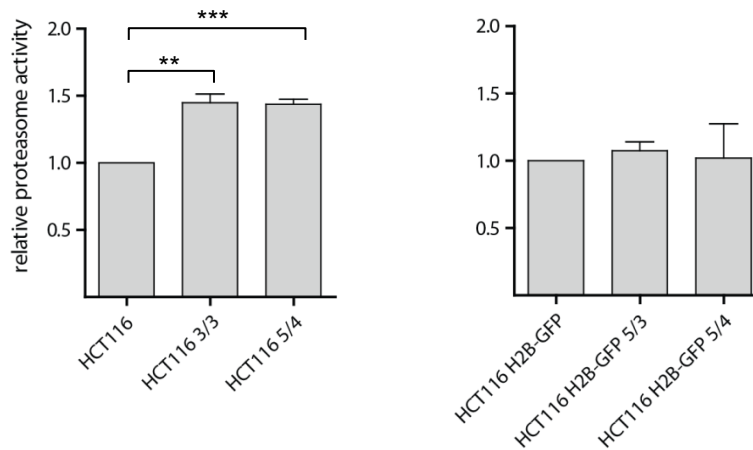


Fig. 25: Proteasomal activity of cell lines with extra chromosome. Proteasome activity was measured by monitoring the chymotrypsin-like protease activity. The disomic cell line was normalized to the value 1. The cell lines HCT116 3/3 and HCT116 5/4 show increased proteasome activity (left panel), whereas H2B-GFP containing cell lines with extra chromosome do not show any increase in proteasome activity (right panel). Experiment was performed in three independent biological triplicates. The mean with SEM is shown. Significance is indicated by the asterisk (unpaired *T*-test), proteasomal activity of cell lines HCT116 H2B-GFP 5/3 and 5/4 was not significantly altered compared to HCT116 H2B-GFP.

4.8.3 Autophagic activity is increased in aneuploid cell lines

Pathway analysis revealed that levels of lysosomal proteins are increased in all analyzed aneuploid cell lines. Furthermore, boxplot analysis of the proteins from the category “autophagy” showed that also autophagic proteins are slightly increased. This suggests a role of autophagy in maintenance of protein homeostasis in aneuploid cell lines. To confirm this hypothesis, we first wanted to show that autophagy activity is indeed increased in aneuploid cell lines. To test this, initial immunoblotting for the autophagic marker LC3 was conducted in various cell lines with extra chromosome. Indeed, LC3-II which is an LC3 isoform that is incorporated into the autophagosomal membrane (Klionsky, Abeliovich et al. 2008) is up-regulated in the tested cell lines HCT116 5/4, HCT116 3/3 and HCT116 H2B-GFP 5/3 and 5/4 (Fig. 26A). Moreover, p62 a marker for selective autophagy (Johansen and Lamark) was found to be up-regulated as well (Fig. 27A). Further immunofluorescence analysis showed distinct patterns of incorporated LC3 into the autophagosomes and confirmed that LC3 is up-regulated in HCT116 5/4, since the mean intensity of LC3 foci was found to be significantly increased (Fig. 26B).

4 RESULTS

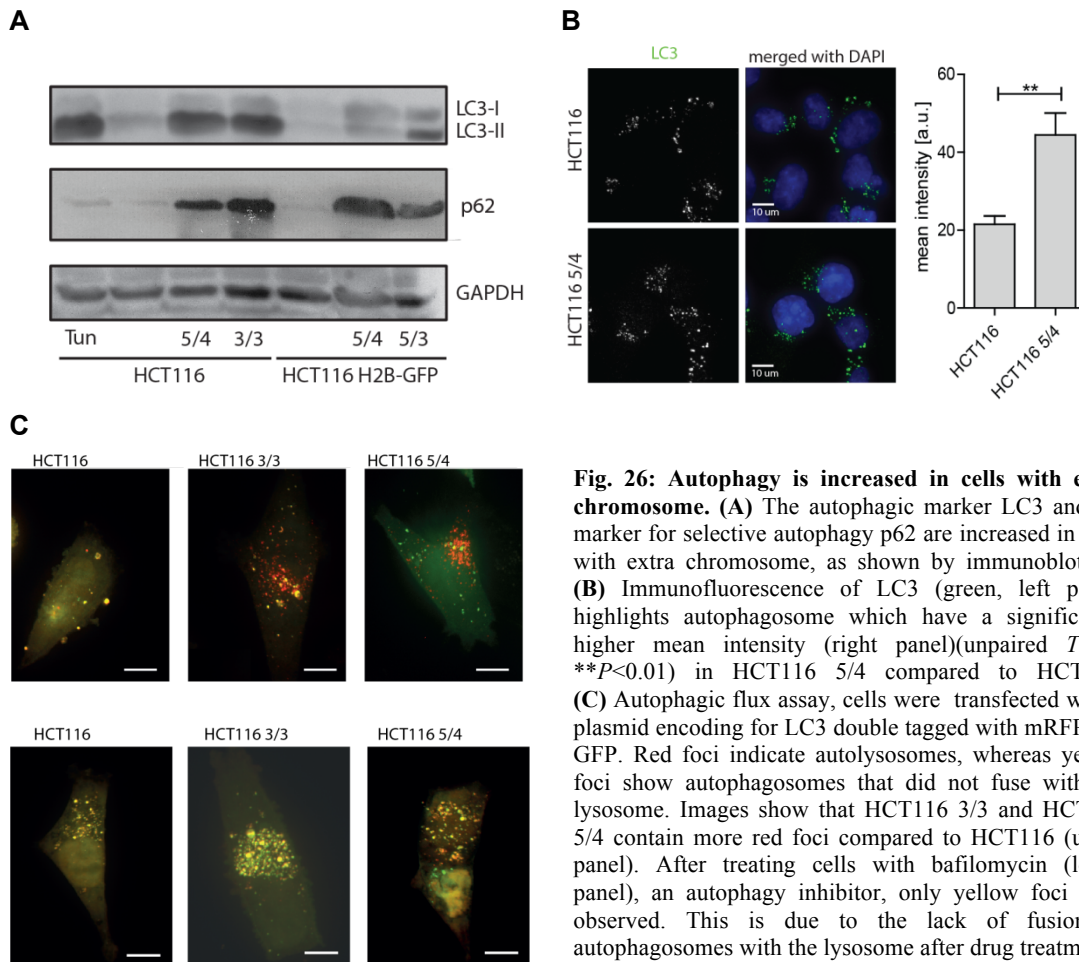


Fig. 26: Autophagy is increased in cells with extra chromosome. (A) The autophagic marker LC3 and the marker for selective autophagy p62 are increased in cells with extra chromosome, as shown by immunoblotting. **(B)** Immunofluorescence of LC3 (green, left panel) highlights autophagosome which have a significantly higher mean intensity (right panel)(unpaired *T*-test, $**P < 0.01$) in HCT116 5/4 compared to HCT116. **(C)** Autophagic flux assay, cells were transfected with a plasmid encoding for LC3 double tagged with mRFP and GFP. Red foci indicate autolysosomes, whereas yellow foci show autophagosomes that did not fuse with the lysosome. Images show that HCT116 3/3 and HCT116 5/4 contain more red foci compared to HCT116 (upper panel). After treating cells with bafilomycin (lower panel), an autophagy inhibitor, only yellow foci were observed. This is due to the lack of fusion of autophagosomes with the lysosome after drug treatment.

Increased levels of LC3 and p62 could also result from a block of autophagy. To test whether the accumulation of p62 and LC3 is due to an increased autophagic activity flux or due to a block in the autophagic pathway, an autophagic flux assay was performed (Kimura, Noda et al. 2007) (Fig. 26C). This assay enables visualization of the dynamics of autophagy by transfecting a construct to the cells that encodes for LC3 double tagged with GFP and mRFP. If LC3 is incorporated into autophagosomes, mRFP and GFP should colocalize and therefore be yellow stained. However, if the autophagosome fuses with the lysosome, the green fluorescence is quenched, and LC3 is then visible in red. Thus, red foci indicate autolysosomes, whereas yellow shows autophagosomes before cell fusion. Comparing the cell lines HCT116 3/3, HCT116 5/4 and HCT116 with each other shows that cell lines with extra chromosome display increased levels of cells with red foci. After treating cells with bafilomycinA1 (hereafter referred to as bafilomycin), an autophagy inhibitor, autophagic flux is perturbed as shown by high level of yellow but only few to none red vesicles. Up-regulation of LC3-II levels and increase autophagic flux leads to the conclusion that autophagic activity is increased in our tested aneuploid cell

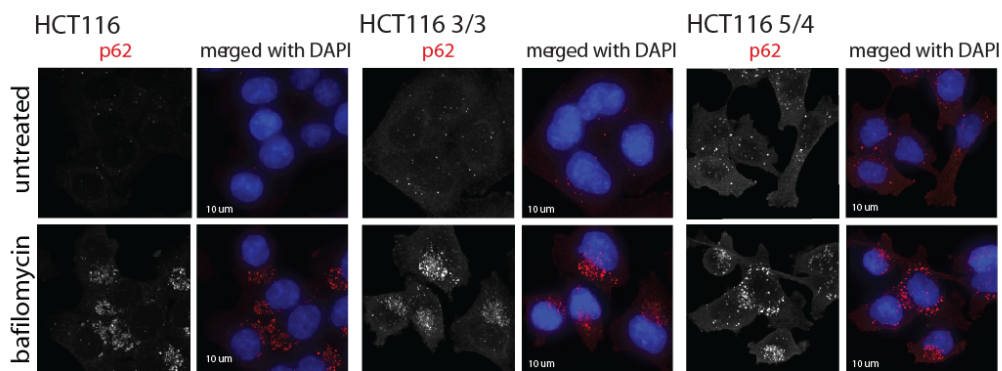
lines. Up-regulation of p62 suggests a role of selective autophagy in regulating aneuploid protein homeostasis.

4.9 Aneuploid cell lines show increased p62-dependent autophagy

4.9.1 p62 levels are increased in aneuploid cells

Since p62 levels were found to be up-regulated in aneuploid cell lines, p62 immunofluorescence experiments were performed to visualize its localization. p62 staining was visible as distinct foci within the cells (Fig. 27A), which confirms that p62 aggregates, as already reported (Kuusisto, Salminen et al. 2001; Bjorkoy, Lamark et al. 2005). Additionally, quantification of the p62 aggregates in the cell lines HCT116, HCT116 3/3 and HCT116 5/4 which was performed by the software cell profiler confirmed that p62 is significantly up-regulated in aneuploid cell lines (Fig. 27B). Moreover, aggregates were more numerous and bigger in size in aneuploid cell lines. As expected, inhibition of autophagy by bafilomycin increased p62 levels further, which was also the case in HCT116. In line with the immunoblot staining, p62 staining by immunofluorescence confirmed that p62 levels are increased in aneuploid cell lines. Moreover, p62 forms aggregates, which are more numerous and bigger in size in aneuploid cell lines.

A



B

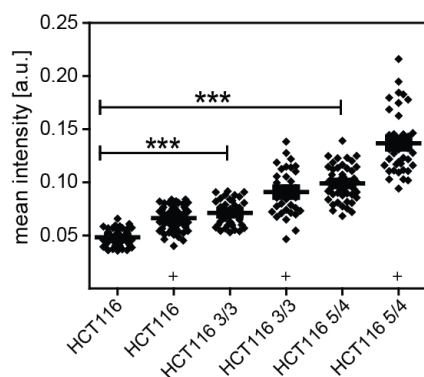


Fig. 27: p62 foci are increased in cell lines with extra chromosome. (A) Staining of p62 (red) shows the distinct p62 foci in HCT116, HCT116 3/3 and HCT116 5/4 cell lines. **(B)** Quantification of p62 foci by cell profiler software. Mean intensity per cell was plotted. p62 was significantly increased in cell lines with extra chromosome (unpaired *T*-test *** $P < 0.001$). Treatment of the cells with Bafilomycin, an autophagy inhibiting agent, showed that p62 levels could be further increased after inhibition.

4.9.2 p62 aggregates colocalize with ubiquitin

It was reported, that p62 binds to ubiquitinated proteins and targets them for autophagic degradation (Pankiv, Clausen et al. 2007; Long, Gallagher et al. 2008; Kirkin, McEwan et al. 2009). Therefore, an immunofluorescence experiment was performed staining for ubiquitin (FITC, shown in green) and p62 (cy5, shown in red) (Fig. 29).

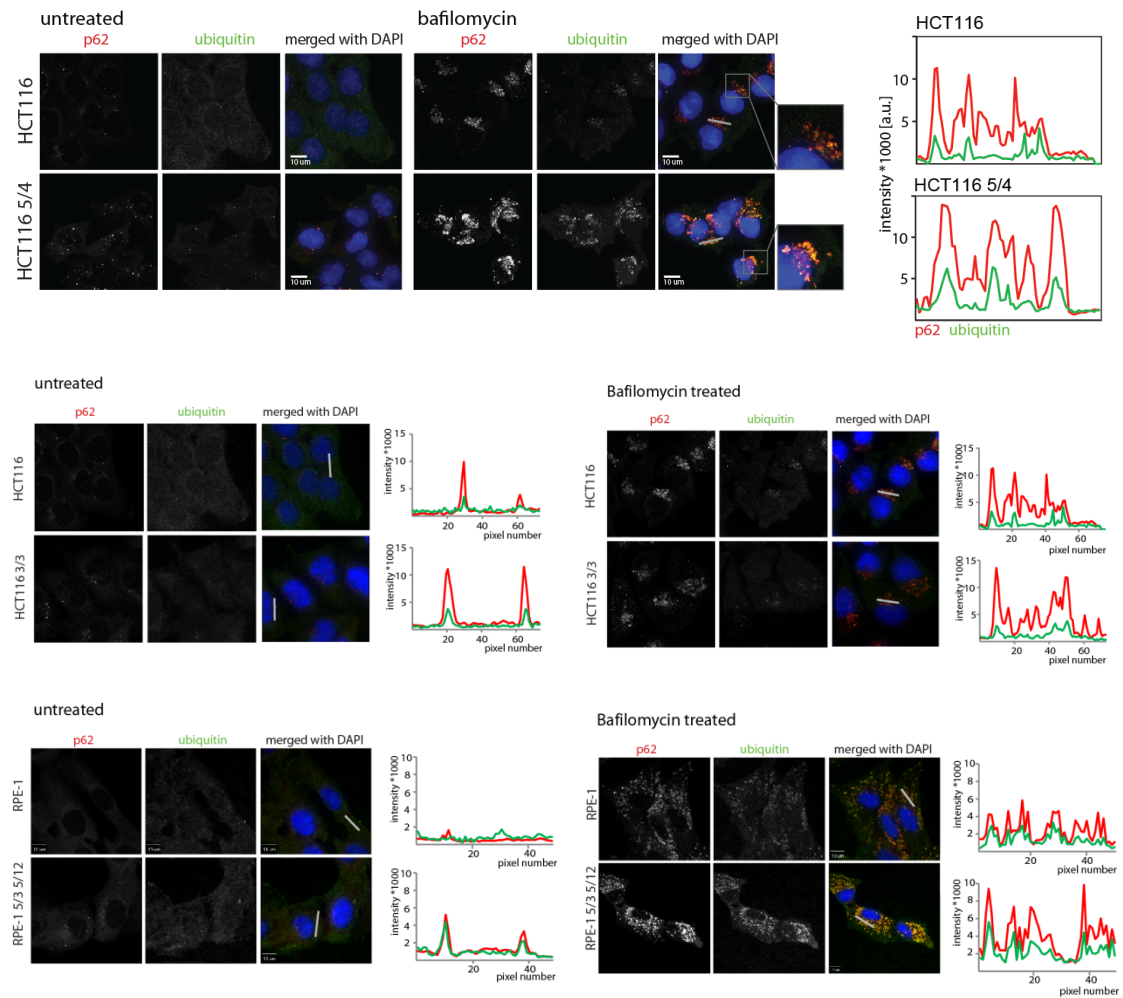


Fig. 28: Ubiquitin and p62 foci are increased and colocalize in cells with extra chromosome. p62 is shown in red and ubiquitin in green. The tested cell lines HCT116 5/4 (upper panel), HCT116 3/3 (middle panel) and RPE1 5/3 12/3 (lower panel) are depicted. Cells were either untreated or treated with bafilomycin to further increase p62 and ubiquitin foci. Line intensities of representative areas are depicted on the right, p62 is indicated in red and ubiquitin in green.

Increased levels of ubiquitin foci were observed in the tested cell lines HCT116 5/4 (Fig. 28A) and HCT116 3/3 (Fig. 28B). These foci colocalized with p62 foci. The same observation was made in the cell line RPE1 5/3 12/3 (Fig. 28C). By using the line intensity tool of the slidebook software, graphs were generated showing the intensity of the cy5 and FITC signal from selected representative areas. To summarize, as expected p62 and ubiquitin colocalized in all cell lines but aneuploid cell lines had a more

pronounced p62 and ubiquitin staining than disomic cell lines. However, if ubiquitinated proteins are proteins encoded on the extra chromosome remains elusive.

4.10 Aneuploid cells do not show increased sensitivity to autophagy inhibition

4.10.1 Sensitivity of aneuploid cells to autophagy inhibiting drugs

The experiments described above show a strong up-regulation of autophagic activity in aneuploid cells. Furthermore, we observed that some proteins, such as subunits of macromolecular protein complex are adjusted towards a level as expected in disomic cell lines. An intriguing speculation would be that proteins that are detrimental to the cells if imbalanced are degraded by autophagy. Therefore, interfering with autophagy should in theory hamper aneuploid cellular growth compared to their disomic counterparts. Moreover, it was reported that aneuploid MEF cells were more sensitive to chloroquine than their diploid counterparts (Tang, Williams et al. 2011). In contrast, another study showed that aneuploid yeasts were not sensitive towards similar drugs but showed distinct sensitivity which was dependent on the extra chromosomes (Pavelka, Rancati et al. 2010). To test if aneuploid cell lines are more sensitive for autophagy inhibiting drugs than their disomic counterparts, cell lines were treated with the autophagy inhibitors bafilomycin and chloroquine (Fig. 29). Live cell imaging analysis was performed while drug treatment was applied. Sensitivities of cell lines towards drug treatments were investigated by monitoring the time of cell death. Data was evaluated by using excel software, generating survival curves.

4.10.2 Knockdown of p62 is not detrimental to aneuploid cells

To study whether aneuploid cell lines are more sensitive to the inhibition of selective autophagy, knockdown of p62 (Fig. 30) was conducted. A live cell imaging experiment was performed after p62 knock down. Time in interphase as well as cell death levels were monitored. However, neither cell death (data not shown) nor time in interphase (Fig. 30A) was significantly altered in the HCT116 5/4 cell line with decreased levels of p62 compared to the cell line treated with control siRNA. Please note that this may be due to the low knock down efficiency (Fig. 30B). However, if p62 amplified levels in aneuploid cells were crucial for their survival, even a knock down towards levels as expected for diploid cell lines should lead to an effect. Therefore, data indicates that increased p62 levels are not required for aneuploid cell survival.

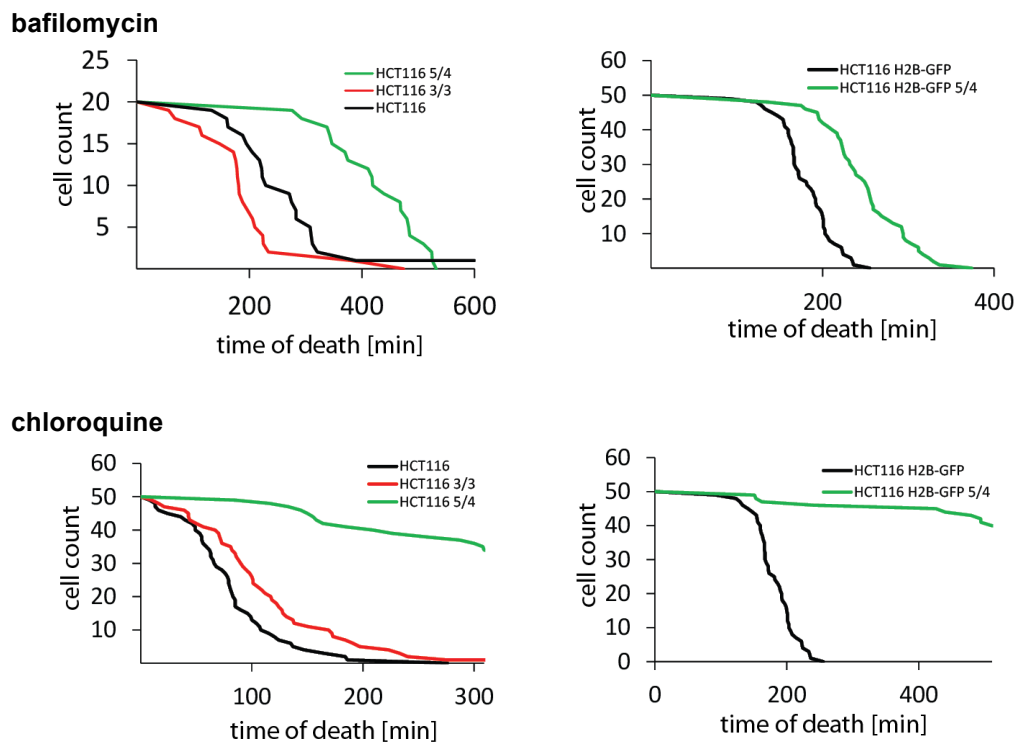


Fig. 29: Cell death after bafilomycin and chloroquine treatment. HCT116 cell lines (left panel) and HCT116 H2B-GFP cell lines (right panel) after bafilomycin (upper panel) and chloroquine (lower panel) treatment. HCT116 are depicted in black, cell lines with extra chromosome 5 in green and cell lines with extra chromosome 3 in red. HCT116 3/3 is more sensitive to bafilomycin, HCT116 5/4 and HCT116 H2B-GFP are less sensitive. Aneuploid cell lines showed all decreased sensitivity to chloroquine.

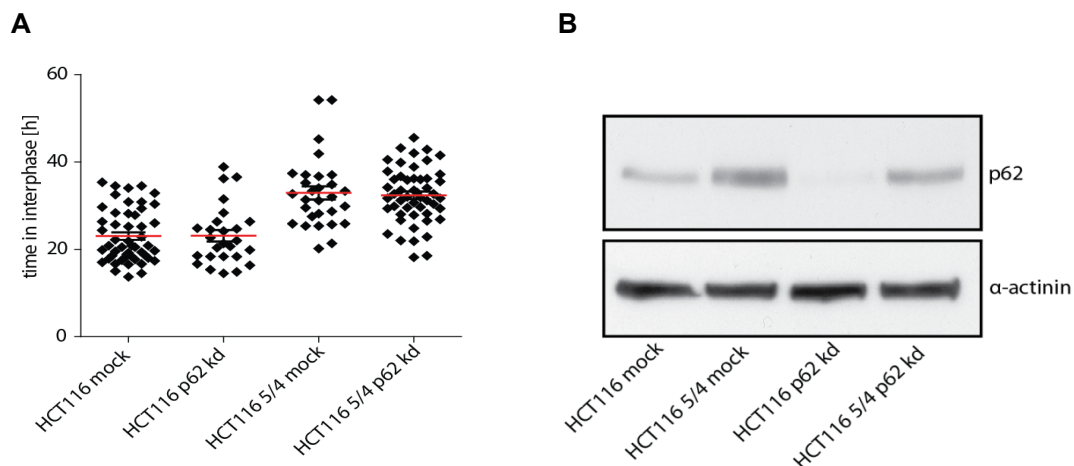


Fig. 30: p2 knockdown is not detrimental to cells with extra chromosome. (A) Time in interphase was measured after knock down of p62. There was no significant increase (unpaired *T*-test) in time of interphase after knockdown for the cell line HCT116 5/4 compared to the control siRNA. **(B)** Western blot of p62 levels. p62 knockdown was only a partial knockdown. Western blot shows that p62 were reduced in HCT116 and HCT116 5/4 p62 siRNA treated cells but not completely knocked down.

4.11 Proteins coded on chromosome 5 are not increased after the inhibition of autophagy

If proteins encoded on the extra chromosome are degraded by autophagy one could speculate that inhibiting autophagy would lead to an accumulation of proteins encoded on the extra chromosome. Ideally, inhibition of autophagy should rescue the phenotype of adjusted protein levels. Therefore, to fully block autophagy 10 nM bafilomycin was added to the cells for 30 hours and protein levels were identified by mass spectrometry. For analysis, untreated as well as well as bafilomycin treated HCT116 5/4 and HCT116 were used and compared with each other.

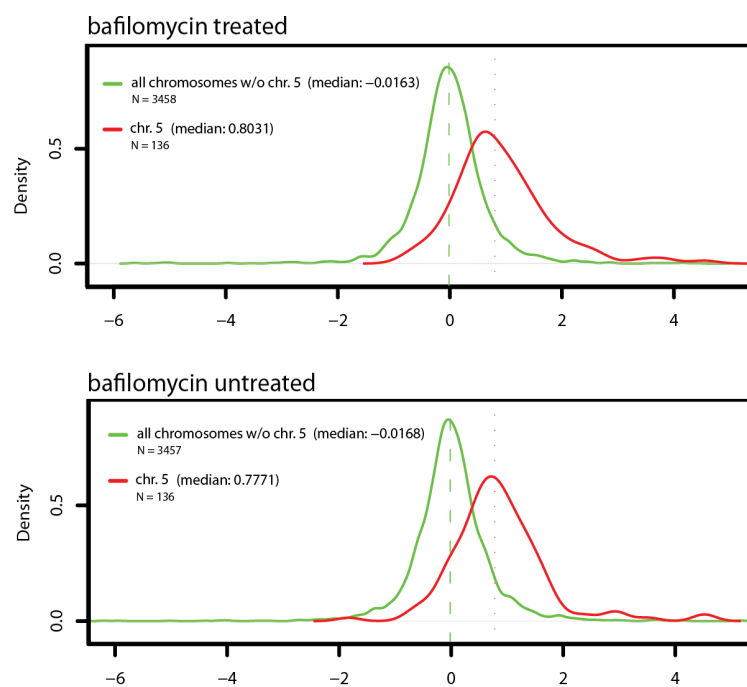


Fig. 31: Changes of protein abundance after inhibition of autophagy. Density distribution graphs of bafilomycin treated HCT116 5/4 (upper panel) and untreated HCT116 5/4 (lower panel) in relation to HCT116 treated and untreated, respectively. Green line shows protein density distribution of proteins encoded on all chromosomes except chromosome 5, red line shows protein distribution of proteins on chromosome 5. Median of proteins encoded on chromosome 5 is at 0.8031 in treated and 0.7771 in untreated cells. Therefore, changes of protein abundance upon bafilomycin treatment do not increase after bafilomycin treatment.

After bafilomycin treatment, abundances of proteins encoded on the extra chromosome do not increase significantly (Fig. 31 “treated” median = 0.8031 vs. “untreated” median = 0.7771). Since the differences may be subtle, proteins encoded on the added chromosome were separated into the categories “CORUM” and “non-CORUM” to filter for proteins that are subunits of complexes which were shown to be significantly down-shifted before (Fig. 32). The graphs “treated” and “untreated” show density distribution graphs of protein abundance changes between treated HCT116 5/4 and treated HCT116 as well as untreated HCT116 5/4 and untreated HCT116, respectively. Subunits of protein complexes show a median of 0.577 in treated HCT116 5/4 compared to treated HCT116 and a median of 0.6023 in untreated HCT116 5/4 compared to untreated HCT116. This shows that subunits of complexes encoded on chromosome 5 are not up-shifted after bafilomycin treatment. Therefore, inhibition of autophagy does not lead to an

4 RESULTS

accumulation of compensated protein indicating that autophagy may not be the cause for the down-regulation of subunits of complexes in cell lines with extra chromosome.

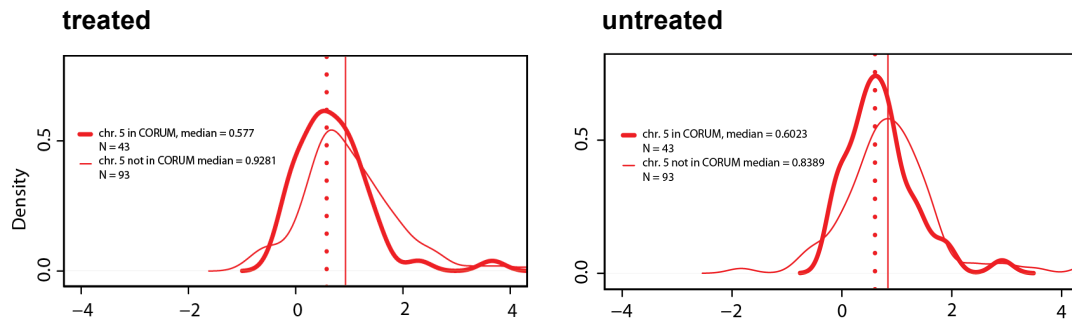


Fig. 33: Inhibition of autophagy does not lead to an upshift of subunit proteins encoded on chromosome 5. Density distribution graph of log₂ ratios of proteins encoded on chromosome 5 from bafilomycin A1 treated HCT116 5/4 vs. treated HCT116 (left panel) as well as untreated HCT116 5/4 vs. untreated HCT116 (right panel) separated into the categories “CORUM” (thick line) and “not in CORUM” (thin line). Medians are depicted in the graph. Subunits of complexes encoded on the added chromosome 5 are not upshifted after bafilomycin treatment.

5 DISCUSSION

Cells with altered chromosome numbers are frequently found in cancerous tissues, miscarried embryos as well as in disabled born children such as trisomy 21 patients (Holland and Cleveland 2012; Nagaoka, Hassold et al. 2012). In the last decades studies on aneuploid tissues and embryos documented that changes in chromosome number lead to growth retardation and in most cases to embryonic lethality (Segal and McCoy 1974; Hodgkin, Horvitz et al. 1979; Magnuson, Debrot et al. 1985; Toikkanen, Joensuu et al. 1993). In contrast, as many cancerous tissues display high levels of cells with altered chromosome number, the idea was born that these cells could benefit from altered protein expression levels due to changes in chromosome number and outcompete cells with normal diploid chromosome content (Li, Yerganian et al. 1997; Storchova and Pellman 2004; Duesberg, Li et al. 2006). Although the phenotypes of cells and tissues with altered chromosome numbers were described for decades, underlying mechanisms that lead to the aneuploidy phenotype remain unknown. To address how aneuploidy affects cellular physiology initial studies were performed to test the effect of altered chromosome number on gene expression levels. Studies employing aneuploid budding yeast, mice and human cells elucidated that cells with extra chromosome scale their mRNA levels according to their gene copy number (Kahlem, Sultan et al. 2004; Upender, Habermann et al. 2004; Torres, Sokolsky et al. 2007; Williams, Prabhu et al. 2008)(Mao, Zielke, Zielke 2003). On protein level buffering mechanisms for subunit proteins of macromolecular complexes in aneuploid maize, yeast and flies were suggested (Birchler and Newton 1981; Devlin, Holm et al. 1982; Torres, Dephoure et al. 2010). Recent developments of Mass spectrometry technology and data analysis tools are emerging allowing more detailed and comprehensive analysis of whole proteomes. Therefore, in depth analysis of dosage dependent proteome levels in comparison to their DNA information of aneuploid cells may lead to new insightful information.

To answer the question how an extra chromosome affects gene expression in human cells, human aneuploid cell lines were constructed and transcriptome as well as proteome were analyzed. This study revealed that, mRNA levels of genes coded on the extra chromosome scale according to gene copy number, whereas protein levels of some proteins encoded on the extra chromosome are adjusted to a level lower than gene copy number. This was especially the case for proteins being a subunit of a protein complex as well as kinases. Analysis of pathways deregulated in cells with extra chromosome revealed a distinct response to aneuploidy, which was found in all analyzed aneuploid cell lines. Interestingly, lysosomal proteins were significantly increased in aneuploid cells and further studies showed that autophagy, a lysosomal degradation pathway, is

activated in all analyzed aneuploid cells. Since also the autophagic receptor p62, which mediates selective degradation of protein was found to be increased in aneuploid cells one may speculate that p62 dependent autophagy is important to maintain adequate protein stoichiometries in aneuploid human cells.

5.1 Mammalian aneuploid model systems

Aneuploid studies have been performed in various sorts of mammalian cell systems. Here I will summarize advantages and disadvantages of different mammalian aneuploid cell systems and compare them to the system which was used in this study.

One possibility to create aneuploid cells is by interfering with the SAC. Mice studies with defective SAC leading to mice with chromosomally instable cells were broadly conducted (Cahill, Lengauer et al. 1998; Dai, Wang et al. 2004; Baker, Jeganathan et al. 2006; Jeganathan, Malureanu et al. 2007; Sotillo, Hernando et al. 2007; Weaver and Cleveland 2007; Weaver, Silk et al. 2007). However, as in this cell model aneuploid cells arise due to chromosomal instability, it is difficult to dissect whether observed phenotypes are caused by aneuploidy or chromosomal instability or may be even caused by the lack of another unknown function of the defective SAC components. To create stable aneuploid cells another study generated aneuploid mouse embryos by crossing mice each containing specific Robertsonian translocations (Williams, Prabhu et al. 2008) and isolated their MEF cells for experiments. Freshly isolated MEF cells display a homogeneous karyotype. However, cultivation of MEF cells quickly leads to polyploidization and immortalization with resulting cell cultures containing various different aneuploid cell types (Todaro and Green 1963). Non-immortalized MEF cells are difficult to cultivate and handle and comparison between cell lines may be difficult, since immortalization occurs quickly. Therefore, aneuploid MEF cells are difficult to use for experiments that require long passaging. One of the earliest studies on mRNA expression levels in aneuploid cells made use of a trisomy 21 mouse model isolating various tissues and performing transcriptional analysis by cDNA array analysis and realtime PCR (Kahlem, Sultan et al. 2004). Tissue cells are suitable for quick endpoint analyses, however using tissue cells for cellular biology assays which require passaging is difficult as primary tissue cells grow poorly and become senescent after few passages. To overcome this problem, we and two other groups (Upender, Habermann et al. 2004; Nawata, Kashino et al. 2011) created aneuploid cell lines by adding an extra chromosome to stable human cell lines by microcell fusion technique (Fournier 1981; Haugen, Goel et al. 2008) resulting in cells that are aneuploid and easy to cultivate. Despite the advantages, one has to note that parental cell lines display already changes

when compared to normal tissue cells. HCT116 is a male, near diploid colorectal cancer cell line with a high level of microsatellite instability but low chromosomal instability (Lengauer, Kinzler et al. 1997). However, the HCT116 cell line already displays some inherent genome alterations (45,X,Y,dup(10)(q24q26),der(16)t(8;16)q13;p13),der(18)t(17;18)(q21;p11.3) (Masramon, Ribas et al. 2000). Thus, we used a second cell line, the RPE-1 cell line that contains fewer changes compared to HCT116 with only a small part of chromosome 10 partially amplified. Moreover, the RPE-1 cell line is a primary epithelial cell line immortalized by h-TERT and therefore closer to normal cells. Despite inherent alterations of HCT116 and RPE-1, these cell lines were used for these experiments as they are already well studied and frequently used as stable cell lines for genome instability research. Present alterations of parental cell lines may weaken specific aneuploid phenotypes of constructed cell lines with extra chromosome, however one would expect that adding a chromosome should lead to a clear enhancement if the phenotype depends on the DNA dosage. Additionally, one has to take into account that adding an extra chromosome may be harmful or lethal to the cell as previously suggested (Thompson and Compton 2010). Therefore, cell lines used may contain alterations that allow propagation of aneuploid cells. To address whether cell lines with extra chromosome contain additional mutations compared to their parental cell line, detailed deep sequencing of cell lines with extra chromosome and their parental cell lines to compare mutations and their corresponding host genes is planned.

To summarize, various mammalian aneuploid cell models were used in the past. Primary tissue cells proliferate poorly and become senescent after passaging. To allow detailed cell biological analysis which requires passaging we made use of a technique called microcell fusion by adding a chromosome to a stable cancerous or hTERT immortalized epithelial cell line. This allowed formation of cell lines which are relatively stable over time and easy to cultivate. One has to note that parental cell lines already differ by karyotype from natural tissue cells which may lessen the phenotypes observed in cell lines with extra chromosome. Moreover, it is possible that the cell lines with extra chromosome proliferate due to the acquisition of aneuploidy tolerating mutations, which will be tested in the future. RPE-1 and HCT116 cell lines containing an extra chromosome are hereafter referred to as aneuploid cell lines and parental cell lines are stated as diploids.

5.2 G1 and S phase delay in aneuploid cell lines

Most whole embryo aneuploidies in humans lead to miscarriages and viable aneuploid humans show mental retardation and growth defects. Accordingly, cultured fibroblasts derived from Down syndrome patients grow slower in comparison to diploid fibroblasts (Segal and McCoy 1974) and hence, multiple other aneuploid organisms show severe growth defects such as yeast (Torres, Sokolsky et al. 2007; Pavelka, Rancati et al. 2010) worm (Hodgkin 2005), fly (Lindsley, Sandler et al. 1972) and mouse (Williams, Prabhu et al. 2008).

Similarly to these findings, this study shows that aneuploid HCT116 cell lines grew significantly slower compared to their parental cell line. This growth delay was caused by an extended time in G1 and S phase, but not by elevated cell death levels or senescence. Similarly, previous findings in aneuploid yeast showed that the growth defect is due to a delay in G1 phase (Torres, Sokolsky et al. 2007) suggesting similar reasons of delayed growth in aneuploid yeast and human cells. However, initial studies in aneuploid MEF cells, analyzing FACS cell cycle profiles, did not show increased number of cells in G1 phase, even though they displayed growth delays (Williams, Prabhu et al. 2008). As cell cycle profiles of aneuploid and diploid cells were similar and no increased level of cells in G1 phase was found the question remains why aneuploid MEF cells grow slower in comparison to diploid MEFs. To summarize, our created aneuploid cell lines grow slower compared to their parental cell line which is in line with previous findings. Aneuploid HCT116 grew slower due to prolonged G1 and S phase.

As discussed later in this chapter cell lines with extra chromosome show a unique pattern of deregulated pathways that is similar in all tested cell lines. Pathways involved in DNA and RNA metabolism were down-regulated. Thus, the question is whether the slow growth of aneuploid cells is a cause or a consequence of the deregulated protein expression in aneuploid cell lines. Two scenarios are possible; aneuploid cell lines may grow slower due to deregulated expression of specific proteins (1) or deregulated expression of some proteins results from a delay which is caused by a specific burden inherent in all aneuploid cells (2) (e.g. DNA damage, protein stress). In the latter case up- and down-regulation of protein levels is a secondary effect due to the growth delay. Proteome data revealed that MCM2-7, which are components of the hexameric helicase are down-regulated in all aneuploid cell lines. Insufficient loading of the MCM complex components was hypothesized to trigger a checkpoint response leading to a delayed entry into S phase (Nguyen, Co et al. 2001; Ge and Blow 2009; Liu, Slater et al. 2009). Therefore, the hexameric helicase may play a role in aneuploids in regard to their cell cycle delay. However, why MCM complex components are down-regulated in aneuploid

cell lines and whether their down-regulation can be linked to the growth delay remains to be addressed in the future.

Another possibility is that the cell cycle delay may be due to an increased need for energy of aneuploid cell lines. It was shown that aneuploid yeast and MEF cells consume more energy metabolites than diploid cells. The same study by Torres et al. showed that adding an untranscribed YAC to yeast cells does not lead to a growth defect as observed for aneuploid cells suggesting that the phenotype is not caused by the extra DNA, but rather by the expression of the extra genes. (Torres, Sokolsky et al. 2007; Williams, Prabhu et al. 2008; Torres, Williams et al. 2010). In conclusion, authors hypothesized that the aneuploid cells require the extra energy for the expression and later degradation of the extra protein. Accordingly, lack of energy in cell lines with extra chromosome may delay multiple cellular functions in cell lines with extra chromosome and therefore delay cell proliferation. Subsequent studies showed that deletion of *UBP6*, coding for a de-ubiquitinating enzyme, improves growth of aneuploid cells to a level similar to their euploid counterparts. Moreover, proteins from the extra chromosome were present at levels more similar to their euploid counterparts after deletion of *UBP6*. As lack of Ubp6 leads to an increase in protein degradation, this indicates that increased protein turn-over can overcome the burden of aneuploid cells, most likely by increased degradation of excess protein from the extra chromosome. Therefore, data suggests that not increased energy need due to overexpression and degradation is the cause of the growth delay but rather the accumulating excess protein encoded on the extra chromosome. In conclusion, aneuploid cells seem to display an increased need for energy. If this is a cause of delayed growth remains unclear, however, recent studies rather pinpoint towards the extra protein as a burden to aneuploid cells. Why the expression of extra proteins is harmful to aneuploid cells is an interesting field of future research.

Slow growth of aneuploids with one extra chromosome is in contrast to the theory that aneuploidization may trigger tumor formation. However, recent studies showed that aneuploid yeast cells display advantages towards certain conditions and moreover, can overcome their growth delay. Pavelka et al. created aneuploid yeast with complex aneuploid karyotypes which displayed growth advantages compared to the euploid control upon treatment with several chemotherapeutic and antifungal drugs such as rapamycin and thiolutin. Interestingly, authors showed a dependency between type of aneuploidy and drug resistance, indicating that aneuploidy can provide certain advantages towards specific conditions (Pavelka, Rancati et al. 2010). In addition aneuploid yeast cells exhibited higher level of chromosomal instability (Sheltzer, Blank et al. 2011), which was lower at levels close to haploidy and increased the more the aneuploidy reached the 2N state. (Zhu, Pavelka et al. 2012). Inherent instability of

aneuploid cells could therefore lead to a mutator phenotype, which may result in fast growing cells over time. Therefore, one may hypothesize that aneuploid cancer cells with highly variable karyotypes and probably frequent doubling events (Carter, Cibulskis et al. 2012) may display an increased inherent chromosomal instability in comparison to normal diploid cells. Due to increased chromosomal instability, cells could gain or lose functions which may make aneuploid cells grow faster. As described above, another study revealed that even less complex aneuploid disomic yeast cells could overcome their growth delay after prolonged cultivation by gaining aneuploidy tolerating mutations e.g. *UBP6* deletion (Torres, Dephoure et al. 2010). As discussed above, *UBP6* deletion was suggested to increase proteasomal turnover and facilitate degradation of excess protein encoded on the extra chromosome (Torres, Dephoure et al. 2010). This indicates that aneuploid cells can overcome their growth delay if additional changes can compensate for their putative burden. Further research is required to dissect the role of aneuploidy towards chromosomal instability and tumorigenesis as well as the function of differentially expressed proteins. Notably, slow growth of freshly generated aneuploid cells does not exclude their evolutionary advantages. Therefore, increased chromosomal instability as well as gain of beneficial mutations may lead to advantages of aneuploid cells towards their diploid counterparts and may provide a model for tumorigenesis caused by aneuploidy.

To summarize, aneuploid cells display a marked growth delay, which was also confirmed by this study. We show that growth delay of human aneuploids is due to prolonged G1 and S phase. Slow growth of aneuploids is in contrast to the hypothesis that aneuploidy can facilitate tumorigenesis. However, other studies showed that aneuploidy can be beneficial under certain conditions e.g. if treated with certain drugs. Moreover, aneuploid cells were shown to display higher levels of chromosomal instability and growth delays, which were abolished upon certain aneuploidy tolerating mutations (e.g. *UBP6* deletion). Increased chromosomal instability in combination with mutations that allow aneuploid cells to grow faster and to gain advantage towards certain stressful conditions could therefore provide an explanation for a role of aneuploidy in cancer formation. Further studies on how aneuploidy can affect evolutionary development of a cell population need to be determined.

5.3 Analysis of transcriptome and proteome in aneuploid cell lines

In the past decades several studies were performed to elucidate dosage dependent gene expression levels in aneuploid cells. First studies in aneuploid plants showed that transcriptional expression levels of most genes do not scale according to gene copy number (Guo and Birchler 1994), similarly as in aneuploid fly cells (Zhang, Malone et al.). However, studies of aneuploid yeast and mouse cells showed that in yeast as well as in mouse cells mRNA are transcribed in a dosage dependent manner (Amano, Sago et al. 2004; Upender, Habermann et al. 2004; Torres, Sokolsky et al. 2007; Williams, Prabhu et al. 2008). Studies on protein levels in aneuploid cells show different outcomes as well. Buffering mechanisms for subunit proteins of macromolecular complexes in aneuploid maize and flies were suggested already more than 30 years ago (Birchler and Newton 1981; Devlin, Holm et al. 1982). Accordingly, a recent study on protein levels in aneuploid yeast showed that proteins scale mostly according to their gene copy number, with the exception of approximately 20% of proteins that are compensated, mainly being subunits of a macromolecular complex (Torres, Dephoure et al. 2010). In contrast, yeasts with complex karyotypes were shown to express protein encoded on extra chromosomes according to gene copy number with no significant compensation of a specific protein group (Pavelka, Rancati et al. 2010).

Recent improvements in depth and analysis of mass spectrometry output allows more detailed and accurate analysis of whole proteomes. When this study was initiated, a detailed global analysis between genome, transcriptome and proteome of different human cell lines was a challenging and pioneering idea. By then whole organism proteome studies were only conducted in yeast comparing the proteome of haploid and diploid yeast (de Godoy, Olsen et al. 2008). Till today this study is the only comprehensive study in human cells comparing genome, transcriptome and proteome with each other. To first analyze how proteome in relation to transcriptome changes in human aneuploid cell lines, mRNA and protein levels were quantitatively analyzed and compared to their genome information. This revealed that mRNA levels in human aneuploid cell lines scale according to gene copy number (cell line with extra chromosome 5; median of 1.09 for mRNA (log2 ratio)) similarly to former mammalian cell studies (Mao, Zielke et al. 2003; Amano, Sago et al. 2004; Williams, Prabhu et al. 2008). As expected, the median aneuploid to diploid ratio of DNA, mRNA and protein of disomic chromosomes ranges around 0 (DNA: 0.005, mRNA: -0.03, proteins: -0.06). Interestingly, average aneuploid to diploid ratio of proteins encoded on the added chromosome did not scale according to gene copy number but were shifted to a value of 0.69. Further analysis revealed that 53 out of 197 proteins (27%) encoded on the extra chromosome 5 or 25% encoded on extra chromosome 3 are not expressed according to gene copy

number. Enrichment analysis of proteins whose abundance change did not scale according to gene copy number revealed that proteins that are subunits of complexes are enriched in this population. Moreover, after analyzing whether other protein groups are preferentially downshifted, we found that kinases show a bimodal distribution, with several kinases present at lower levels, whereas other kinases were up-shifted. These were associated with pathways up-regulated in cell lines with extra chromosome (e.g. JNK2) (for pathway analysis see the chapter “Pathways analysis of aneuploid cell lines”). Analysis of complexes with at least one subunit coded on the extra chromosome 5 revealed that some subunits coded on the extra chromosome seem to be regulated to a level closer to diploid level (8 out of 14, 57%). This result is in line with the hypothesis that dosages of subunits of the same macromolecular complexes are tightly regulated (Veitia, Bottani et al. 2008; Birchler 2010). The dosage balance hypothesis states that stoichiometry imbalances of subunits of macromolecular complexes can lead to dosage-dependent detrimental phenotypes (Veitia, Bottani et al. 2008). As overexpression of an dosage-sensitive gene will lead to dosage changes of the whole complex (Birchler, Bhadra et al. 2001; Veitia 2002; Veitia 2003), proteins from the same complex are expressed at similar levels (Jansen, Greenbaum et al. 2002; Papp, Pal et al. 2003; Ettwiller and Veitia 2007). Accordingly, compensation of macromolecular subunits in aneuploid yeast was described before (Torres, Sokolsky et al. 2007; Torres, Dephore et al. 2010) and this study shows that compensation of subunits encoded on the extra chromosome seems to be conserved from yeast to human. In contrast, Pavelka et al. could only see an insignificant compensation of specific protein groups such as subunit proteins in aneuploid yeast (Pavelka, Rancati et al. 2010). This could be caused by technical differences between their proteome analysis (MudPIT versus SILAC) as well as using yeast with more complex aneuploidies, which could hide compensatory protein changes in the analysis. The dosage balance hypothesis has been recently expanded to proteins that are required to maintain normal function of cellular physiology (Veitia 2005), which is in concordance with the compensation of kinase proteins in our study. Thus, regulation of subunits of macromolecular complexes and kinases encoded on the extra chromosome is in line with the dosage balance hypothesis and with former studies performed in yeast and suggests that dosage compensation of certain proteins is conserved between yeast and humans. Transcription factors showed similar trends, but could not be evaluated because of the small number in our data set.

The mechanism by which subunits and kinases are compensated remain speculative. Regulation of gene transcription can be excluded as transcripts scale according to gene copy number in human cells. Therefore, protein expression of subunit proteins and kinases is only achieved by modulating protein levels, which could be done at several levels (e.g. protein degradation, modulating translation rates). It was shown that

incorporation of proteins into a complex may increase their thermal stability (Buchler, Gerland et al. 2005) and disorder of proteins was shown to correlate with protein half-life (Tompa, Prilusky et al. 2008). Moreover, it was suggested that proteins that are incorporated into a complex most likely escape from proteasomal degradation (Asher, Reuven et al. 2006). Function of the subunit, the topology and the kinetics between interacting subunits may affect the dosage dependent phenotype (Veitia, Bottani et al. 2008) when a subunit for example forms a bridge between other subunits, overexpression of this subunit may result in the formation of inactive sub-complexes (Veitia, Bottani et al. 2008), which may lead to more detrimental phenotypes if over-expressed. Therefore, subunits may be differentially regulated depending on their function and kinetics. Whether regulation could be facilitated actively or is a result from its instability remains elusive. Instability of free subunits as well as differences in kinetics and subunit function could lead to various types of regulation of subunits from the same complex. This may explain different patterns of subunit expression in analyzed complexes with at least one subunit encoded on the extra chromosome as observed in this study. However, studies on subunits encoded on the extra chromosome and their specific function in a macromolecular complex would require higher protein numbers as detailed information is not available for all subunits.

In conclusion, our study shows that transcripts scale according to gene copy number whereas some proteins are adjusted towards lower levels, more similar to the abundance as expected for disomes. This is the case for most subunits of complexes as well as some protein kinases coded on the extra chromosome. Therefore, this study confirms that compensation of subunit proteins in aneuploid cells is conserved between yeast (Torres, Dephoure et al. 2010) and humans and supports the long standing hypothesis that subunits of complexes are compensated as overexpression leads to detrimental phenotypes (Veitia, Bottani et al. 2008). Compensation mechanisms remain elusive, however it was shown that proteins with high disorder that are not incorporated into complexes have a lower half-life than their incorporated counterparts and most likely escape proteasomal degradation (Asher, Reuven et al. 2006; Tompa, Prilusky et al. 2008).

5.4 Pathway analysis in aneuploid cell lines

As described above, aneuploid cells display severe growth defects, indicating that the addition of the extra chromosome is a burden to these cells. As we show here, aneuploid cell lines express proteins encoded on the extra chromosome. Many of them according to their gene copy number. This differential protein expression could lead to up or down-regulation of other proteins or pathways. These pathways could either be altered similarly in various aneuploid cell lines or specifically depending on the type of extra chromosome. In other words, the pathway may be altered as a reaction to the set of amplified proteins or being a reaction to a common burden that the aneuploid cells face (e.g. protein stress, DNA damage)

To test how cellular physiology is globally affected by an extra chromosome, pathway analysis was performed by creating 2-D annotation enrichment analysis (Cox and Mann 2012). Remarkably, all tested HCT116 cell lines with extra chromosome show similar regulation patterns of up- and down-regulated pathways. Similar trends are also present in all RPE-1 cell lines with extra chromosomes. These effects are also clearly visible when proteins from up- and down-regulated pathways of different cell lines were plotted next to each other. Pathways involved in DNA and mRNA metabolism are down-regulated (e.g.: replication, DNA repair, transcription and mRNA processing). Up-regulated pathways involve lipid and membrane biogenesis, endoplasmic reticulum, Golgi vesicles, lysosome function as well as energy metabolism. Notably, observed pathway changes in aneuploid cell lines were not due to proteins encoded on the extra chromosome since removing this data from the analyzed dataset did not lead to any changes in pathway regulation. Moreover, effects were also not caused by labeling artifacts or a bias in protein detection as a reverse labeling experiment and mRNA pathway analysis showed similar results. The specific functions of most altered pathways in cell lines with extra chromosome remain speculative. Interestingly, proteins involved in energy metabolism were in average up-regulated, which is in line with former data, showing that aneuploid yeasts assimilate higher levels of glucose (Torres, Sokolsky et al. 2007) and aneuploid MEFs increase their lactate up-take (Williams, Prabhu et al. 2008). Authors hypothesize that transcription and translation as well as degradation of the extra encoded proteins in aneuploid cells, require energy and that this leads to an increased need for energy metabolism.

Most comprehensive studies on deregulated pathways in aneuploid cells were performed in yeast (Torres, Sokolsky et al. 2007; Pavelka, Rancati et al. 2010) with contradictory outcome. Pavelka et al. could not find a common pattern of pathway regulation in aneuploid yeast. In contrast, Torres et al. observed a transcriptional regulation pattern similar to the environmental stress response (ESR) in most aneuploid yeast cells. Here in

this study we did not identify a pattern similar to the yeast ESR in aneuploid cell lines. However, direct comparison of mRNA data would be needed to allow accurate comparison. Besides these yeast studies, the effect of aneuploidy on cellular physiology was tested in human transformed as well as cancerous cells with a transferred additional chromosome. Authors showed that multiple transcripts were deregulated across the whole genome however, no common aneuploidy specific deregulation pattern of pathways was reported (Upender, Habermann et al. 2004). Moreover, studies in *Drosophila* cells did not reveal any aneuploidy specific response (Zhang, Malone et al. ; Stenberg, Lundberg et al. 2009). However, just recently, gene expression of aneuploid yeast, plant, mice and human cells were directly compared to each other showing highly related expression patterns (Sheltzer, Torres et al. 2012). As Sheltzer et al. also showed that complex aneuploid yeasts display similar altered pathway patterns than yeast with single chromosome aneuploidies (Sheltzer, Torres et al. 2012) contradictory yeast data, described above are probably due to differences in data analyses. Differences between our study and the study by Upender et al. may also be caused by differing analyses as comparing their cDNA array data to our mRNA data revealed equally deregulation patterns (performed by Milena Dürrbaum, data not shown).

As aneuploid cell lines grow slower we cannot exclude that the observed pathway pattern is due to their G1 and S phase delay. However, it is difficult to dissect pathways that are altered due to aneuploidy and pathways that are altered as a secondary effect due to their cell cycle delay. One possibility could be to grow cell lines in minimal medium or to synchronize cell lines to a level where aneuploid cell lines and control cell lines grow similarly and perform an mRNA or SILAC analysis. Similarly, aneuploid yeast cells which showed common pathway patterns similar to the ESR were grown under phosphate limiting conditions in a chemostat before mRNA array analysis. In contrast to cells under nutrient rich condition the only differences of aneuploid yeast in comparison to haploid yeast grown in the chemostat were down-regulation of carbohydrate metabolism and up-regulation of ribosome biogenesis. Thus, authors hypothesize that pathways observed under normal growth conditions were due to the differences in doubling time. However, depletion of nutrients may lead to strong phenotypic responses that may alter or hide aneuploidy specific phenotypes as the aneuploidy phenotype is likely a combination of an increased energy demand and a changed protein turnover rate, and depletion of nutrition likely affects multiple similar functions. Therefore, these results may be even more difficult to interpret. In conclusion, the underlying reasons for common pathway deregulation patterns in aneuploid cells are difficult to interpret. Detailed answers may only be provided by further cell biological and biochemical research dissecting the molecular mechanisms underlying the changes of specific pathways.

Since aneuploid cell lines were shown to express protein encoded on the extra chromosome, we verified whether proteins involved in the protein stress response are increased. However, neither chaperones nor the category “heat shock response” was found to be significantly up-regulated. This finding supports the hypothesis that chronic protein overexpression does not induce the same response in cells as an acute protein stress (Gidalevitz, Ben-Zvi et al. 2006). Moreover, we could not find any up-regulation of proteins involved in unfolded protein response or ER-associated degradation (ERAD).

To summarize, aneuploid cell lines show distinct common patterns of deregulated pathways. Further studies may elucidate why specific pathways in aneuploid cells are differentially regulated and how they affect cellular phenotype and what is their distinct function. Altered pathway regulation of aneuploid cells could open a new and exciting field of study to find therapeutics to treat aneuploid related pathologies. Therefore, treating aneuploid cancer cells with inhibitors targeting specific pathway that are required for aneuploid cell proliferation/survival may lead to aneuploid cell death. Finding treatments that allows aneuploid cells to grow faster may be beneficial for Down syndrome treatments.

5.5 Analysis of protein degradation mechanisms in aneuploid cell lines

2-D Annotation enrichment analysis revealed that proteins from the category “lysosome” are more abundant in all aneuploid cell lines. The lysosome is known to degrade proteins that are either delivered via autophagosomes or directly directed to the lysosome. Up-regulation of protein degradation pathways makes sense in the light of amplified protein expression with partial down-regulation of specific protein groups in cell lines with extra chromosome. Therefore, we analyzed proteins of the two major degradation mechanisms, autophagy and proteasome in our SILAC data in detail. This revealed that the abundances of autophagosomal proteins are slightly increased in all aneuploid cell lines. Moreover, the cell lines with two extra chromosomes 5 or the RPE-1 cell line with extra chromosome 5 and 12 also showed increased levels of proteasomal proteins, whereas other tested cell lines did not show any remarkable increase. The autophagic marker LC3-II was also up-regulated in all analyzed HCT116 cell lines with extra chromosome. It should be noted that an increase of proteasomal and autophagic protein levels does not generally mean that these degradation processes are more active or degrade the proteins that were shown to be downshifted towards diploid level. Further experiments revealed that also autophagic activity was increased in the cell lines HCT116 3/3, HCT116 5/4, HCT116 H2B-GFP 5/3 and HCT116 H2B-GFP 5/4, whereas proteasome activity was increased in HCT116 3/3 and HCT116 5/4. However, turnover by the proteasome may be modulated at multiple stages, such as increase of ubiquitin conjugation levels, increased transport to the proteasome or decrease of de-ubiquitinating enzymes (Hoeller and Dikic 2009) which was not addressed in this study. Therefore, it may be possible that the proteasome activity is not altered itself but that turnover by the proteasome is still increased due to orchestrating ubiquitination and delivery to the proteasome. In conclusion, autophagic proteins as well as autophagic flux were increased in all tested aneuploid cell lines, whereas proteasomal proteins and proteasomal activity were only increased in some cell lines. However degradation by the proteasome may be modulated at multiple stages.

Studies by Torres et al. indicate that aneuploid cells likely suffer from proteotoxic stress (Torres, Sokolsky et al. 2007). Moreover, the same group found that aneuploid yeast cells with a deletion for *UBP6*, a gene encoding for the de-ubiquitinating enzyme Ubp6 (Borodovsky, Kessler et al. 2001; Leggett, Hanna et al. 2002; Guterman and Glickman 2004) grow as fast as haploid yeast (Torres, Dephoure et al. 2010). Intriguingly, authors hypothesize that the extra proteins encoded on the added chromosome leads to the observed growth delay and after increasing proteasomal turnover the excess protein is effectively degraded, allowing these cells to overcome their growth delay. Moreover, it

was shown that aneuploid MEF cells were sensitive to the autophagy inhibitor chloroquine (Tang, Williams et al. 2011), suggesting that autophagy is important for aneuploid MEF cells. Surprisingly, sensitivity to rapamycin as well as any tested proteasome inhibitor (lactacystin and MG132) was not significantly altered in aneuploid MEF cells, which would be expected if aneuploid cells require proteasomal or autophagic activity for survival or growth. In contrast to the data obtained with aneuploid MEFs or budding yeast, we could not find any aneuploidy specific response after drug treatment. Inhibition of USP14, the mammalian Ubp6 homologue, by 1-[1-(4-fluorophenyl)-2,5-dimethyl-1H-pyrrol-3-yl]-2-(1-pyrrolidinyl)-ethanone (IU1) (Lee, Lee et al. 2010) did not improve cellular growth of aneuploid cell lines in a similar way as reported for aneuploid cells with the deletion of *UBP6* in yeast (data not shown). Moreover, experiments performed during this study using autophagy inhibitors such as bafilomycin and chloroquine did not reveal any unique response. Some cell lines with extra chromosome showed increased sensitivity compared to their parental cell lines, whereas others were less sensitive. This observation is rather in accordance with data obtained by Pavelka et al. describing that depending on the type of aneuploidy some yeast strains were less and some more sensitive to certain drugs than their euploid counterparts (Pavelka, Rancati et al. 2010). Therefore, the question remains if altered protein expression is more important for drug sensitivity of aneuploid cells than targeting e.g. their protein degradation pathways. Moreover, autophagy and the proteasome system work synergistically as it was shown that autophagy activity is stimulated after inhibition of the proteasome (Iwata, Riley et al. 2005; Pandey, Nie et al. 2007). Therefore, inhibition of one degradation mechanism may be compensated by the other and may not affect cellular survival, which influences the experimental result. Testing the sensitivity of aneuploid cell lines towards combined treatment of bafilomycin and MG132 could provide interesting insight into this question. What may be the reason for increased autophagic or proteasome activity is further discussed in the following chapter.

To summarize, recent research illustrated that the extra protein encoded on the extra chromosome may be a burden for aneuploid cells. Yeast cells seem to circumvent this problem by degrading protein by proteasomal degradation whereas this study reveals that mainly autophagic degradation is up-regulated in aneuploid human cell lines.

5.6 p62 dependent autophagy is increased in aneuploid cell lines

This study shows that p62, a selective autophagy receptor, is up-regulated in cell lines with extra chromosomes, which increased even more after treatment with the autophagy inhibitor bafilomycin. p62 sequesters misfolded or damaged ubiquitinated proteins and targets them to the autophagosome by interacting with LC3 (Bjorkoy, Lamark et al. 2005; Pankiv, Clausen et al. 2007). Immunofluorescence analysis revealed that in cell lines with extra chromosome, the p62 co-localization to ubiquitin is increased, suggesting a specific degradation mechanism in aneuploid cell lines.

As described, p62 foci in aneuploid cell lines are increased compared to their parental cell lines. Since p62 sequesters ubiquitinated proteins and forms aggregates (Pankiv, Clausen et al. 2007; Kuusisto, Kauppinen et al. 2008; Wooten, Geetha et al. 2008), one can speculate about the nature of these foci. One appealing possibility could be that the extra proteins in aneuploid cell lines is sequestered by p62 and degraded via autophagy. Proteins from the extra chromosome might be harmful to the cell by perturbing cellular protein homeostasis. Moreover, proteins of cell lines with extra chromosome may be misfolded due to high load on the protein folding machinery as chaperones are not increased in cell lines with extra chromosome, but effectively more protein has to be folded. In line, protein degradation mechanisms were shown to play an important role in aggregate based neurodegenerative diseases (Alves-Rodrigues, Gregori et al. 1998; Webb, Ravikumar et al. 2003; Harris and Rubinsztein 2012). Recently, a more dominant role for autophagy in neurodegenerative diseases was proposed. Proteasomal degradation requires unfolding of the substrate to pass through the pore of the proteasome (Verhoef, Lindsten et al. 2002), therefore, aggregated proteins may be rather degraded by autophagy, which was shown to degrade e.g. bulk proteins, mitochondria and protein complexes (Johansen and Lamark). This could be an explanation why autophagy was shown to be up-regulated in all analyzed human cell aneuploids, whereas the proteasome is up-regulated only in some aneuploid cell lines with higher chromosome load (tetrasomic cell lines).

Interestingly, p62 was shown to play a role in neurodegenerative diseases displaying accumulation of malformed or toxic proteins. Therefore, sequestered p62 is used as a marker for neuropathologies (Kuusisto, Salminen et al. 2001; Kuusisto, Kauppinen et al. 2008) and overexpressed huntingtin was shown to be degraded via p62-dependent autophagy (Bjorkoy, Lamark et al. 2005). p62 colocalized with expressed huntingtin in human cell lines and interference with p62 function lead to a huntingtin dependent cell death (Bjorkoy, Lamark et al. 2005). As also cell lines with extra chromosome may accumulate extra proteins, the role of p62 in these cell lines could be similar as for neurodegenerative diseases. In line, signs of mental retardation are present in

neurodegenerative diseases and patients with Down syndrome. Moreover, Down syndrome patients suffer from Alzheimer disease earlier and more often in life than healthy humans (Olson and Shaw 1969; Glenner and Wong 1984) and number of aneuploid cells is increased in Alzheimer diseased brain (Petrozzi, Lucetti et al. 2002). Research on neurodegenerative diseases pinpointed to the aggregates being the toxic species of neurodegenerative phenotypes. However, recently it was discussed that aggregates may be rather protective to the cell (Behrends, Langer et al. 2006; Douglas, Treusch et al. 2008; Douglas and Dillin 2010), as aggregation provides a tool to store harmful proteins in an inactive form. Effects of aggregates on cellular physiology e.g. as shown by Olzscha and colleagues may thus be tolerated by the cell as a protection from the worse. In this study authors could show that expression of artificial amyloids lead to the formation of aggregates, which attract other proteins. These proteins were reported to be relatively large in size and significantly enriched in predicted unstructured regions. Interestingly, aggregates were shown to contain in addition to the artificial amyloid multiple important cytosolic proteins such as proteins involved in chromatin organization, transcription, translation, maintenance of cell architecture and protein quality control (Olzscha, Schermann et al.). Conclusively, authors could show that indeed aggregates itself have an effect on the cell independent of their origin. If the sequestration of important cytosolic proteins by aggregates would be a general phenomenon, one could speculate that p62 associated aggregates arising in aneuploids can attract other proteins important for cellular function as well. This might be a possible explanation for the growth delay observed in aneuploid cells. Therefore, a general higher demand of protein degradation and an overload of the proteasome could lead to accumulation of either proteins from the extra chromosome or misfolded and damaged proteins that attract cytosolic proteins which are important for cellular function. Interestingly, a recent study showed that p62 increases in autophagy deficient mice, which leads to an increased in ROS levels, DNA damage and subsequently tumorigenesis (Mathew, Karp et al. 2009). A former study by the same group showed that autophagy suppresses chromosomal instability (Mathew, Kongara et al. 2007). Authors hypothesized that deficiency in autophagy leads to an accumulation of mitochondria and damaged proteins, which causes an increase in ROS. Interestingly, Sheltzer and colleagues could show that genome instability as well as DNA damage is increased in aneuploid yeast (Sheltzer, Blank et al. 2011) and also our cell lines with extra chromosomes show higher chromosomal instability than their parental cell lines (data not shown). Further studies should address whether aneuploid cell display increased ROS levels (1), show elevated levels of DNA damage (2), and accumulate mitochondria (3). If these experiments result in positive data, it may be interesting to test how activation of autophagy affects these factors.

Even though p62 as well as LC3-II are increased in aneuploid cell lines, it remains unclear whether proteins encoded on the extra chromosome are sequestered by p62 and actively degraded via p62 mediated autophagy. If p62 was important for cell lines with extra chromosome, its depletion should have detrimental effects. Knockdown of p62 in cell lines with extra chromosome did not lead to an increased delay in interphase nor did it lead to increased cell death levels. However, knockdown was only partial and another specific autophagy receptor NBR, which was shown to have a similar function as p62 (Kirkin, Lamark et al. 2009) could compensate decreased p62 levels. Therefore, future experiments with double knockdown of p62 and NBR should be performed. To elucidate which proteins are associated with p62, p62 immunoprecipitation experiments followed by mass spectrometry analysis were performed (data not shown). Unfortunately, this technically challenging experiment did not lead to interpretable data since associated proteins were only present in very low concentrations. For mass spectrometric analysis, only the soluble fraction was used, however, aggregates may be rather present in the insoluble fraction. Therefore, it would be interesting to follow this path further in the future, either by optimizing the p62 immunoprecipitation conditions or by trying to use the insoluble fraction for analysis. Moreover, immunoprecipitation of ubiquitin in combination with subsequent SILAC analysis could identify, whether proteins from the tri- or tetrasomic chromosome are differentially ubiquitinated. Identifying proteins by ubiquitin pull-down however, does not answer the question how proteins are degraded. If the ubiquitination of proteins from the extra chromosome is significantly increased above the expected level, this may pinpoint to a function of ubiquitination in regard to protein degradation. Another possibility could be that other proteins are preferentially ubiquitinated in aneuploid cells (e.g. aggregation of damaged or old protein due to a higher demand to protein degradation machineries). However, analysis of ubiquitinated proteins may be difficult since as reported multiple pathways are altered in aneuploid cells. Therefore, ubiquitination status of proteins may be changed by the physiological response to aneuploidy but may not provide a clear answer which proteins are degraded via p62.

To test whether the extra proteins encoded on the added chromosome accumulate after autophagy inhibition, bafilomycin was added to the cells for 30 hours followed by a quantification of protein levels by SILAC. Analysis of the levels of proteins encoded on the added chromosome did not reveal any significant difference as their levels were increased as in untreated conditions. This may have many reasons. First, proteins from the added chromosome may not be degraded by autophagy. As described above, the UPS could degrade protein encoded on the extra chromosome. Due to the overload of the proteasome by the extra proteins, autophagy would be needed to compensate the degradation of other misfolded or damaged proteins to maintain protein homeostasis.

Second, activation of autophagy could have secondary reasons. Aneuploid cell lines show up-regulated energy metabolism pathways and former studies showed that aneuploid cells have a higher demand of energy sources. Since autophagy is known to be activated due to starvation, increased p62 and LC3 levels may result out of nutrient deprivation. However, p62 was shown to accumulate with proteins specifically and increased p62 aggregation does not fit to the starvation hypothesis. Third, experimental setup is not suitable to test the hypothesis that proteins from the extra chromosome are degraded by autophagy. Bafilomycin was shown to inhibit autophagy. One study showed that bafilomycin inhibits the fusion of autophagosome and lysosome (Yamamoto, Tagawa et al. 1998), this was also confirmed in this study by autophagy flux assay, thus almost only yellow fluorescence was detected indicating that autophagosomes did not fuse with lysosomes. However, it is unclear whether prolonged bafilomycin treatment and therefore autophagy inhibition alters other pathways and metabolism besides autophagy. Therefore, it is possible that after inhibition alternative pathways such as proteasomal degradation are increased. As described above, the proteasome and autophagy were shown to work synergistically (Clague and Urbe 2010). Notably, as inhibition of the proteasome was shown to induce autophagic activity (Pandey, Nie et al. 2007) and vice versa (Zhu, Dunner et al. 2010), autophagy inhibition could lead to induced proteasome activity, which could bypass the lack of autophagic degradation. In conclusion, cell lines with extra chromosome show increased levels of p62, a receptor for selective autophagy. Why p62 is up-regulated and whether proteins from the extra chromosome are preferentially sequestered by p62 remains the subject of future research. The suggested role of p62 targeting over-expressed or malformed proteins may pinpoint to a function of p62 in sequestering excess protein encoded on the extra chromosome for degradation.

To summarize, this study shows that aneuploid cell lines express mRNAs according to gene copy number, whereas some proteins encoded on the extra chromosome are compensated. These compensated proteins are mainly subunits of protein complexes as well as kinases. Compensation of subunits and kinases suggests that over-expression of these proteins may be harmful and compensation is required to maintain cellular physiology. In line, former studies proposed that protein imbalances of subunits and kinases are detrimental to the cellular homeostasis and that compensation of these proteins may be a common mechanism for deregulated proteins (Veitia, Bottani et al. 2008). Moreover, 2-D pathway enrichment analysis revealed that cell lines with extra chromosomes display a common pattern of deregulated pathways when compared to their parental cell lines. This aneuploidy-response pattern was found in all analyzed cell lines, which shows that cellular physiology of aneuploid cells is not affected by the

specific set of over-expressed proteins according to the extra chromosome but rather by a common burden displayed in all aneuploid cells. The lysosomal pathway was up-regulated in all cell lines, pinpointing towards a function of the lysosome in degrading excess protein. Testing for autophagy, a lysosomal degradation pathway revealed that p62 dependent autophagy is up-regulated in aneuploid cell lines, which implies a role of p62 in degrading excess protein in aneuploid cell lines. However, inhibiting autophagy did not lead to an accumulation of proteins encoded on the extra chromosome nor did the p62 knock down negatively affect the aneuploid cell line HCT116 5/4. p62 may also sequester proteins that are deregulated in aneuploids independently of proteins encoded on the extra chromosome. Aneuploid yeast cells, lacking the de-ubiquitinating enzyme Ubp6, displayed lower levels of proteins encoded on the disomic chromosome indicating that extra protein in yeast is degraded via the proteasome. In this study we only tested protein levels of proteasomal proteins and proteasome activity; however proteasomal degradation can also be modulated by other factors such as ubiquitin ligases. Therefore, we cannot exclude that proteasomal degradation plays a role in degrading excess proteins in human aneuploid cell lines and enhanced autophagic activity may be needed to compensate for the increased load of proteins on the proteasome. On the other hand, one may speculate that unfolded and non-incorporated subunit proteins might be prone to be aggregated. Furthermore, it was proposed that aggregated proteins may be rather degraded by autophagy as by the proteasome (Johansen and Lamark) providing an appealing model how protein compensation is achieved. Further research is needed to clarify the roles of autophagy and proteasome in aneuploid cells and may reveal interesting targets for aneuploidy based pathologies.

6 EXPERIMENTAL PROCEDURES

6.1 Material

Reagents and consumables not listed below were purchased from the listed companies: Abcam (Cambridge, UK), Beckman Coulter (Krefeld, Germany), Becton Dickinson (Heidelberg, Germany), Bio-Rad Laboratories (Munich, Germany), Cell Signaling Technologies (Frankfurt a. M., Germany), GE Healthcare (Munich, Germany), Invitrogen (Karlsruhe, Germany), Ibbidi (Martinsried, Germany), Lonza (Basel, Switzerland), MBL (Woburn, USA), Merck Biosciences (Darmstadt, Germany), Nunc (Wiesbaden, Germany), Progen (Heidelberg, Germany), Promega (Madison, USA), QIAGEN (Hilden, Germany), R&D Systems (Minneapolis, USA), Roche (Mannheim, Germany), Roth (Karlsruhe, Germany), Santa Cruz Biotechnology (Heidelberg, Germany), Sarstedt (Nümbrecht, Germany), SERVA Electrophoresis (Heidelberg, Germany), Sigma (Taufkirchen, Germany), TPP (Trasadingen, Switzerland), VWR (Darmstadt, Germany).

Microbiological, molecular biological, cell biological and biochemical techniques were based on standard protocols (Sambrook et al., 1998) or conducted after manufacturer's instructions.

6.1.1 Chemicals, media and reagents

4',6-diamidino-2-phenylindole	(DAPI, Roth)
β -mercaptoethanol	(Merck)
acetic acid	(Sigma-Aldrich)
acrylamide (30% w/v)	(Serva)
ammoniumpersulfate	(APS, Merck)
bafilomycin A1	(Sigma-Aldrich)
blastidicinS	(AppliChem)
bromphenol blue	(Merck)
bovine serum albumine (BSA)	(Sigma-Aldrich)
colchicine	(Fluka)
cytochalasin D	(Sigma-Aldrich)
dimethylsulfoxide (DMSO)	(Serva)
DMEM + GlutaMAX TM -I	(Invitrogen)
ethanol	(Sigma-Aldrich)
fetal bovine serum (FBS)	(Gibco)
formaldehyde	(AppliChem)
formamide	(Merck)
G418	(Invitrogen)
glycerol	(Sigma-Aldrich)
HCl	(Merck)
isopropanol	(Sigma-Aldrich)
KCl	(Roth)

6 EXPERIMENTAL PROCEDURES

KH ₂ PO ₄	(Merck)
methanol	(Merck)
MgCl ₂	(Merck)
NaCl	(VWR)
NaF	(Sigma)
Na ₄ HPO ₄	(Merck)
Na ₄ P ₂ O ₇	(Sigma)
N,N,N'-tertramethylethylene diamine (TEMED)	(Serva)
NP-40	(Sigma-Aldrich)
Opti-MEM I + GlutaMAX™-I	(Invitrogen)
paint probes	(Chrombios)
penicillin/ streptomycin (Pen-Strep, 100x)	(PAA)
Plus™ Reagent	(Invitrogen)
polyvinylidene fluoride membrane (PVDF)	(Roche)
Protease inhibitor cocktail tablets	(Roche Diagnostics)
sodium azide	(Merck)
sodium dodecyl sulfate (SDS)	(Serva)
Tris-(hydroxymethyl)-aminomethane (Tris)	(Sigma)
trisodium citrate	(Sigma-Aldrich)
Triton-X-100	(Roth)
trypsin-EDTA (1x)	(PAA)
tunicamycin	(Sigma-Aldrich)
Tween 20	(Applichem)
Vecta shield	(Vector Labs)
L-arginine (Arg0),	(Sigma-Aldrich)
L-lysine (Lys0),	(Sigma-Aldrich)
L-13C615N4-arginine (Arg10)	(Sigma-Aldrich)
L-13C615N2-lysine (Lys8)	(Sigma-Aldrich)
dialyzed FCS	(Invitrogen)
DMEM without arginine and lysine	(Invitrogen)

6.1.2 Buffers

Lämmli buffer	62.5 mM Tris/HCl pH 6.8 2% (w/v) SDS 10% (v/v) glycerol 0.002% (w/v) bromphenole blue 2.5% β- mercaptoethanol
Lower running gel (15%), pH 8.8	7.5 ml 30% (w/v) acrylamide 3.75 ml lower SDS-buffer pH 8.8 3.75 ml H ₂ O 150 µl APS 15 µl TEMED
Lower SDS buffer, pH 8.8	1.5 M Tris/HCl 0.4% (w/v) SDS
Lysis buffer (RIPA), pH 7.5	50 ml 10% NP-40 5 ml 10% natriumdeoxycholate 15 ml 5 M NaCl 1 ml 0,5 M EDTA 25 ml 1 M Tris, pH 7,5

6 EXPERIMENTAL PROCEDURES

PBS(-T), pH 7.5	137 mM NaCl 2.7 mM KCl 10 mM Na ₄ HPO ₄ 2.0 mM KH ₂ PO ₄ (0.1% Tween 20)
Propidium iodide solution	69 µM propidium iodide 100 µg/ml RNase in 38 mM sodium citrate
SDS- running buffer	25 mM Tris/HCl 200 mM glycine 0.1% (w/v) SDS
20xSSC, pH 7.0	3 M sodium chloride 300 mM trisodium citrate
Staining solution (β-gal-assay)	5 mM K ₃ Fe(CN) ₆ , 2 mM MgCl ₂ , 150 mM NaCl, 30 mM citric acid/ phosphate buffer 5 mM K ₄ Fe(CN) ₆ , 1 mg/ml X-Gal)
TBS(-T)	50 mM Tris.HCl, pH 7.4 150 mM NaCl (0.1% Tween 20)
Transfer buffer	25 mM Tris/HCl 1.44% (w/v) glycerol 20% (v/v) methanol
Upper SDS buffer, pH 6.8	0.5 M Tris/HCl 0.4% (w/v) SDS
Upper stacking gel (7.5%), pH 6.8	1.25 ml 30% (w/v) acrylamide 1.25 ml upper SDS-buffer pH 6.8 2.5 ml H ₂ O 50 µl APS

6.1.3 Plasmids and bacteria**6.1.3.1 Plasmids**

pBOS-H2B-GFP	(BD Pharmingen)
ptfLC3 plasmid (mRFG-GFP-LC3)	(Addgene)

6.1.3.2 Bacteria

XL-1 blue competent cells	(Stratagene)
---------------------------	--------------

6.1.4 Kits

ECLplus™ kit proteins	(GE Healthcare)
GenElute™ HP Plasmid Maxiprep Kit	(Sigma-Aldrich)
Genra Puregene Kit	(Qiagen)
Lipofectamin LTX and plus reagent	(Invitrogen)
mRNeasy mini kit	(Qiagen)
Plasmid mini kit	(Qiagen)
Proteasome-Glo™ Chymotrypsin-Like Cell-Based Assay	(Promega)

6.1.5 Technical equipment

Electrophoresis Power Supply EPS 301	(GE Healthcare Biosciences, USA)
Eppendorf centrifuge 5415R, 5417 C	(Eppendorf, Germany)
FACScalibur	(Becton Dickinson)
Fluoroscanner Ascent FL	(Labsystems, Australia)
Hera Cell, Hera Safe, Megafuge 3.0R	(Thermo Fisher Scientific, Germany)
Mini-PROTEAN II electrophoresis system	(Bio-Rad Laboratories, Germany)
MUPID ONE electrophoresis unit	(Advance Co., Japan)
Nanodrop ND-1000 spectrophotometer	(PEQLAB, Germany)
Rotina 420R centrifuge, Micro centrifuge SD220	(Hettich, Germany)
SmartSpec 3000	(Biorad, Germany)
Thermomixer comfort	(Eppendorf, Germany)
Vortex Genie 2	(Scientific industries, USA)
VWR Digital Heat Block	(VWR, Germany)
X-ray film processor MI-5	(Medical Index, Germany)
Z2 Coulter Particle Count and Size Analyzer	(Beckman Coulter, Germany).

6.1.5.1 Microscopy

Confocal spinning disc microscope

Confocal microscopy was performed using a fully automated Zeiss inverted microscope (AxioObserver Z1) equipped with a MS-2000 stage (Applied Scientific Instrumentation, Eugene, OR), the CSU-X1 spinning disk confocal head (Yokogawa), LaserStack Launch with selectable laser lines (Intelligent Imaging Innovations, Denver, CO) and an X-CITE Fluorescent Illumination System. Images were captured using a CoolSnap HQ camera (Roper Scientific) under the control of the Slidebook software (Intelligent Imaging Innovations, Denver, CO).

Live cell imaging microscope

Live cell imaging was performed using a Zeiss Axio Observer Z1 microscope equipped with a Plan Neofluar 20 × air objective. The microscope contains a sample stage with an incubator chamber (EMBLEM, Heidelberg, Germany) maintained at a 37° C, 40 % humidity, in an atmosphere of 5 % CO₂. Metamorph 7.1 software (Molecular Devices) was used to control the microscope.

6.1.6 Software

Adobe Illustrator CS3 (13.0.0)	(Adobe Systems Incorporated, USA)
Ascent software (2.6)	(Thermo Scientific)
CellProfiler (2.0)	(BROAD Institute)
Cell Quest Pro 5.2.1	(BD Bio Sciences)
FlowJo 7.6.1	(Tree Star, Inc.)
GraphPad Prism 5	(GraphPad Software, La Jolla, USA)
Metamorph 7.1	(Molecular Devices, Germany)
Slidebook 5.0	(Intelligent Imaging Innovations, USA)

6.1.7 Antibodies

6.1.7.1 Primary antibodies

anti-LC3 (115-3)	(Medical & Biological Laboratories)
anti-p62 (610832) (for immunoblotting)	(BD Transduction Laboratories)
anti-p62 (GP62-C) (for immunofluorescence)	(Progen)
anti-Ubiquitin (P4D1)	(Santa Cruz)
anti-β-Tubulin (ab21057)	(Abcam)
anti-GAPDH (ab9483)	(Abcam)

6.1.7.2 Secondary antibodies

goat anti-mouse IgG HRP affinity purified PAb (HAF007)	(R&D systems, US)
donkey anti-goat IgG HRP affinity purified PAb (HAF109)	(R&D systems, US)
anti-mouse FITC	(Abcam)
anti-guinea pig dylight 649	(Jackson ImmunoResearch)
anti-mouse dylight649	(Jackson ImmunoResearch)

6.2 Methods

6.2.1 Cell culture

6.2.1.1 Cell lines

Cell lines HCT116 (ATCC No. CCL-247), HCT116 5/4 and HCT116 3/3 were a kind gift of M. Koi (Baylor University Medical Centre, USA). The cell line RPE-1 hTERT (hereafter referred to as RPE-1) and RPE-1 hTERT H2B-GFP (hereafter referred to as RPE-1 H2B-GFP) were kindly provided by Stephen Taylor (University of Manchester, UK). Cell lines with extra chromosomes were created adding a chromosome by microcell fusion technique (see Experimental procedures, chapter: “microcell fusion technique”). As donor cell lines, mouse A9 cell lines were used containing the appropriate human chromosome which was purchased from the Health Science Research Resources Bank (HSRRB), Osaka 590-0535, Japan. HCT116 H2B-GFP was created by Christian Kuffer transfecting HCT116 with pBOS-H2B-GFP by lipofection (FugeneHD, Roche) according to manufacturer’s protocols.

6.2.1.2 Cultivation

Used cell lines were cultivated in Dulbecco’s Modified Eagle Medium (DMEM) supplemented with 10% fetal bovine serum (FBS), 100U penicillin and 100U streptomycin (pen-strep) at 37°C and 5% CO₂ atmosphere. HCT116 3/3, HCT116 H2B-GFP 5/3, HCT116 H2B-GFP 5/4, RPE1 5/3 12/3, RPE1 3/3, RPE1 H2B-GFP 21/3 and A9 cell lines were grown in medium with 400 µg/ml G418. The cell lines HCT116 5/4 and HCT116 with stable transfected H2B-GFP were grown in media with 6 µg/ml blasticidinS. BlasticidinS and G418 were omitted at least two passages before any experiment to avoid possible side effects on the experimental outcome.

6.2.1.3 Sub-culturing and passaging

Cell lines were grown in 10 or 15 cm cell culture dishes for 2-3 days at 37°C in a 5% CO₂ atmosphere to a confluency between 70 and 80%. Then, cells were washed with 1x PBS, afterwards trypsin-EDTA was added to the cells and incubated for 5 min at 37°C in 5% CO₂ atmosphere. Cells were then resuspended in DMEM supplemented with FCS and pen-strep as described for cultivation and splitted in ratios between 1/5 to 1/10 to a new 10 or 15 cm cell culture dish. The appropriate amount of fresh medium was added to the cells (a total of 10 ml for 10 cm dish and 20 ml for 15 cm dish). As observed during this study, cells with extra chromosome are less chromosomal stable as their parental cell

lines. Therefore, cells used for experiments did not exceed passage 15 after cryopreservation of cell lines generated by microcell fusion.

6.2.1.4 Cryopreservation and recultivation

Cells were grown as described to a confluency of 70-80%. Then cells were collected by trypsinization as mentioned above and carefully centrifuged at 1500 rpm for 3 min. The supernatant was removed and cells were resuspended in FCS/10% DMSO. 0.5-1 ml of suspension was added to cryotubes and frozen at -80°C using a freezing chamber filled with isopropanol. For long time storage, cells were placed in liquid nitrogen. To recultivate cells from frozen stocks, filled and frozen cryotubes were thawed in a 37°C water bath and cell suspension was pipetted into 10 ml of fresh and 37°C warm cell culture medium. After careful centrifugation at 1500 rpm for three minutes, cell pellets were again resuspended in appropriate amounts of suitable cell culture medium and seeded on a cell culture dish.

6.2.1.5 siRNA transfection using Oligofectamine

Cells were seeded one day before transfection on a 6 well plate. At the day of transfection, cells were between 50-60% confluent. At the day of transfection media was exchanged to 4 ml DMEM without FCS and antibiotics. At least two hours later, 8 µl siRNA (100 pmol/µl) and 175 µl OptiMEM were combined as well as 5 µl Oligofectamine was added to 15 µl OptiMEM. After 20 min both liquids were mixed and incubated for 5 min at room temperature. Then mixture was added to the cells and cells were incubated till further processing.

6.2.2 Molecular biology standard techniques

6.2.2.1 Agarose gel electrophoresis

Quality of genomic DNA was evaluated first by measuring 260/280 nm ratio using the Nanodrop ND-1000 and second by applying the gelelectrophoresis technique. Therefore, 5 µl of genomic DNA was mixed with 1 µl of electrophoresis running dye and loaded on a 1% agarose gel in TBS-T. The gel was run in a MUPID ONE electrophoresis unit at 100V for 20 min. Only high quality genomic DNA was used for arrayCGH analysis.

6.2.2.2 Bacteria transformation

Competent XL-1 blue cells were thawed on ice and aliquoted at 50 µl into 1.5 ml eppendorf tubes. 1-5 µl plasmid DNA was added to the cells and mixed gently. Tubes were incubated on ice for 30 min. Then, cells were heat shocked at 42°C for 30 sec. Afterwards, tubes were placed on ice for two minutes and then 250 µl of pre-warmed LB medium was added. Samples were shaken at 37°C for one hour and 100 µl of each transformation was spread onto LB plates with appropriate antibiotics. Plates were then incubated overnight. Single colonies were used to create overnight cultures in 500 ml LB media plus appropriate antibiotics for plasmid extraction by maxi prep.

6.2.2.3 Cell lysis

Cells were grown to 70-80% confluency, collected by trypsinization and afterwards pelleted by centrifugation. Supernatant was removed and cells were lysed in appropriate amounts of RIPA buffer supplemented with a Protease inhibitor cocktail tablet (Roche) (one tablet/10 ml of buffer).

6.2.2.4 Bio-Rad protein assay

Bio-Rad Protein assay was conducted as described in the manufacturer's protocol. In brief, Bio-Rad solution was diluted 1:5. To 1 µl of lysed cells resuspended in RIPA buffer 999 µl of diluted BioRad solution was added. As blank 1 µl pure RIPA buffer was added to 999 µl of diluted BioRad solution. Samples were added to plastic cuvettes and absorbance at 595 nm was measured using the spectrophotometer SmartSpec 3000. Samples were measured in triplicates. Protein concentration was evaluated by comparing gained values to a standard curve previously generated using the same assay with known concentrations of BSA in solution.

6.2.2.5 SDS-polyacrylamide gel electrophoresis (PAGE)

After the protein concentration was evaluated by Bio-Rad protein assay, 20-50 µg of protein was mixed with 6x Lämmli-buffer and loaded on an appropriate, self-made SDS-polyacrylamide gel. Gel was run using the Mini-PROTEAN II electrophoresis system at 200V for 45 min using SDS-running buffer.

6.2.2.6 Immunoblot

After SDS-PAGE, the separated proteins were transferred to a methanol soaked PVDF membrane at 100V for one hour using the Mini-PROTEAN II electrophoresis system. The membrane was blocked in either 5% skimmed milk in TBS-T or 1% BSA in PBS-T (for LC3 and p62 antibodies). Primary antibodies were incubated at 4°C overnight whereas secondary antibodies were incubated at room temperature for one hour. Buffers used for antibodies were applied as described in the manufacturer's protocols. As secondary antibody HRP-conjugates antibodies were used in a 1:5000 dilution. To visualize stained proteins, the ECLplus™ reagent was applied to the membrane as described in the manufacturer's instructions. An Amersham hyperfilm ECL was incubated on the membrane using various, appropriate time points and developed using the X-ray film processor MI-5.

6.2.3 Generation and characterization of cell lines

6.2.3.1 Microcell fusion technique

To generate aneuploid cell lines with, microcell fusion technique was performed as described (Fournier 1981). Therefore, Mouse A9 cells that contain in addition to their mouse chromosome content one human chromosome with an antibiotic resistance gene were used as donor cells. To induce mitotic slippage cells were treated for 48 h with colchicine (final concentration: 60 ng/ml). Then, cells were collected by trypsinisation and applied on plastic bullets. After attachment of the cells, bullets were centrifuged at 30-34°C and 15000 rpm for 30 min in DMEM containing 10 µg/ml cytochalasin B. Pellets were resuspended in serum free DMEM and later on filtered using first Whatman, pore size 8 µm and later 5 µm to remove mouse cells from the suspension. Phytohemagglutinin (PHA-P) was applied to the mouse cells and applied to the recipient cell lines (HCT116 H2B-GFP, RPE1 or RPE1 H2B-GFP). Then, polyethylene glycol 1500 (PEG 1500) was added to induce fusion of microcells with the recipient cells. Using medium supplemented with corresponding antibiotics enabled selection of cells containing the added chromosome. The cell line RPE1 5/3 12/3 contains an extra chromosome 12, which was not intentionally added to the cell line. This chromosome may be added to the recipient cell by chromosome missegregation before fusion.

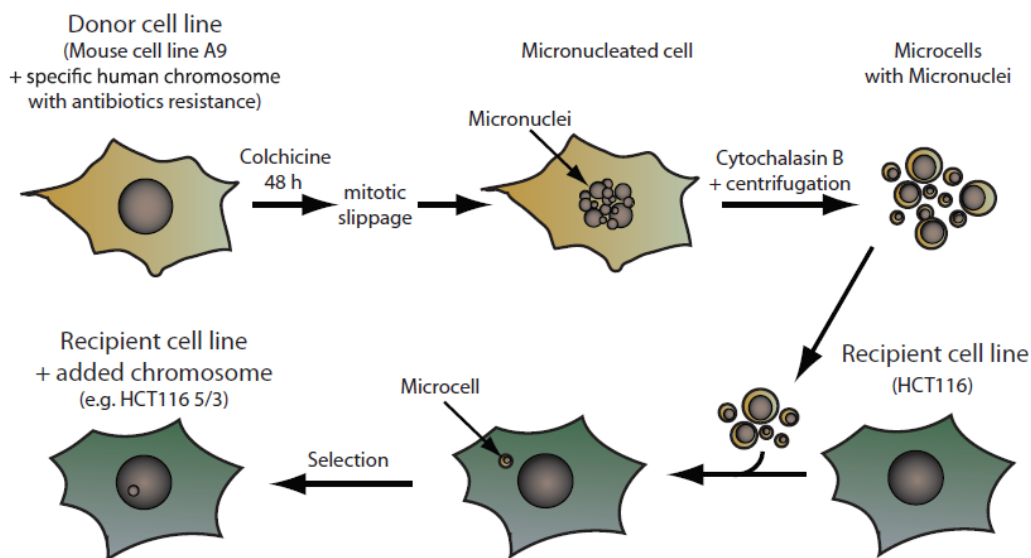


Fig. 34: Generating aneuploid cells by microcell fusion technique. After colchicine treatment of Donor cell lines for 48 h micronuclei containing the extra human chromosome were extracted and fused to recipient cells. As recipient cells HCT116 and RPE-1 cell lines were used. Cell lines were selected by adding the appropriate antibiotics. (Figure adapted from: (Killary and Lott)).

6.2.3.2 Chromosome spreads

Cells were cultivated as described. After reaching 70-80% confluency, cells were treated with 50 ng/ml colchicine for 3-5 h. Then, cells were collected by trypsinization and centrifuged for 10 min at 1000 rpm. Cell pellets were carefully resuspended in 75 mM KCl and kept at 37°C for 10-15 min. Carefully at 800 rpm for 10 min centrifuged cell pellets were fixed in 3:1 methanol/acetic acid after removing most but leaving some remaining supernatant. After washing the cell pellets several times with 3:1 methanol/acetic acid, dead and swollen cells were spread on a wet glass slide that was later air dried at 42° C for 5 min.

6.2.3.3 Paints

Chromosome spreads were carried out as described. Then, chromosomes spreads were labeled with paints probes (Chrombios GmbH, Raubling, Germany) for chromosome 2, 3, 5 and 21 tagged with TAMRA, FITC, Cy-5 and TAMRA, respectively. Cell lines were always stained with two probes. One probe that stained the expected added chromosome and one probe that stained a control chromosome that was not added to the cells. The experimental procedure was carried out according to the manufacturer's instructions. Before imaging, chromosomes were counterstained with DAPI. Images were taken by the confocal spinning disc microscope using a 100x oil objective and the

appropriate laser (561 nm (TAMRA), 473 nm (FITC) or 660 nm (Cy-5) laser). The DAPI signal was detected using the UV channel.

6.2.3.4 Multiplex FISH (M-FISH)

Chromosome spreads were prepared as described above. M-FISH analysis was performed by Chrombios GmbH (Raubling, Germany)

6.2.4 Growth and Cell Cycle Studies

6.2.4.1 Growth curves

Cells that reached 70-80% confluency were trypsinized and counted in triplicates either by haemocytometer or by a Beckman Coulter Particle Count and Size Analyzer Z2. After seeding exactly 300000 cells in each well of a six well plate time points were taken for 5 days every day. Cells were counted as described. The experiment was performed in triplicates. The mean values were taken to generate the growth curves. The error bars indicate the standard deviation. Cell lines with extra chromosome were always compared to their parental cell lines that were cultivated in parallel.

6.2.4.2 Cell death analysis

Cells were trypsinized after three days, reaching a confluency of 70-80% and resuspended in DMEM/10% FCS/1% pen-strep. After collection cells were kept on ice throughout the whole experimental procedure and propidium iodide was added (final concentration: 69 μ M). Incorporated propidium iodide was measured in the FL-3 channel by FACS using the FACScalibur (Becton Dickinson) operated by the Cell Quest Pro software. Later analysis was performed by using the FlowJo software. The experiment was performed in triplicates. The mean values are depicted; error bars represent standard error of mean.

6.2.4.3 β -galactosidase assay

Cells were grown in a 6 well plate dish until reaching 70-90% confluency. After washing the cells three times with PBS, 3% formaldehyde/1x PBS was added for fixation. To remove the formaldehyde, cells were again washed twice with 1x PBS. Staining solution was applied for two hours at 37°C and images were taken using 20x bright field (spinning disc microscope). β -galactosidase positive and negative cells were counted. The

experiment was performed in triplicates. The mean value is displayed in the graph, the error bars indicate the standard error of mean. As a positive control cells were treated with 0.2 μM doxorubicin for 7 days. Most cells treated with doxorubicin were β -galactosidase positive.

6.2.4.4 DNA content measurements using fluorescence activated cell sorting (FACS)

Cells were grown for three days after splitting in a 10 cm dish to 70-80% confluence and collected by trypsination. After gentle centrifugation cells were resuspended in 70% ice cold ethanol and fixed for 20 min. Afterwards, cells were centrifuged, then washed with 1x PBS and finally resuspended in propidium iodide solution (69 μM propidium iodide and 100 $\mu\text{g/ml}$ RNase in 38 mM sodium citrate). Samples were measured using the FL-2 or FL-3 channel by FACS analysis (FACScalibur (Becton Dickinson) controlled by the Cell Quest Pro software. FACS profiles were later evaluated by FlowJo software and graphs were generated using the Prism software. The experiment was conducted in triplicates. Cell lines with extra chromosome were always compared to their parental cell lines which were grown in parallel. All experiments were performed in three biological replicates; the error bars represent the standard error. Unpaired *T*-test was used to evaluate the statistical significance.

6.2.4.5 Thymidine release

For thymidine release experiment 1×10^6 cells were seeded on a 6 cm dish. After attachment of the cells the medium was exchanged to medium containing 2 mM thymidine. After 30 h cells were released from the thymidine block by washing 3x with PBS. Cell culture medium was added and cells were incubated at 37°C and 5% CO_2 . For the time course samples were taken every hour. Samples were measured as described for the DNA content measurement by FACS. Gained profiles were later evaluated by fitting the curve to the Watson model included in the FlowJo software. As a parameter to calculate the length of each phase, the distance between the time where 50% of the cells reach the corresponding DNA content was calculated.

6.2.4.6 Live cell imaging

HCT116 H2B-GFP and HCT116 H2B-GFP 5/4 cell lines were seeded sparsely on a 6 channel μ -slide (Ibidi, Martinsried, Germany). 24 h after seeding time laps imaging was started in a 10 min (for time in interphase) or 4 min (for time in mitosis) interval for 72 or

48 h, respectively. Therefore, the slide was placed onto the sample stage of the live cell imaging microscope (using the incubator chamber maintained at a 37°C, 40% humidity, in an atmosphere of 5% CO₂). Images were taken by the 20× air objective. The microscope was controlled by Metamorph software. Later evaluation of images was conducted using the ImageJ software. Time in interphase was measured from first observed nuclear envelope breakdown (NEB) to the second observed NEB. Time in mitosis was measured from NEB to the onset of anaphase (OA). Experiment was carried out in biological triplicates. Graphs were generated with Prism. Mean values are indicated in the graph; error bars indicate the standard error of mean.

6.2.5 Autophagy and proteasome studies

6.2.5.1 Proteasome activity assay

In parallel 2x10⁴ trypsinized and washed HCT116, HCT116 3/3 and HCT116 5/4 were seeded in triplicates on a 96 well plate. 40 min later Proteasome-Glo™ Chymotrypsin-Like Cell-Based Assay (Promega) was added according to manufacturer's protocol. Luminescence was detected using a Fluoroskan Ascent FL plate reader operated by the Ascent software. Experiment was conducted three times. For evaluation the mean with SEM of the biological triplicates was calculated and depicted using Prism software. Unpaired *T*-test was used to calculate significances.

6.2.5.2 Immunofluorescence experiments

Cells were seeded on glass objectives or ibidi 8 well slides and cultivated for two days to 50-70% confluency. Cells were washed with 1x PBS-T and fixed by 3.7% paraformaldehyde. Fixed cells were washed twice with PBS and permeabilized with 0.5% Triton X-100 in PBS. Then cells were blocked in 2% BSA in PBS-T and afterwards stained with anti-LC3 (1:100), anti-p62 (1:100) or anti-ubiquitin (1:50) antibodies. After staining with primary antibody cells were again washed three times with 1x PBS-T. The fluorescent secondary antibodies: anti-mouse dylight649, anti-guinea pig dylight649, anti-mouse FITC and anti-guinea pig dylight649 were applied (1:1000) for one hour at room temperature. Cells were washed three times with PBS-T, counterstained with 50 ng/ml DAPI in PBS-T and washed once with PBS-T. If glass objectives were used objective was mounted on glass slides using Vecta shield. Cells seeded on ibidi slides were imaged through PBS-T supplemented with sodium azide (0.1%) to avoid bacterial growth. For amplification of the signal autophagy of some cells was additionally inhibited to allow accumulation of p62 and ubiquitin. Therefore, cells were treated for 16-18 hours before fixation with 50 nM bafilomycin A1.

For LC3 immunofluorescence intensity analysis images were analyzed using the Slidebook software. The background of each image was identified and subtracted. To allow comparison levels were adjusted equally for all analyzed samples. Cells were marked as objects and then fluorescence mean intensity of the identified objects were used for evaluation. Graph was generated using the Prism software. Mean with SEM is shown in the graph. Significance was calculated by unpaired *T*-test.

To evaluate the p62 mean intensity/cell the cell profiler software was used. Therefore, the cell cytoplasm was additionally stained by HCS cell mask red dye (Invitrogen) before fixation to allow proper automated cell segmentation. Then, the mean intensity of p62/cell was analyzed automated by the software. Given values were plotted by using the Prism software. Mean is depicted in the graph, error bars indicate the SD. Unpaired *T*-test was conducted to test for significance.

To evaluate p62 and ubiquitin co-localization cells were stained with p62 and anti-ubiquitin. To compare images, the background was subtracted and fluorescence intensity levels were adjusted equally for each image. Line intensities were evaluated using the “line intensity” tool of the Slidebook software. To allow in parallel comparison of ubiquitin and p62 signal, the ubiquitin signal intensity of all images was multiplied by the factor 40 since ubiquitin signals were in general low.

6.2.5.3 Autophagy flux assay

HCT116, HCT116 3/3 and HCT116 5/4 cell lines were seeded one day before transfection and grown to 40% confluency. Then, the ptfLC3 plasmid (mRFG-GFP-LC3,) was transfected using Lipofectamin LTX and plus reagent as described before. Cells were fixed two days later when mRFP-GFP-LC3 was fully expressed and images were taken by spinning disc microscopy. Images were taken by 100x oil objective applying the 561 nm (mRFP) and 473 nm (GFP) lasers. Due to transient transfection levels differ in every cell. Therefore, fluorescence levels of cells were individually adjusted.

6.2.5.4 Evaluation of cell survival after autophagy inhibition

HCT116-derived cell lines were seeded the day before the experiment on a 96 well plate. Shortly, before the experiment was started cells were treated with the autophagy inhibiting drugs bafilomycin and chloroquine to test if aneuploid cell lines are more sensitive towards the drugs than their disomic counterparts. To all cells treated with bafilomycin a concentration of 5 nM was applied. Chloroquine was added in a concentration of 10 μ M for HCT116 H2B-GFP and HCT116 H2B-GFP 5/4 and 50 μ M for

HCT116, HCT116 5/4 and HCT116 3/3, as a 10 μ M concentration was too low for cell death studies. After treatment, the 96 well plate was mounted on the live cell imaging microscope. Time laps imaging was started imaging in bright field in a 10 min interval for at least 52 h. Then, movies were evaluated by Slidebook software, monitoring the time of cell death. Survival curves were generated by Excel software.

6.2.5.4 Evaluation of time in interphase after p62 knockdown

HCT116-derived cell lines were seeded three days before the experiment on a 6 well plate. One day later, when cells were around 30-50% confluent they were transfected with p62 and scrambled siRNA by Oligofectamin as described above. Then, one day later, cells were seeded on a 6 well plate for western blot analysis and on an 8 well ibidi slide for live cell imaging. One day after seeding, cells for western blot were collected and lysed and 8 well ibidi slide was mounted on the live cell imaging microscope for time lapse imaging in a humidified 37°C chamber in 10 min intervals. Movies were evaluated using the slidebook software. Cells were tracked and time in interphase was evaluated by monitoring the time from the first observed nuclear envelope breakdown (NEB) to the second NEB. Data was evaluated by the Prism software. An unpaired *T*-test was performed to evaluate significances. Time in interphase of cells with p62 knockdown was not significantly altered compared to cells treated with scrambled siRNA.

6.2.6 Experimental setup for genome, transcriptome and proteome analysis

6.2.6.1 Array comparative genomic hybridization (CGH)

Genomic DNA (gDNA) for arrayCGH (aCGH) analysis was extracted from 70-80% confluent cells after trypsinization and pelleting using the Qiagen Genra Puregene Kit following manufacturer's instructions. gDNA quality and quantity was measured by DNA absorbance and 260nm/280nm ratio measured by NanoDrop spectral photometer. gDNA quality was also tested on a 1.0% agarose gel stained with ethidium bromide. 1 μ g of gDNA was used for each aCGH analysis. The genomic DNA was sent to IMGm laboratories, Martinsried, Germany, who performed the aCGH experiment. As a reference sample commercially available human gDNA (Promega) was used for all 4x44K array based analyses (conducted with gDNA extracted from HCT116, HCT116 3/3, HCT116 5/4, HCT116 H2B-GFP 5/3, HCT116 H2B-GFP 5/4). aCGH analysis from gDNA of the cell line RPE1 H2B-GFP 21/3 was carried out by SurePrint 4x180K G3 Human CGH Microarray. gDNA of HCT116 and HCT116 5/4 cell lines were used for the high density CGH analysis in direct comparison using the 2x400K array.

6.2.6.2 mRNA array

mRNA was extracted from 70-80% confluent cells after trypsinization and pelleting using the Qiagen mRNAeasy mini kit. mRNA array analysis was performed in biological triplicates. mRNA array was carried out by IMG laboratories. mRNA quality and quantity was identified by NanoDrop spectral photometer. mRNA quality was also tested on a 1.0% agarose gel stained with ethidium bromide. 500 ng of total RNA was used for the experiment according to IMG laboratories standard protocol. Agilent Whole Human Genome Oligo Microarrays (4x44K format) were used for experiments in combination with a One-Color based hybridization protocol. Microarray signals were detected using the Agilent DNA Microarray Scanner. Finally, raw data was quantile normalized.

6.2.6.3 SILAC labeling

DMEM lacking arginine and lysine with 10% dialyzed FBS with a cutoff of 10 kDa and 1% pen-strep was used as a basis medium. For labeling, arginine and lysine were added either as light (Arg0; Lys0) or as heavy (Arg10; Lys8) isotope (final concentration: 33.6 µg/ml for arginine and 73 µg/ml for lysine). RPE1 and HCT116 cells were grown in heavy (Arg10; Lys8) SILAC medium for 8 to 10 passages. Aneuploid cell lines were grown for 3-4 passages in light (Arg0; Lys0) medium. For the SILAC analysis after autophagy inhibition (description see below) a SuperSILAC mix experiment was conducted labeling HCT116 treated and untreated with bafilomycin with light, medium (Arg6 and LysD4) and heavy isotopes.

HCT116, HCT116 5/4, HCT116 H2B-GFP 5/4, HCT116 H2B-GFP 5/3, HCT116 3/3 and all RPE-1 derived cell lines were conducted as double labeling experiments. HCT116 and HCT116 5/4 labeling was performed in biological triplicates including 6 measurements with one of them as label switch experiment, to exclude that observed phenotypes are due to labeling side effects. SILAC experiments with RPE-1 derived cell lines were also conducted as biological triplicates.

6.2.6.4 SILAC analysis after autophagy inhibition

Cells were labeled for 7 passages in light, medium and heavy SILAC medium. 30 h before cell collection 10 nM bafilomycin was added to inhibit autophagy. Treated as well as untreated HCT116 and HCT116 5/4 cell lines were labeled in light, medium and heavy medium. Then, a SuperSILAC mix (Geiger, Cox et al. 2010) was generated by mixing all medium labeled conditions. Then, equal protein amounts of the SuperSILAC mix (medium label), the untreated cells and the treated cells were mixed. To compare all conditions directly with each other, the SuperSILAC mix serves as an internal standard.

6.2.6.5 Sample processing for SILAC experiments

Labeled cells were collected by trypsinization and washed twice with PBS. After collection cells were kept on ice. After washing cell pellet was stored at -80°C. Sample processing after collection and data analysis of Mass spectrometry data was conducted by Gabriele Stoehr. For detailed information see experimental procedures of this published data (Stingele, Stoehr et al. 2012).

6.2.7 Analysis of genome, transcriptome and proteome data

Processing of DNA, mRNA and protein raw data as well as generation of 2-D annotations, boxplots of categories and density distribution graphs were performed by Gabriele Stoehr.

6.2.7.1 Analysis of CGH data

To subtract the background the raw values of CGH signal ("r BGSubSignal") from HCT116 and cell lines with extra chromosome were divided by their control background signal ("g BGSubSignal"). Then, ratios of ratios between the signal of cell lines with extra chromosome and their corresponding parental cell line were calculated. These values were afterwards converted into log₂ ratios. The median of the whole population was subtracted to allow centering around zero.

6.2.7.2 Analysis of the mRNA data

mRNA array analysis were performed in biological triplicates. Ratios were transformed in log₂ values and then the triplicates were averaged using their median. The value of HCT116 was subtracted from the values of HCT116 5/4.

6.2.7.3 Analysis of protein data

First, the protein list output file was filtered for contaminants and reverse entries. Ratios were transformed in log₂ values. For technical replicates median values were calculated. Then, median ratios for the biological replicas of the HCT116 5/4 experiments were calculated. Only median ratios derived from at least two biological replicas were taken for further analyses. For the other cell lines with extra chromosome, normalized protein ratios were used. SuperSILAC HCT116 and bafilomycin treated samples were filtered as

described for HCT116 5/4. Median ratios obtained based on the SuperSILAC mix were calculated and used for further analyses.

6.2.7.4 Combination of the pre-processed DNA, mRNA and protein results

All described CGH and mRNA log₂ entries were matched to their corresponding protein entries (median values). CGH data and protein data were combined by their chromosomal location (position information from Ensembl (<http://www.ensembl.org/index.html>)). mRNA and protein data were combined using specific “Probe set” names and their corresponding Uniprot entries. Cell line HCT116 5/4 contains parts of chromosome 5 at level as expected for diploid cell lines. These parts were removed from the analysis. Therefore, thresholds to remove data from analysis were set at 0.65 and 0.6 for HCT116 5/4 and HCT116 H2B-GFP 5/4.

6.2.7.5 Two-dimensional (2-D) annotation analysis

Significant regulations of categorical annotations between two different cell lines were analyzed using a 2-D annotation distribution analysis (Geiger, Cox et al. 2010). For analysis, Gene Ontology (GO) biological processes (GOBP), molecular functions (GOMF) and cellular components (GOCC), KEGG pathways, proteins within complexes (CORUM) and chromosomes have been taken into account. To test, whether the expression of proteins of a given category is significantly different from the remaining population a non-parametric two-sided Wilcoxon-Mann-Whitney test was applied, using Benjamini-Hochberg false discovery rate (threshold 2%) for multiple hypothesis testing. The algorithm calculates relative regulation values between -1 and 1 for each significant category.

6.2.7.6 Density histograms for different populations

Density histograms were generated by using the R software. Interesting populations were plotted in one figure using the *density* function. Median ratios of the subpopulation and numbers of the populations are depicted within the plots. Proteins that are a subunit of a complex were extracted applying the CORUM database (<http://mips.helmholtz-muenchen.de/genre/proj/corum/>). The subpopulation *Kinase Activity* was extracted from the GOMF terms (entries: “kinase activity”). Relative protein abundance of single proteins is depicted below the graph with black vertical lines.

6.2.7.7 Detailed analysis of kinases and complexes

Complex proteins as well as proteins with kinase activity from the HCT116 5/4 data were extracted as described above.

For complex analysis, complexes that contain at least one protein and corresponding mRNA and DNA entries coded on the tetrasomic chromosome 5 were analyzed. Depicted are all analyzed complexes with at least 5 total protein entries of subunits.

To compare all kinases encoded on chromosome 5, all DNA, mRNA and kinase entries that are present in 4 DNA copies were plotted. Scatter plots of DNA, mRNA and proteins were generated by the Prism Software. Medians with their interquartile range were calculated by the Prism software.

6.2.7.8 Boxplot analysis

For boxplot analysis the category GOBP autophagy or KEGG proteasome were extracted from dataset. Then, the ratios between different cell lines with extra chromosome were compared by using the *geom_boxplot* function from the R package ggplot2. The median of the population is depicted as black line. The 25% and 75% quantiles are depicted in the graph.

7 REFERENCES

- Akerfelt, M., R. I. Morimoto, et al. "Heat shock factors: integrators of cell stress, development and lifespan." *Nat Rev Mol Cell Biol* **11**(8): 545-555.
- Akhtar, A. and P. B. Becker (2000). "Activation of transcription through histone H4 acetylation by MOF, an acetyltransferase essential for dosage compensation in *Drosophila*." *Mol Cell* **5**(2): 367-375.
- Alves-Rodrigues, A., L. Gregori, et al. (1998). "Ubiquitin, cellular inclusions and their role in neurodegeneration." *Trends Neurosci* **21**(12): 516-520.
- Amano, K., H. Sago, et al. (2004). "Dosage-dependent over-expression of genes in the trisomic region of Ts1Cje mouse model for Down syndrome." *Hum Mol Genet* **13**(13): 1333-1340.
- Amerik, A. Y. and M. Hochstrasser (2004). "Mechanism and function of deubiquitinating enzymes." *Biochim Biophys Acta* **1695**(1-3): 189-207.
- Asher, G., N. Reuven, et al. (2006). "20S proteasomes and protein degradation "by default"." *Bioessays* **28**(8): 844-849.
- Backer, J. M. and J. F. Dice (1986). "Covalent linkage of ribonuclease S-peptide to microinjected proteins causes their intracellular degradation to be enhanced during serum withdrawal." *Proc Natl Acad Sci U S A* **83**(16): 5830-5834.
- Baker, D. J., K. B. Jeganathan, et al. (2006). "Early aging-associated phenotypes in Bub3/Rae1 haploinsufficient mice." *The Journal of cell biology* **172**(4): 529-540.
- Balch, W. E., R. I. Morimoto, et al. (2008). "Adapting proteostasis for disease intervention." *Science* **319**(5865): 916-919.
- Barber, T. D., K. McManus, et al. (2008). "Chromatid cohesion defects may underlie chromosome instability in human colorectal cancers." *Proc Natl Acad Sci U S A* **105**(9): 3443-3448.
- Behrends, C., C. A. Langer, et al. (2006). "Chaperonin TRiC promotes the assembly of polyQ expansion proteins into nontoxic oligomers." *Mol Cell* **23**(6): 887-897.
- Belote, J. M. and J. C. Lucchesi (1980). "Control of X chromosome transcription by the maleless gene in *Drosophila*." *Nature* **285**(5766): 573-575.
- Beroukhim, R., C. H. Mermel, et al. (2010). "The landscape of somatic copy-number alteration across human cancers." *Nature* **463**(7283): 899-905.
- Birchler, J. A. (2010). "Reflections on studies of gene expression in aneuploids." *Biochem J* **426**(2): 119-123.
- Birchler, J. A., U. Bhadra, et al. (2001). "Dosage-dependent gene regulation in multicellular eukaryotes: implications for dosage compensation, aneuploid syndromes, and quantitative traits." *Dev Biol* **234**(2): 275-288.
- Birchler, J. A. and K. J. Newton (1981). "Modulation of protein levels in chromosomal dosage series of maize: the biochemical basis of aneuploid syndromes." *Genetics* **99**(2): 247-266.

7 REFERENCES

- Bjorkoy, G., T. Lamark, et al. (2005). "p62/SQSTM1 forms protein aggregates degraded by autophagy and has a protective effect on huntingtin-induced cell death." *J Cell Biol* **171**(4): 603-614.
- Borodovsky, A., B. M. Kessler, et al. (2001). "A novel active site-directed probe specific for deubiquitylating enzymes reveals proteasome association of USP14." *EMBO J* **20**(18): 5187-5196.
- Bossy-Wetzel, E., R. Schwarzenbacher, et al. (2004). "Molecular pathways to neurodegeneration." *Nature medicine* **10 Suppl**: S2-9.
- Boveri, T. (1912). "Anton Dohbn." *Science* **36**(928): 453-468.
- Buchler, N. E., U. Gerland, et al. (2005). "Nonlinear protein degradation and the function of genetic circuits." *Proc Natl Acad Sci U S A* **102**(27): 9559-9564.
- Cahill, D. P., C. Lengauer, et al. (1998). "Mutations of mitotic checkpoint genes in human cancers." *Nature* **392**(6673): 300-303.
- Carter, S. L., K. Cibulskis, et al. (2012). "Absolute quantification of somatic DNA alterations in human cancer." *Nat Biotechnol* **30**(5): 413-421.
- Chiang, H. L., S. R. Terlecky, et al. (1989). "A role for a 70-kilodalton heat shock protein in lysosomal degradation of intracellular proteins." *Science* **246**(4928): 382-385.
- Chiti, F., M. Stefani, et al. (2003). "Rationalization of the effects of mutations on peptide and protein aggregation rates." *Nature* **424**(6950): 805-808.
- Choi, C. M., K. W. Seo, et al. (2009). "Chromosomal instability is a risk factor for poor prognosis of adenocarcinoma of the lung: Fluorescence in situ hybridization analysis of paraffin-embedded tissue from Korean patients." *Lung Cancer* **64**(1): 66-70.
- Ciechanover, A. (2005). "Proteolysis: from the lysosome to ubiquitin and the proteasome." *Nature reviews. Molecular cell biology* **6**(1): 79-87.
- Cimini, D. (2008). "Merotelic kinetochore orientation, aneuploidy, and cancer." *Biochimica et biophysica acta* **1786**(1): 32-40.
- Cimini, D., B. Howell, et al. (2001). "Merotelic kinetochore orientation is a major mechanism of aneuploidy in mitotic mammalian tissue cells." *The Journal of cell biology* **153**(3): 517-527.
- Clague, M. J. and S. Urbe (2010). "Ubiquitin: same molecule, different degradation pathways." *Cell* **143**(5): 682-685.
- Coenen, S., B. Pickering, et al. (2005). "The relevance of sequence insertions in the Mcl-1 promoter in chronic lymphocytic leukemia and in normal cells." *Haematologica* **90**(9): 1285-1286.
- Corton, J. M., J. G. Gillespie, et al. (1995). "5-aminoimidazole-4-carboxamide ribonucleoside. A specific method for activating AMP-activated protein kinase in intact cells?" *Eur J Biochem* **229**(2): 558-565.
- Cox, J. and M. Mann (2008). "MaxQuant enables high peptide identification rates, individualized p.p.b.-range mass accuracies and proteome-wide protein quantification." *Nat Biotechnol* **26**(12): 1367-1372.
- Cox, J. and M. Mann (2012). "1D and 2D annotation enrichment: a statistical method integrating quantitative proteomics with complementary high-throughput data." *BMC Bioinformatics* **13 Suppl 16**: S12.

7 REFERENCES

- Crasta, K., N. J. Ganem, et al. (2012). "DNA breaks and chromosome pulverization from errors in mitosis." Nature **482**(7383): 53-58.
- Cuervo, A. M. and J. F. Dice (1996). "A receptor for the selective uptake and degradation of proteins by lysosomes." Science **273**(5274): 501-503.
- Cuervo, A. M., E. Knecht, et al. (1995). "Activation of a selective pathway of lysosomal proteolysis in rat liver by prolonged starvation." Am J Physiol **269**(5 Pt 1): C1200-1208.
- Dai, W., Q. Wang, et al. (2004). "Slippage of mitotic arrest and enhanced tumor development in mice with BubR1 haploinsufficiency." Cancer research **64**(2): 440-445.
- de Godoy, L. M., J. V. Olsen, et al. (2008). "Comprehensive mass-spectrometry-based proteome quantification of haploid versus diploid yeast." Nature **455**(7217): 1251-1254.
- Devlin, R. H., D. G. Holm, et al. (1982). "Autosomal dosage compensation *Drosophila melanogaster* strains trisomic for the left arm of chromosome 2." Proc Natl Acad Sci U S A **79**(4): 1200-1204.
- Dice, J. F. (2007). "Chaperone-mediated autophagy." Autophagy **3**(4): 295-299.
- Dimri, G. P., X. Lee, et al. (1995). "A biomarker that identifies senescent human cells in culture and in aging skin in vivo." Proc Natl Acad Sci U S A **92**(20): 9363-9367.
- Dobles, M., V. Liberal, et al. (2000). "Chromosome missegregation and apoptosis in mice lacking the mitotic checkpoint protein Mad2." Cell **101**(6): 635-645.
- Dorsey, F. C., K. L. Rose, et al. (2009). "Mapping the phosphorylation sites of Utk1." J Proteome Res **8**(11): 5253-5263.
- Douglas, P. M. and A. Dillin (2010). "Protein homeostasis and aging in neurodegeneration." J Cell Biol **190**(5): 719-729.
- Douglas, P. M., S. Treusch, et al. (2008). "Chaperone-dependent amyloid assembly protects cells from prion toxicity." Proc Natl Acad Sci U S A **105**(20): 7206-7211.
- Drummond, D. A. and C. O. Wilke (2008). "Mistranslation-induced protein misfolding as a dominant constraint on coding-sequence evolution." Cell **134**(2): 341-352.
- Duesberg, P., R. Li, et al. (2006). "Aneuploidy and cancer: from correlation to causation." Contrib Microbiol **13**: 16-44.
- Ellgaard, L. and A. Helenius (2003). "Quality control in the endoplasmic reticulum." Nature reviews. Molecular cell biology **4**(3): 181-191.
- Elliott, F.C. (1958). "Plant breeding and cytogenetics." McGraw Hill Book Company, Inc. NY
- Ellis, R. J., S. M. van der Vies, et al. (1989). "The molecular chaperone concept." Biochemical Society symposium **55**: 145-153.
- Escot, C., C. Theillet, et al. (1986). "Genetic alteration of the c-myc protooncogene (MYC) in human primary breast carcinomas." Proc Natl Acad Sci U S A **83**(13): 4834-4838.
- Ettwiller, L. and R. A. Veitia (2007). "Protein coevolution and isoexpression in yeast macromolecular complexes." Comp Funct Genomics: 58721.

7 REFERENCES

- Fournier, R. E. (1981). "A general high-efficiency procedure for production of microcell hybrids." *Proc Natl Acad Sci U S A* **78**(10): 6349-6353.
- Fujiwara, T., M. Bandi, et al. (2005). "Cytokinesis failure generating tetraploids promotes tumorigenesis in p53-null cells." *Nature* **437**(7061): 1043-1047.
- Ganem, N. J., S. A. Godinho, et al. (2009). "A mechanism linking extra centrosomes to chromosomal instability." *Nature* **460**(7252): 278-282.
- Gao, C., K. Furge, et al. (2007). "Chromosome instability, chromosome transcriptome, and clonal evolution of tumor cell populations." *Proc Natl Acad Sci U S A* **104**(21): 8995-9000.
- Ge, X. Q. and J. J. Blow (2009). "The licensing checkpoint opens up." *Cell Cycle* **8**(15): 2320-2322.
- Gebauer, F. and M. W. Hentze (2004). "Molecular mechanisms of translational control." *Nature reviews. Molecular cell biology* **5**(10): 827-835.
- Geiger, T., J. Cox, et al. (2010). "Proteomic changes resulting from gene copy number variations in cancer cells." *PLoS Genet* **6**(9).
- Geiger, T., J. Cox, et al. (2010). "Super-SILAC mix for quantitative proteomics of human tumor tissue." *Nat Methods* **7**(5): 383-385.
- Gidalevitz, T., A. Ben-Zvi, et al. (2006). "Progressive disruption of cellular protein folding in models of polyglutamine diseases." *Science* **311**(5766): 1471-1474.
- Gidalevitz, T., T. Krupinski, et al. (2009). "Destabilizing protein polymorphisms in the genetic background direct phenotypic expression of mutant SOD1 toxicity." *PLoS Genet* **5**(3): e1000399.
- Glenner, G. G. and C. W. Wong (1984). "Alzheimer's disease and Down's syndrome: sharing of a unique cerebrovascular amyloid fibril protein." *Biochem Biophys Res Commun* **122**(3): 1131-1135.
- Glickman, M. H. and A. Ciechanover (2002). "The ubiquitin-proteasome proteolytic pathway: destruction for the sake of construction." *Physiol Rev* **82**(2): 373-428.
- Guacci, V., D. Koshland, et al. (1997). "A direct link between sister chromatid cohesion and chromosome condensation revealed through the analysis of MCD1 in *S. cerevisiae*." *Cell* **91**(1): 47-57.
- Guidotti, J. E., O. Bregerie, et al. (2003). "Liver cell polyploidization: a pivotal role for binuclear hepatocytes." *The Journal of biological chemistry* **278**(21): 19095-19101.
- Guo, M. and J. A. Birchler (1994). "Trans-acting dosage effects on the expression of model gene systems in maize aneuploids." *Science* **266**(5193): 1999-2002.
- Guterman, A. and M. H. Glickman (2004). "Complementary roles for Rpn11 and Ubp6 in deubiquitination and proteolysis by the proteasome." *J Biol Chem* **279**(3): 1729-1738.
- Gutierrez, M. G., D. B. Munafo, et al. (2004). "Rab7 is required for the normal progression of the autophagic pathway in mammalian cells." *Journal of cell science* **117**(Pt 13): 2687-2697.
- Hara, T., K. Nakamura, et al. (2006). "Suppression of basal autophagy in neural cells causes neurodegenerative disease in mice." *Nature* **441**(7095): 885-889.

7 REFERENCES

- Harris, H. and D. C. Rubinsztein (2012). "Control of autophagy as a therapy for neurodegenerative disease." *Nat Rev Neurol* **8**(2): 108-117.
- Haugen, A. C., A. Goel, et al. (2008). "Genetic instability caused by loss of MutS homologue 3 in human colorectal cancer." *Cancer Res* **68**(20): 8465-8472.
- Hayashi-Nishino, M., N. Fujita, et al. (2009). "A subdomain of the endoplasmic reticulum forms a cradle for autophagosome formation." *Nature cell biology* **11**(12): 1433-1437.
- Hernando, E., Z. Nahle, et al. (2004). "Rb inactivation promotes genomic instability by uncoupling cell cycle progression from mitotic control." *Nature* **430**(7001): 797-802.
- Hershko, A. and A. Ciechanover (1998). "The ubiquitin system." *Annu Rev Biochem* **67**: 425-479.
- Hicke, L. and R. Dunn (2003). "Regulation of membrane protein transport by ubiquitin and ubiquitin-binding proteins." *Annual review of cell and developmental biology* **19**: 141-172.
- Hochstrasser, M. (1996). "Ubiquitin-dependent protein degradation." *Annu Rev Genet* **30**: 405-439.
- Hochstrasser, M. (2009). "Origin and function of ubiquitin-like proteins." *Nature* **458**(7237): 422-429.
- Hodgkin, J. (2005). "Karyotype, ploidy, and gene dosage." *WormBook*: 1-9.
- Hodgkin, J., H. R. Horvitz, et al. (1979). "Nondisjunction Mutants of the Nematode CAENORHABDITIS ELEGANS." *Genetics* **91**(1): 67-94.
- Hoegel, C., B. Pfander, et al. (2002). "RAD6-dependent DNA repair is linked to modification of PCNA by ubiquitin and SUMO." *Nature* **419**(6903): 135-141.
- Hoeller, D. and I. Dikic (2009). "Targeting the ubiquitin system in cancer therapy." *Nature* **458**(7237): 438-444.
- Holland, A. J. and D. W. Cleveland (2009). "Boveri revisited: chromosomal instability, aneuploidy and tumorigenesis." *Nature reviews. Molecular cell biology* **10**(7): 478-487.
- Holland, A. J. and D. W. Cleveland (2012). "Losing balance: the origin and impact of aneuploidy in cancer." *EMBO Rep* **13**(6): 501-514.
- Hosokawa, N., T. Hara, et al. (2009). "Nutrient-dependent mTORC1 association with the ULK1-Atg13-FIP200 complex required for autophagy." *Molecular biology of the cell* **20**(7): 1981-1991.
- Huang, D. and D. Koshland (2003). "Chromosome integrity in *Saccharomyces cerevisiae*: the interplay of DNA replication initiation factors, elongation factors, and origins." *Genes & development* **17**(14): 1741-1754.
- Hurtley, S. M., D. G. Bole, et al. (1989). "Interactions of misfolded influenza virus hemagglutinin with binding protein (BiP)." *The Journal of cell biology* **108**(6): 2117-2126.
- Itakura, E., C. Kishi, et al. (2008). "Beclin 1 forms two distinct phosphatidylinositol 3-kinase complexes with mammalian Atg14 and UVRAG." *Molecular biology of the cell* **19**(12): 5360-5372.
- Iwata, A., B. E. Riley, et al. (2005). "HDAC6 and microtubules are required for autophagic degradation of aggregated huntingtin." *J Biol Chem* **280**(48): 40282-40292.

7 REFERENCES

- Jansen, R., D. Greenbaum, et al. (2002). "Relating whole-genome expression data with protein-protein interactions." Genome Res **12**(1): 37-46.
- Jeganathan, K., L. Malureanu, et al. (2007). "Bub1 mediates cell death in response to chromosome missegregation and acts to suppress spontaneous tumorigenesis." The Journal of cell biology **179**(2): 255-267.
- Jiang, X. R., G. Jimenez, et al. (1999). "Telomerase expression in human somatic cells does not induce changes associated with a transformed phenotype." Nat Genet **21**(1): 111-114.
- Johansen, T. and T. Lamark "Selective autophagy mediated by autophagic adapter proteins." Autophagy **7**(3): 279-296.
- Jung, C. H., C. B. Jun, et al. (2009). "ULK-Atg13-FIP200 complexes mediate mTOR signaling to the autophagy machinery." Molecular biology of the cell **20**(7): 1992-2003.
- Kahlem, P., M. Sultan, et al. (2004). "Transcript level alterations reflect gene dosage effects across multiple tissues in a mouse model of down syndrome." Genome research **14**(7): 1258-1267.
- Kalitsis, P., E. Earle, et al. (2000). "Bub3 gene disruption in mice reveals essential mitotic spindle checkpoint function during early embryogenesis." Genes Dev **14**(18): 2277-2282.
- Kaufman, M. H. (1991). "New insights into triploidy and tetraploidy, from an analysis of model systems for these conditions." Human reproduction **6**(1): 8-16.
- Kaushik, S., U. Bandyopadhyay, et al. "Chaperone-mediated autophagy at a glance." J Cell Sci **124**(Pt 4): 495-499.
- Kiffin, R., C. Christian, et al. (2004). "Activation of chaperone-mediated autophagy during oxidative stress." Mol Biol Cell **15**(11): 4829-4840.
- Kim, P. K., D. W. Hailey, et al. (2008). "Ubiquitin signals autophagic degradation of cytosolic proteins and peroxisomes." Proc Natl Acad Sci U S A **105**(52): 20567-20574.
- Kimura, S., T. Noda, et al. (2007). "Dissection of the autophagosome maturation process by a novel reporter protein, tandem fluorescent-tagged LC3." Autophagy **3**(5): 452-460.
- Kirkin, V., T. Lamark, et al. (2009). "A role for NBR1 in autophagosomal degradation of ubiquitinated substrates." Mol Cell **33**(4): 505-516.
- Kirkin, V., D. G. McEwan, et al. (2009). "A role for ubiquitin in selective autophagy." Mol Cell **34**(3): 259-269.
- Klionsky, D. J., H. Abeliovich, et al. (2008). "Guidelines for the use and interpretation of assays for monitoring autophagy in higher eukaryotes." Autophagy **4**(2): 151-175.
- Klionsky, D. J., J. M. Cregg, et al. (2003). "A unified nomenclature for yeast autophagy-related genes." Dev Cell **5**(4): 539-545.
- Koi, M., A. Umar, et al. (1994). "Human chromosome 3 corrects mismatch repair deficiency and microsatellite instability and reduces N-methyl-N'-nitro-N-nitrosoguanidine tolerance in colon tumor cells with homozygous hMLH1 mutation." Cancer Res **54**(16): 4308-4312.
- Komatsu, M., S. Waguri, et al. (2006). "Loss of autophagy in the central nervous system causes neurodegeneration in mice." Nature **441**(7095): 880-884.

7 REFERENCES

- Komatsu, M., S. Waguri, et al. (2007). "Homeostatic levels of p62 control cytoplasmic inclusion body formation in autophagy-deficient mice." *Cell* **131**(6): 1149-1163.
- Kuusisto, E., T. Kauppinen, et al. (2008). "Use of p62/SQSTM1 antibodies for neuropathological diagnosis." *Neuropathol Appl Neurobiol* **34**(2): 169-180.
- Kuusisto, E., A. Salminen, et al. (2001). "Ubiquitin-binding protein p62 is present in neuronal and glial inclusions in human tauopathies and synucleinopathies." *Neuroreport* **12**(10): 2085-2090.
- Kuusisto, E., A. Salminen, et al. (2002). "Early accumulation of p62 in neurofibrillary tangles in Alzheimer's disease: possible role in tangle formation." *Neuropathol Appl Neurobiol* **28**(3): 228-237.
- Lamark, T., M. Perander, et al. (2003). "Interaction codes within the family of mammalian Phox and Bem1p domain-containing proteins." *J Biol Chem* **278**(36): 34568-34581.
- Lee, B. H., M. J. Lee, et al. (2010). "Enhancement of proteasome activity by a small-molecule inhibitor of USP14." *Nature* **467**(7312): 179-184.
- Leggett, D. S., J. Hanna, et al. (2002). "Multiple associated proteins regulate proteasome structure and function." *Mol Cell* **10**(3): 495-507.
- Lengauer, C., K. W. Kinzler, et al. (1997). "Genetic instability in colorectal cancers." *Nature* **386**(6625): 623-627.
- Li, R., G. Yerganian, et al. (1997). "Aneuploidy correlated 100% with chemical transformation of Chinese hamster cells." *Proc Natl Acad Sci U S A* **94**(26): 14506-14511.
- Lindquist, S. and E. A. Craig (1988). "The heat-shock proteins." *Annu Rev Genet* **22**: 631-677.
- Lindsley, D. L., L. Sandler, et al. (1972). "Segmental aneuploidy and the genetic gross structure of the Drosophila genome." *Genetics* **71**(1): 157-184.
- Lingle, W. L., S. L. Barrett, et al. (2002). "Centrosome amplification drives chromosomal instability in breast tumor development." *Proceedings of the National Academy of Sciences of the United States of America* **99**(4): 1978-1983.
- Lister, L. M., A. Kouznetsova, et al. (2010). "Age-related meiotic segregation errors in mammalian oocytes are preceded by depletion of cohesin and Sgo2." *Curr Biol* **20**(17): 1511-1521.
- Liu, P., D. M. Slater, et al. (2009). "Replication licensing promotes cyclin D1 expression and G1 progression in untransformed human cells." *Cell Cycle* **8**(1): 125-136.
- Long, J., T. R. Gallagher, et al. (2008). "Ubiquitin recognition by the ubiquitin-associated domain of p62 involves a novel conformational switch." *J Biol Chem* **283**(9): 5427-5440.
- Magnuson, T., S. Debrot, et al. (1985). "The early lethality of autosomal monosomy in the mouse." *The Journal of experimental zoology* **236**(3): 353-360.
- Magnuson, T., S. Smith, et al. (1982). "The development of monosomy 19 mouse embryos." *J Embryol Exp Morphol* **69**: 223-236.
- Mao, R., C. L. Zielke, et al. (2003). "Global up-regulation of chromosome 21 gene expression in the developing Down syndrome brain." *Genomics* **81**(5): 457-467.

7 REFERENCES

- Masramon, L., M. Ribas, et al. (2000). "Cytogenetic characterization of two colon cell lines by using conventional G-banding, comparative genomic hybridization, and whole chromosome painting." *Cancer Genet Cytogenet* **121**(1): 17-21.
- Mathew, R., C. M. Karp, et al. (2009). "Autophagy suppresses tumorigenesis through elimination of p62." *Cell* **137**(6): 1062-1075.
- Mathew, R., S. Kongara, et al. (2007). "Autophagy suppresses tumor progression by limiting chromosomal instability." *Genes & development* **21**(11): 1367-1381.
- Matsunaga, K., T. Saitoh, et al. (2009). "Two Beclin 1-binding proteins, Atg14L and Rubicon, reciprocally regulate autophagy at different stages." *Nature cell biology* **11**(4): 385-396.
- Mayer, V. W. and A. Aguilera (1990). "High levels of chromosome instability in polyploids of *Saccharomyces cerevisiae*." *Mutation research* **231**(2): 177-186.
- Michaelis, C., R. Ciosk, et al. (1997). "Cohesins: chromosomal proteins that prevent premature separation of sister chromatids." *Cell* **91**(1): 35-45.
- Michel, L. S., V. Liberal, et al. (2001). "MAD2 haplo-insufficiency causes premature anaphase and chromosome instability in mammalian cells." *Nature* **409**(6818): 355-359.
- Mizushima, N. "The role of the Atg1/ULK1 complex in autophagy regulation." *Curr Opin Cell Biol* **22**(2): 132-139.
- Mizushima, N. and B. Levine "Autophagy in mammalian development and differentiation." *Nat Cell Biol* **12**(9): 823-830.
- Mizushima, N., B. Levine, et al. (2008). "Autophagy fights disease through cellular self-digestion." *Nature* **451**(7182): 1069-1075.
- Mizushima, N., H. Sugita, et al. (1998). "A new protein conjugation system in human. The counterpart of the yeast Apg12p conjugation system essential for autophagy." *The Journal of biological chemistry* **273**(51): 33889-33892.
- Morimoto, R. I. (2008). "Proteotoxic stress and inducible chaperone networks in neurodegenerative disease and aging." *Genes Dev* **22**(11): 1427-1438.
- Muratani, M. and W. P. Tansey (2003). "How the ubiquitin-proteasome system controls transcription." *Nature reviews. Molecular cell biology* **4**(3): 192-201.
- Nagaoka, S. I., T. J. Hassold, et al. (2012). "Human aneuploidy: mechanisms and new insights into an age-old problem." *Nat Rev Genet* **13**(7): 493-504.
- Nawata, H., G. Kashino, et al. (2011). "Dysregulation of gene expression in the artificial human trisomy cells of chromosome 8 associated with transformed cell phenotypes." *PLoS One* **6**(9): e25319.
- Nesbit, C. E., J. M. Tersak, et al. (1999). "MYC oncogenes and human neoplastic disease." *Oncogene* **18**(19): 3004-3016.
- Nguyen, V. Q., C. Co, et al. (2001). "Cyclin-dependent kinases prevent DNA re-replication through multiple mechanisms." *Nature* **411**(6841): 1068-1073.
- Nijman, S. M., M. P. Luna-Vargas, et al. (2005). "A genomic and functional inventory of deubiquitinating enzymes." *Cell* **123**(5): 773-786.
- Novak, I., V. Kirkin, et al. "Nix is a selective autophagy receptor for mitochondrial clearance." *EMBO Rep* **11**(1): 45-51.

7 REFERENCES

- Olson, M. I. and C. M. Shaw (1969). "Presenile dementia and Alzheimer's disease in mongolism." Brain **92**(1): 147-156.
- Olzscha, H., S. M. Schermann, et al. "Amyloid-like aggregates sequester numerous metastable proteins with essential cellular functions." Cell **144**(1): 67-78.
- Orenstein, S. J. and A. M. Cuervo "Chaperone-mediated autophagy: molecular mechanisms and physiological relevance." Semin Cell Dev Biol **21**(7): 719-726.
- Pandey, U. B., Z. Nie, et al. (2007). "HDAC6 rescues neurodegeneration and provides an essential link between autophagy and the UPS." Nature **447**(7146): 859-863.
- Pankiv, S., E. A. Alemu, et al. (2010). "FYCO1 is a Rab7 effector that binds to LC3 and PI3P to mediate microtubule plus end-directed vesicle transport." The Journal of cell biology **188**(2): 253-269.
- Pankiv, S., T. H. Clausen, et al. (2007). "p62/SQSTM1 binds directly to Atg8/LC3 to facilitate degradation of ubiquitinated protein aggregates by autophagy." J Biol Chem **282**(33): 24131-24145.
- Papp, B., C. Pal, et al. (2003). "Dosage sensitivity and the evolution of gene families in yeast." Nature **424**(6945): 194-197.
- Paulsson, K. and B. Johansson (2007). "Trisomy 8 as the sole chromosomal aberration in acute myeloid leukemia and myelodysplastic syndromes." Pathol Biol (Paris) **55**(1): 37-48.
- Pavelka, N., G. Rancati, et al. (2010). "Aneuploidy confers quantitative proteome changes and phenotypic variation in budding yeast." Nature **468**(7321): 321-325.
- Peters, J. M. (2012). "The many functions of cohesin--different rings to rule them all?" EMBO J **31**(9): 2061-2063.
- Petrozzi, L., C. Lucetti, et al. (2002). "Cytogenetic alterations in lymphocytes of Alzheimer's disease and Parkinson's disease patients." Neurol Sci **23 Suppl 2**: S97-98.
- Raslova, H., L. Roy, et al. (2003). "Megakaryocyte polyploidization is associated with a functional gene amplification." Blood **101**(2): 541-544.
- Ried, T., Y. Hu, et al. (2012). "The consequences of chromosomal aneuploidy on the transcriptome of cancer cells." Biochim Biophys Acta **1819**(7): 784-793.
- Rieder, C. L., R. W. Cole, et al. (1995). "The checkpoint delaying anaphase in response to chromosome monoorientation is mediated by an inhibitory signal produced by unattached kinetochores." The Journal of cell biology **130**(4): 941-948.
- Rodriguez, A., A. Duran, et al. (2006). "Mature-onset obesity and insulin resistance in mice deficient in the signaling adapter p62." Cell Metab **3**(3): 211-222.
- Salvador, N., C. Aguado, et al. (2000). "Import of a cytosolic protein into lysosomes by chaperone-mediated autophagy depends on its folding state." J Biol Chem **275**(35): 27447-27456.
- Sambrook, J., Maniatis, T., and Fritsch, E.F. (1989). *Molecular cloning: a laboratory manual*, 2nd edn (Cold Spring Harbor, N.Y., Cold Spring Harbor Laboratory Press)
- Sarto, F., I. Cominato, et al. (1982). "Increased incidence of chromosomal aberrations and sister chromatid exchanges in workers exposed to chromic acid (CrO₃) in electroplating factories." Carcinogenesis **3**(9): 1011-1016.

7 REFERENCES

- Sato, N., K. Mizumoto, et al. (2001). "Correlation between centrosome abnormalities and chromosomal instability in human pancreatic cancer cells." *Cancer Genet Cytogenet* **126**(1): 13-19.
- Schroder, M. and R. J. Kaufman (2005). "The mammalian unfolded protein response." *Annual review of biochemistry* **74**: 739-789.
- Segal, D. J. and E. E. McCoy (1974). "Studies on Down's syndrome in tissue culture. I. Growth rates and protein contents of fibroblast cultures." *Journal of cellular physiology* **83**(1): 85-90.
- Sheltzer, J. M., H. M. Blank, et al. (2011). "Aneuploidy drives genomic instability in yeast." *Science* **333**(6045): 1026-1030.
- Sheltzer, J. M., E. M. Torres, et al. (2012). "Transcriptional consequences of aneuploidy." *Proc Natl Acad Sci U S A* **109**(31): 12644-12649.
- Sherman, M. Y. and A. L. Goldberg (2001). "Cellular defenses against unfolded proteins: a cell biologist thinks about neurodegenerative diseases." *Neuron* **29**(1): 15-32.
- Sijts, E. J. and P. M. Kloetzel (2011). "The role of the proteasome in the generation of MHC class I ligands and immune responses." *Cell Mol Life Sci* **68**(9): 1491-1502.
- Solomon, D. A., T. Kim, et al. (2011). "Mutational inactivation of STAG2 causes aneuploidy in human cancer." *Science* **333**(6045): 1039-1043.
- Sotillo, R., E. Hernando, et al. (2007). "Mad2 overexpression promotes aneuploidy and tumorigenesis in mice." *Cancer cell* **11**(1): 9-23.
- Stefani, M. and C. M. Dobson (2003). "Protein aggregation and aggregate toxicity: new insights into protein folding, misfolding diseases and biological evolution." *J Mol Med (Berl)* **81**(11): 678-699.
- Stenberg, P., L. E. Lundberg, et al. (2009). "Buffering of segmental and chromosomal aneuploidies in *Drosophila melanogaster*." *PLoS Genet* **5**(5): e1000465.
- Stingele, S., G. Stoehr, et al. (2012). "Global analysis of genome, transcriptome and proteome reveals the response to aneuploidy in human cells." *Mol Syst Biol* **8**: 608.
- Stingele, S., G. Stoehr, et al. (2012). "Activation of autophagy in cells with abnormal karyotype." *Autophagy* **9**(2).
- Storchova, Z. and C. Kuffer (2008). "The consequences of tetraploidy and aneuploidy." *Journal of cell science* **121**(Pt 23): 3859-3866.
- Storchova, Z. and D. Pellman (2004). "From polyploidy to aneuploidy, genome instability and cancer." *Nature reviews. Molecular cell biology* **5**(1): 45-54.
- Suzuki, K., M. Ojima, et al. (2003). "Radiation-induced DNA damage and delayed induced genomic instability." *Oncogene* **22**(45): 6988-6993.
- Tabas, I. and D. Ron (2011). "Integrating the mechanisms of apoptosis induced by endoplasmic reticulum stress." *Nature cell biology* **13**(3): 184-190.
- Tang, Y. C., B. R. Williams, et al. (2011). "Identification of aneuploidy-selective antiproliferation compounds." *Cell* **144**(4): 499-512.

7 REFERENCES

- Tanida, I., E. Tanida-Miyake, et al. (2002). "Human Apg3p/Aut1p homologue is an authentic E2 enzyme for multiple substrates, GATE-16, GABARAP, and MAP-LC3, and facilitates the conjugation of hApg12p to hApg5p." The Journal of biological chemistry **277**(16): 13739-13744.
- Tanida, I., E. Tanida-Miyake, et al. (2001). "The human homolog of *Saccharomyces cerevisiae* Apg7p is a Protein-activating enzyme for multiple substrates including human Apg12p, GATE-16, GABARAP, and MAP-LC3." The Journal of biological chemistry **276**(3): 1701-1706.
- Tanida, I., T. Ueno, et al. (2008). "LC3 and Autophagy." Methods in molecular biology **445**: 77-88.
- Taylor, R. C. and A. Dillin (2011). "Aging as an event of proteostasis collapse." Cold Spring Harbor perspectives in biology **3**(5).
- Thompson, S. L. and D. A. Compton (2010). "Proliferation of aneuploid human cells is limited by a p53-dependent mechanism." The Journal of cell biology **188**(3): 369-381.
- Todaro, G. J. and H. Green (1963). "Quantitative studies of the growth of mouse embryo cells in culture and their development into established lines." J Cell Biol **17**: 299-313.
- Toikkanen, S., H. Joensuu, et al. (1993). "DNA aneuploidy in ectopic pregnancy and spontaneous abortions." European journal of obstetrics, gynecology, and reproductive biology **51**(1): 9-13.
- Tompa, P., J. Prilusky, et al. (2008). "Structural disorder serves as a weak signal for intracellular protein degradation." Proteins **71**(2): 903-909.
- Torres, E. M., N. Dephoure, et al. (2010). "Identification of aneuploidy-tolerating mutations." Cell **143**(1): 71-83.
- Torres, E. M., T. Sokolsky, et al. (2007). "Effects of aneuploidy on cellular physiology and cell division in haploid yeast." Science **317**(5840): 916-924.
- Torres, E. M., B. R. Williams, et al. (2010). "Thoughts on aneuploidy." Cold Spring Harbor symposia on quantitative biology **75**: 445-451.
- Uppender, M. B., J. K. Habermann, et al. (2004). "Chromosome transfer induced aneuploidy results in complex dysregulation of the cellular transcriptome in immortalized and cancer cells." Cancer Res **64**(19): 6941-6949.
- Veitia, R. A. (2002). "Exploring the etiology of haploinsufficiency." Bioessays **24**(2): 175-184.
- Veitia, R. A. (2003). "Nonlinear effects in macromolecular assembly and dosage sensitivity." J Theor Biol **220**(1): 19-25.
- Veitia, R. A. (2005). "Gene dosage balance: deletions, duplications and dominance." Trends Genet **21**(1): 33-35.
- Veitia, R. A., S. Bottani, et al. (2008). "Cellular reactions to gene dosage imbalance: genomic, transcriptomic and proteomic effects." Trends Genet **24**(8): 390-397.
- Verhoef, L. G., K. Lindsten, et al. (2002). "Aggregate formation inhibits proteasomal degradation of polyglutamine proteins." Hum Mol Genet **11**(22): 2689-2700.
- Walter, P. and D. Ron (2011). "The unfolded protein response: from stress pathway to homeostatic regulation." Science **334**(6059): 1081-1086.

7 REFERENCES

- Weaver, B. A. and D. W. Cleveland (2007). "Aneuploidy: instigator and inhibitor of tumorigenesis." Cancer research **67**(21): 10103-10105.
- Weaver, B. A., A. D. Silk, et al. (2007). "Aneuploidy acts both oncogenically and as a tumor suppressor." Cancer cell **11**(1): 25-36.
- Webb, J. L., B. Ravikumar, et al. (2003). "Alpha-Synuclein is degraded by both autophagy and the proteasome." J Biol Chem **278**(27): 25009-25013.
- Williams, B. R., V. R. Prabhu, et al. (2008). "Aneuploidy affects proliferation and spontaneous immortalization in mammalian cells." Science **322**(5902): 703-709.
- Wooten, M. W., T. Geetha, et al. (2008). "Essential role of sequestosome 1/p62 in regulating accumulation of Lys63-ubiquitinated proteins." J Biol Chem **283**(11): 6783-6789.
- Xie, Z. and D. J. Klionsky (2007). "Autophagosome formation: core machinery and adaptations." Nat Cell Biol **9**(10): 1102-1109.
- Yamamoto, A., Y. Tagawa, et al. (1998). "Bafilomycin A1 prevents maturation of autophagic vacuoles by inhibiting fusion between autophagosomes and lysosomes in rat hepatoma cell line, H-4-II-E cells." Cell Struct Funct **23**(1): 33-42.
- Yang, Z. and D. J. Klionsky "Mammalian autophagy: core molecular machinery and signaling regulation." Curr Opin Cell Biol **22**(2): 124-131.
- Yang, Z. and D. J. Klionsky (2010). "Mammalian autophagy: core molecular machinery and signaling regulation." Current opinion in cell biology **22**(2): 124-131.
- Yla-Anttila, P., H. Vihinen, et al. (2009). "3D tomography reveals connections between the phagophore and endoplasmic reticulum." Autophagy **5**(8): 1180-1185.
- Yurov, Y. B., I. Y. Iourov, et al. (2007). "Aneuploidy and confined chromosomal mosaicism in the developing human brain." PloS one **2**(6): e558.
- Yurov, Y. B., S. G. Vorsanova, et al. (2009). "GIN'n'CIN hypothesis of brain aging: deciphering the role of somatic genetic instabilities and neural aneuploidy during ontogeny." Molecular cytogenetics **2**: 23.
- Zhang, N., G. Ge, et al. (2008). "Overexpression of Separase induces aneuploidy and mammary tumorigenesis." Proceedings of the National Academy of Sciences of the United States of America **105**(35): 13033-13038.
- Zhang, Y., J. H. Malone, et al. "Expression in aneuploid Drosophila S2 cells." PLoS Biol **8**(2): e1000320.
- Zhang, Y. and B. Oliver (2007). "Dosage compensation goes global." Current opinion in genetics & development **17**(2): 113-120.
- Zhu, J., N. Pavelka, et al. (2012). "Karyotypic determinants of chromosome instability in aneuploid budding yeast." PLoS Genet **8**(5): e1002719.
- Zhu, K., K. Dunner, Jr., et al. (2010). "Proteasome inhibitors activate autophagy as a cytoprotective response in human prostate cancer cells." Oncogene **29**(3): 451-462.

8 ABBREVIATIONS

2-D	two-dimensional
μ	micro
aa	amino acid
aCGH	array-comparative genomic hybridization
ADP	adenosine 5'-diphosphate
AML	acute myeloid leukaemia
AMP	adenosine 5'-monophosphate
APS	ammonium-peroxo-disulfate
Arg	arginine
ATG	autophagy related genes
ATP	adenosine 5'-triphosphate
β-Gal	beta-galactosidase
bp	base pairs
β-ME	beta-mercaptoethanol
BSA	bovine serum albumin
C	DNA content
C-terminal	carboxyterminal
°C	degree Celsius
<i>C. elegans</i>	<i>Caenorhabditis elegans</i>
chr.	chromosome
CIN	chromosomal instability
CORUM	KEGG pathways, molecular complexes
DMEM	Dulbecco's modified Eagle medium
DMSO	dimethylsulfoxide
DNA	deoxyribonucleic acid
DTT	dithiothreitol
DUB	de-ubiquitinating enzyme
E1	ubiquitin activation enzyme
E2	ubiquitin conjugating enzyme
E3	ubiquitin ligase
<i>E. coli</i>	<i>Escherichia coli</i>
EDTA	ethylenediaminetetraacetic acid
e.g.	exempli gratia, for example
ER	endoplasmic reticulum
ERAD	endoplasmic-reticulum-associated protein degradation
ESR	environmental stress response
FACS	fluorescence-activated cell sorting
FBS	fetal bovine serum
Fig.	Figure
FISH	fluorescence in situ hybridization
g	gram; gravitational constant
G1 phase	gap 1 phase of the cell cycle
G2 phase	gap 2 phase of the cell cycle
G418	geneticine disulfate
GCR	gross chromosomal rearrangements
gDNA	genomic DNA
GFP	green fluorescent protein
GO	gene ontology
GOBP	GO biological processes
GOCC	GO cellular components
GOMF	GO molecular functions

8 ABBREVIATIONS

h	hour(s)
H	histone
γH2AX	phosphorylated histone 2A variant X
H2B	histone 2B
HCT116 3/3	cell line HCT116 plus one chr. 3
HCT116 5/4	cell line HCT116 plus two chr. 5
HCT116 H2B-GFP 5/3	cell line HCT116 H2B-GFP plus one chr. 5
HCT116 H2B-GFP 5/4	cell line HCT116 H2B-GFP plus two chr. 5
HSFs	heat shock transcription factors
HSPs	heat shock proteins
HU	hydroxyurea
hTERT	human telomerase reverse transcriptase
IP	immunoprecipitation
K	lysine, kilo (for aCGH)
k	kilo
kb	kilo base pairs
kDa	kilo Daltons
KEGG	Kyoto Encyclopedia of Gene and Genomes
l	liter
LB-media	Luria-Bertani media
LIR	LC3 interacting region
Lys	lysine
m	mili
M	molar
M-FISH	Multiplex-FISH
MIN	microsatellite instability
min	minute(s)
MEF	mouse embryonic fibroblasts
mRFP	monomeric red fluorescent protein
mRNA	messenger RNA
MSL	male-specific lethal
MW	molecular weight
N	chromosome content
n	nano
NEB	nuclear envelope breakdown
OA	onset of anaphase
OD	optical density
p	pico
PB1	Phox and Bem1p
PHA-P	phytohemagglutinin
PI	propidium iodide
PAGE	polyacrylamide gel electrophoresis
PBS	phosphate-buffered saline
PE	phosphatidyl ethanolamine
PEG	polyethylene glycol
PVDF	polyvinylidenfluorid
RNase	ribonuclease
ROS	reactive oxygen species
RPE-1	cell line RPE-1 hTERT
RPE-1 5/3 12/3	RPE-1 cell line plus one chr. 5 and one chr. 12
RPE-1 H2B-GFP 21/3	RPE-1 H2B-GFP cell line plus one long arm of chr. 21
rpm	rounds per minute
s	seconds
S	sedimentation coefficient (Svedberg)
SAC	spindle assembly checkpoint

8 ABBREVIATIONS

SCNAs	small site specific changes
SD	standard deviation
SDS	sodium dodecylsulfate
SEM	standard error of mean
SILAC	stable isotope labeling of amino acids in cell culture
TBS	tris-buffered saline
TEMED	N,N,N',N'- tetramethylethylene diamine
Tris	tris (hydromethyl) aminomethane
U	unit
UBA	ubiquitin associated
UPR	unfolded protein response
UPS	ubiquitin proteasome system
UV	ultra violet
V	volt
v/v	volume per volume
w/v	weight per volume
X	times
X-Gal	5-bromo-4-chloro-indolyl- β -D-galactopyranoside
YAC	yeast artificial chromosome

9 ACKNOWLEDGEMENTS

First, I would like to thank my PhD supervisor Zuzana Storchova for her trust in my work and her active support. Her exceptional passion for science and her intellect creates a motivating working atmosphere which provides space for inspiring discussions. Zuzana, I also want to thank you for your good company during lunch time.

I also want to thank Stefan Jentsch for being such a generous and kind host. Thank you for being my “Doktorvater” and for reading my thesis.

Additionally, my thanks go to our collaborators who contributed significantly to the success of this project. Thank you very much, Matthias, for your constant support. Thank you, Gabi, for the never ending data supply and for your good company.

Furthermore, I would like to thank the members of the doctoral thesis committee for refereeing my thesis. Especially, I would like to give thanks to the members of my thesis defense committee Peter Becker, John Parsch and Kirsten Jung. Peter Becker, thank you for co-refereeing this thesis, despite your busy time schedule.

Many thanks go also to the members of my thesis advisory committee for fruitful discussions. Thank you, Silke, that you came all the way from Tübingen.

Moreover, I am grateful to the IMPRS coordinators Maxi and Hans-Jörg, who always had an open ear for their PhDs.

I would like to thank the whole Storchova lab for exceptionally good company during my PhD. Chris, thanks for all your help, I think you are the most helpful person I have ever met. Anastasia, thanks for the fun you bring! Karolina, thank you for being a good company in “our” office. Especially, I would like to thank Susanne, who one can rely on, not only as technical support but also in everyday live. Thanks go also to my former diploma student Sarah for technical help.

There are a few people I would like to name, because they became very good friends during my PhD: Carina Frauer, Leila Khouri and Anne Wöllmer. Thank you for your friendship and the time we had here in Munich.

A great and warm thank you goes to my family, especially to my parents who always supported me in my life. I greatly appreciate how you care for me and at the same time leave me the freedom to find my own way in life. Of course I would like to thank my brother Claudius and my sister Anja, who are very important to me. Especially, I want to express my gratitude to my grandfather for his support and just for the way he is.

Finally, I would like to say thank you to my own small family. First, to my son Tom who, quoting Zuzana, was probably the best result during my PhD (also requiring the longest incubation time) and second, my husband Julian for many open ears, his support and his love. Thank you for the way you are and the way you changed my life for the better!

10 CURRICULUM VITAE

Name: Silvia Stingele (geb. Coenen)
Contact: Theresienstraße 156
80333 Munich
Germany

Date of birth: 10.08.1980
Nationality: German
Marital status: female, married
Email: coenen@biochem.mpg.de
Phone: 0177/6708897

Education and professional experience

Since February 2008 PhD Student Max Planck Institute of Biochemistry

February 2006 - St. Jude Children's Research Hospital, Memphis, Tennessee
May 2007 Master Thesis: February 2006 - November 2006 Department:
Biochemistry
Principal Investigator: Dr. John L. Cleveland (now: Scripps Institute,
Florida)
Project: Ulk1 in the regulation of autophagy in mammals

September 2004 - Internship, University of Southampton, England
April 2005 Department: Cancer Research UK, Oncology Division
Principal Investigator: Dr. Graham Packham
Project: Relevance of sequence insertions in the Mcl-1 promoter in
chronic lymphocytic leukemia (CLL)

October 2000 - Johannes Gutenberg University, University of Mainz, Germany
November 2006 Field of study: biology

Publications

- Stingele S.***, Stoehr G.*, Peplowska K., Cox J., Mann M., Storchova Z. (2012). "Global analysis of genome, transcriptome and proteome reveals the response to aneuploidy in human cells." *Mol Syst Biol* **8**: 608.
- Stingele S.**, Stoehr G., Storchova Z. (2012). "Activation of autophagy in cells with abnormal karyotype." *Autophagy* **9**(2).
- Dorsey, F. C., Rose K. L., **Coenen S.**, Prater S.M., Cavett V., Cleveland J.L., Caldwell-Busby J. (2009). "Mapping the phosphorylation sites of Ulk1." *J Proteome Res* **8**(11): 5253-5263.
- Coenen S.**, Pickering B., Potter K.N., Johnson P.W., Stevenson F.K., Packham G. (2005). "The relevance of sequence insertions in the Mcl-1 promoter in chronic lymphocytic leukemia and in normal cells." *Haematologica* **90**(9): 1285-1286.

